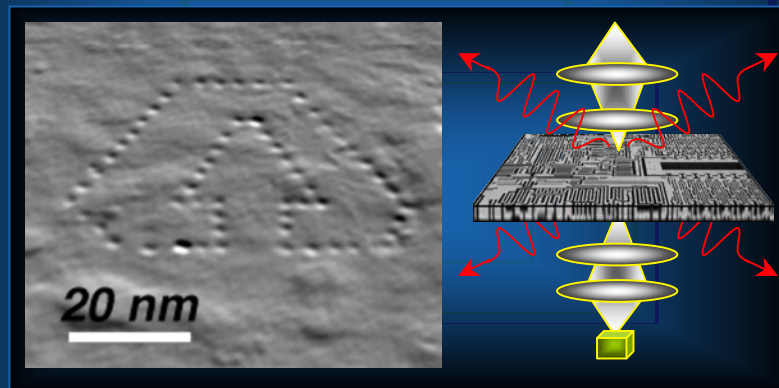


Introduction to EELS in the AEM

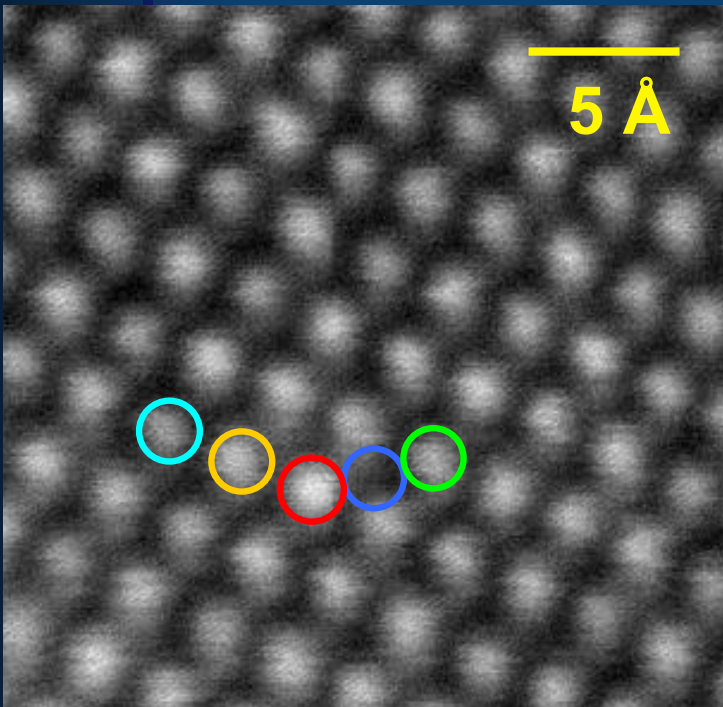


Nestor J. Zaluzec

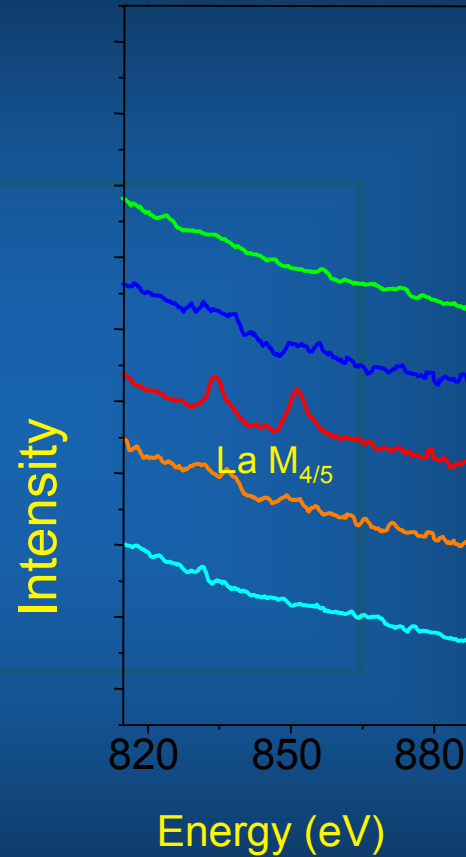
zaluzec@microscopy.com

zaluzec@aaem.amc.anl.gov

What are the Limits - Today?



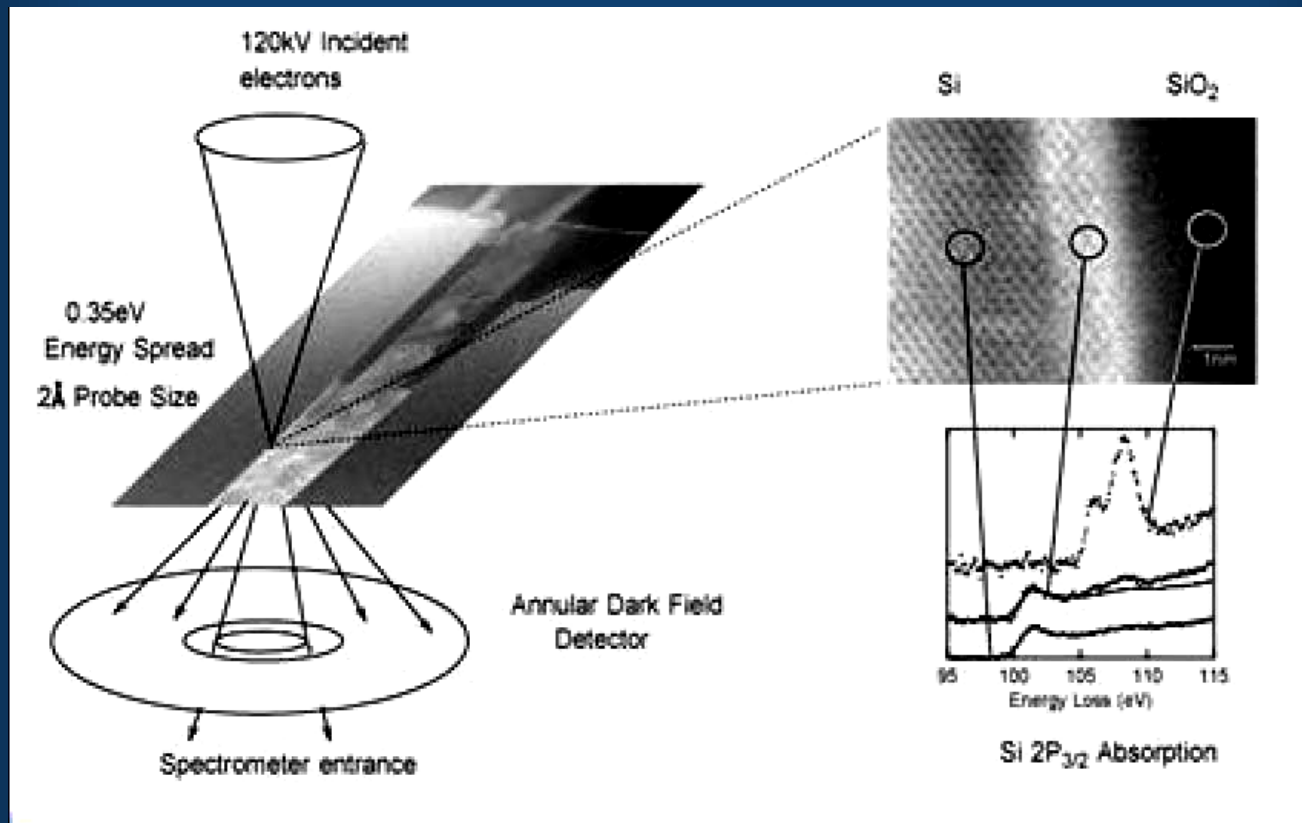
**La in CaTiO₃
grown by MBE**



Spectroscopic
identification at
subnanometer
resolution.

8% collection
efficiency

AEM - High Spatial Resolution Analysis



Electronic Structure changes at the Si/SiO₂ Interface

Brief Review of Energy Loss Processes

Instrumentation: Detector Systems

Instrumentation: AEM Systems

Data Analysis and Quantification:

Advanced Topics

Brief Review of Energy Loss Processes

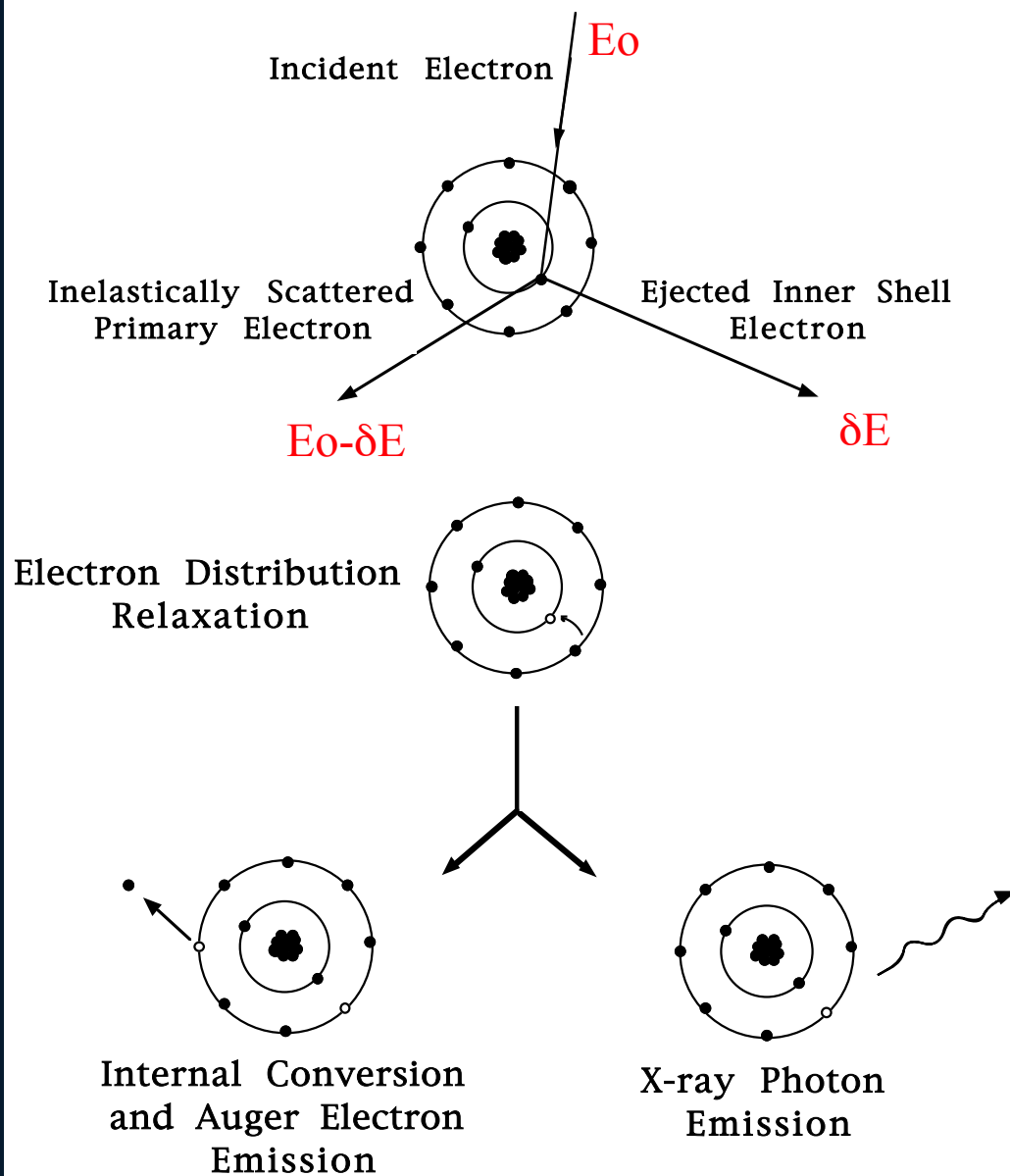
Electron Excitation of Inner Shell & Continuum Processes

Spectral Shapes

Notation of Edges

Electron Scattering Angular Distributions

Electron Excitation of Inner Shell Processes



The Emission Process:

- 1-Excitation
- 2-Relaxation
- 3-Emission

Electron Energy Loss Spectroscopy

Measure the changes in the energy distribution of an electron beam transmitted through a **thin** specimen.

Each type of interaction between the electron beam and the specimen produces a **characteristic** change in the energy and angular distribution of scattered electrons.

The energy loss process is the **primary** interaction event. All other sources of analytical information (i.e. X-rays, Auger electrons, etc.) are **secondary** products of the initial inelastic event. Thus, EELS has the highest potential yield of information/inelastic event

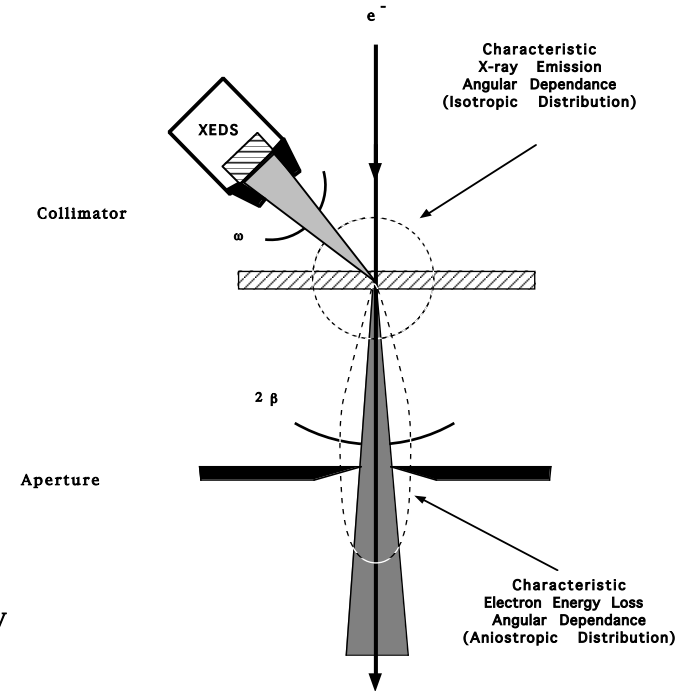
Geometrical Collection Efficiency in XEDS

$$\epsilon_{\omega} = \frac{\omega}{4\pi} = \frac{1}{4\pi} \frac{A}{R^2}$$

Geometrical Collection Efficiency in EELS

$$\epsilon_{\beta} = \frac{\ln \left(1 + \left[\frac{\beta}{\theta_E} \right]^2 \right)}{\ln \left(\frac{2}{\theta_E} \right)}$$

$$\theta_E = \frac{\Delta E}{2\gamma_0 T_0}; \quad \gamma_0 = \frac{1}{\sqrt{1-\beta^2}}; \quad T_0 = \frac{1}{2} m_0 v^2 = 255.530 \left[1 - \left(\frac{1}{1 + \frac{V_0(\text{kV})}{511.060}} \right)^2 \right] \text{ keV}$$



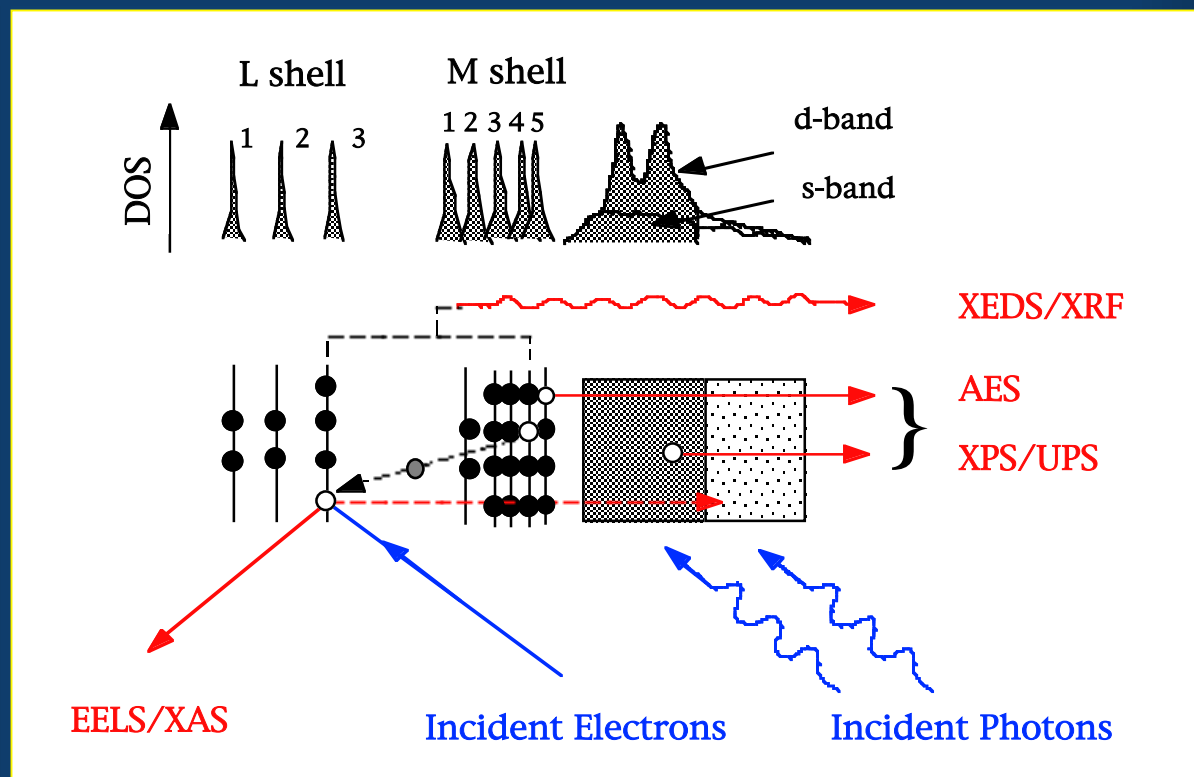
Accelerating Voltage V ₀ (kV)
50
100
120
150
200
250
300
350
400
1000

T ₀ = 1/2 m ₀ v ² (keV)•
43.5
76.8
87.9
102.8
123.5
140.3
153.8
165.5
175.1
226.3

Energy Loss ΔE (eV)
10
100
200
500
1000
500
500
500
500
500

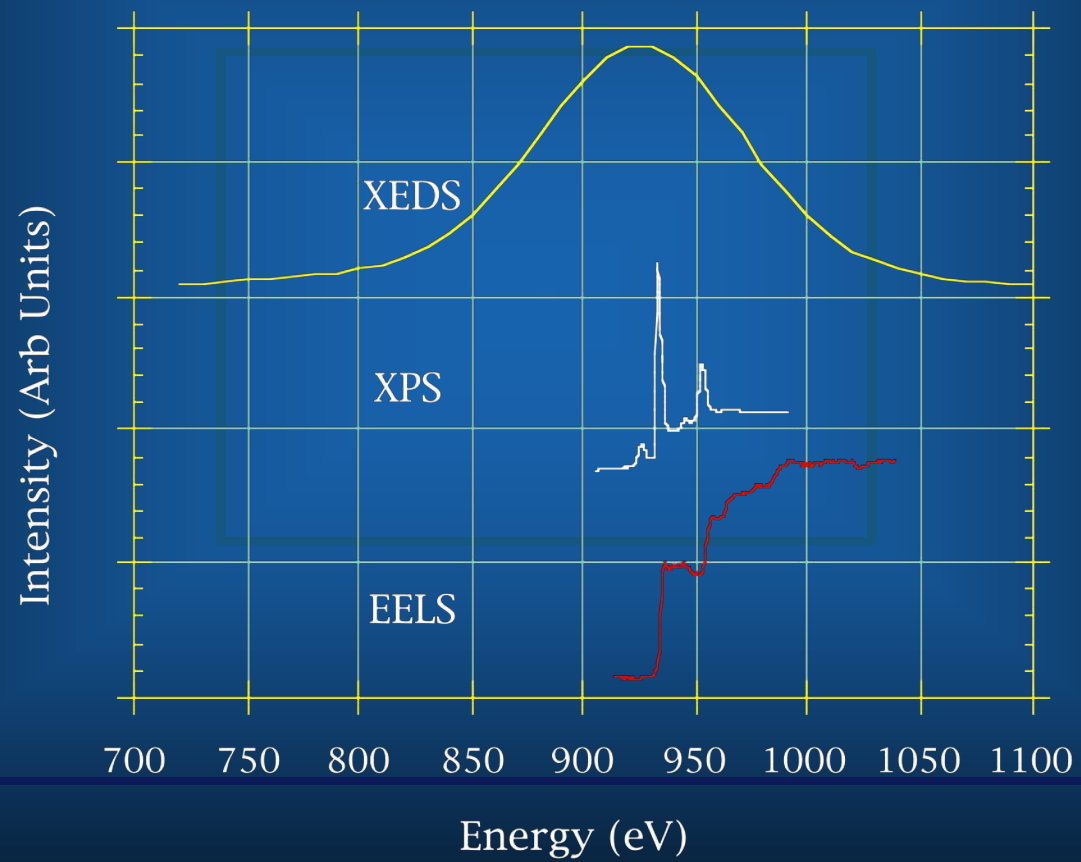
Accelerating Voltage (kV)
120
120
120
120
120
100
200
300
400
1000

Scattering Angle θ _E (mr)
0.057
0.569
1.14
2.84
5.69
3.26
2.02
1.62
1.43
1.10



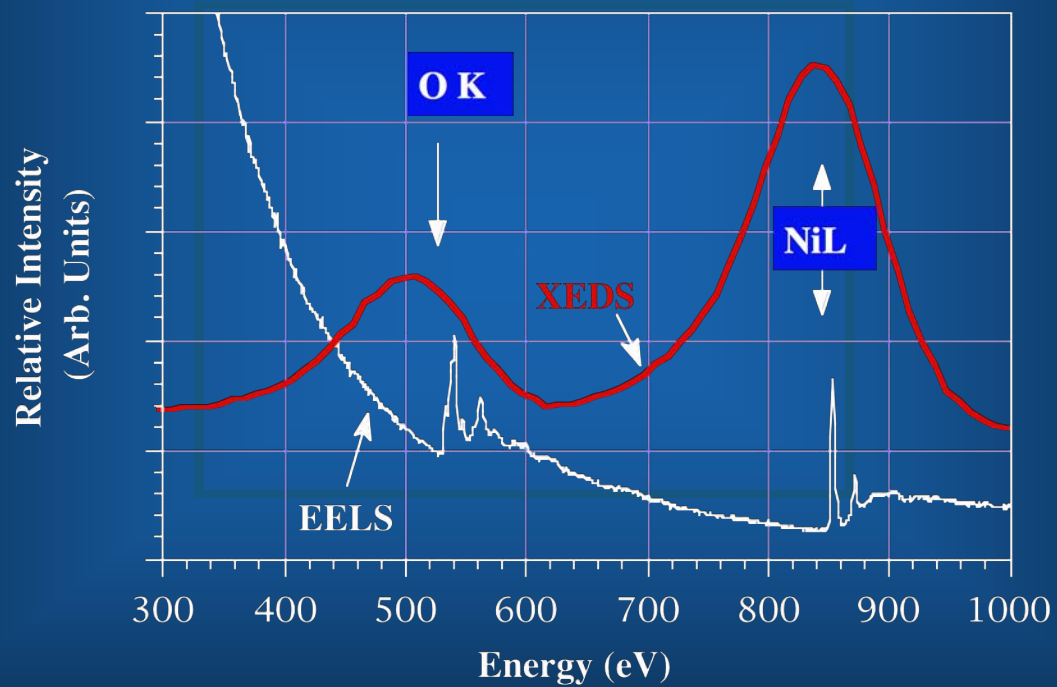
Schematic Diagram Illustrating Sources of Inelastic Scattering Signals

Experimental XEDS, XPS, and EELS data from the Copper L shell. Note the differences in energy resolution, and spectral features.



Comparison Light Element Spectroscopy Resolution XEDS vs EELS

Comparison of WL XEDS Detector and EELS spectra
taken from the same NiO specimen



Note the enhanced spectral information in the EELS data. Vertical scale is arbitrary and chosen for clarity of presentation.

Edges for EELS Microanalysis (0 - 3 keV)

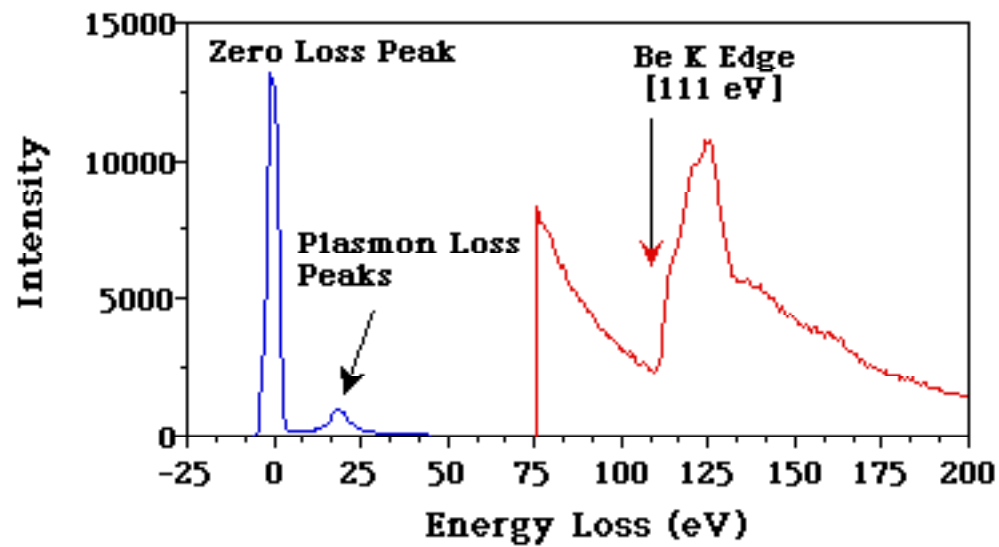


Table 1. Edges Suitable for EELS Microanalysis
for the Energy Range 0-3 keV

Atomic Number	Inner Shell	Spectroscopic Notation
Z = 1-11	K	1s
Z = 12-17	K L ₃ ,L ₂ ,L ₁	1s 2p _{3/2} ,2p _{1/2} ,2s
Z = 19-45	L ₃ ,L ₂ ,L ₁ M ₅₄ ,M ₃₂ ,M ₁	2p _{3/2} ...--> 3d _{5/2} ,3d _{3/2} ,3d _{1/2} , 3p _{3/2} ,3p _{1/2} ,3s
Z = 46-79	M ₅₄ ,M ₃₂ ,M ₁ N ₄₅ ,N ₃₂ ,N ₁ O ₃₂ ,O ₁	3d _{5/2} ...--> 4d _{5/2} ,4d _{3/2} ,4d _{1/2} , 4p _{3/2} ,4p _{1/2} ,4s 5p _{3/2} ,5p _{1/2} ,5s
Z > 80	N ₆₇ ,N ₄₅ ,N ₃₂ ,N ₁ O ₄₅ ,O ₃₂ ,O ₁	4f _{7/2} ...--> 5p _{3/2} ...-->

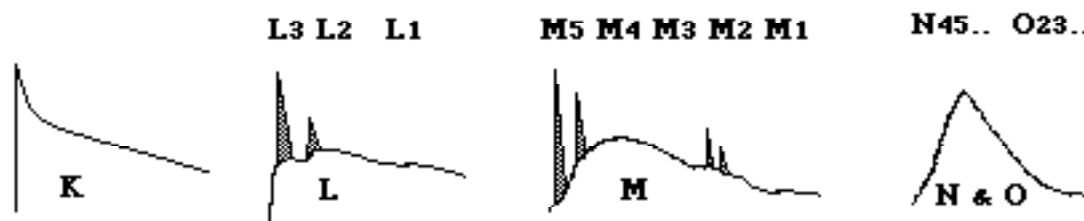


Figure 5. Schematic illustration of K, L, M, N and O Edge shapes, the "white lines" sometimes detected on L and M shells are shown shaded peaks at the edge onsets. In all sketches the background shape has been omitted for clarity. These profiles should be compared with experimental profiles of figure 6.

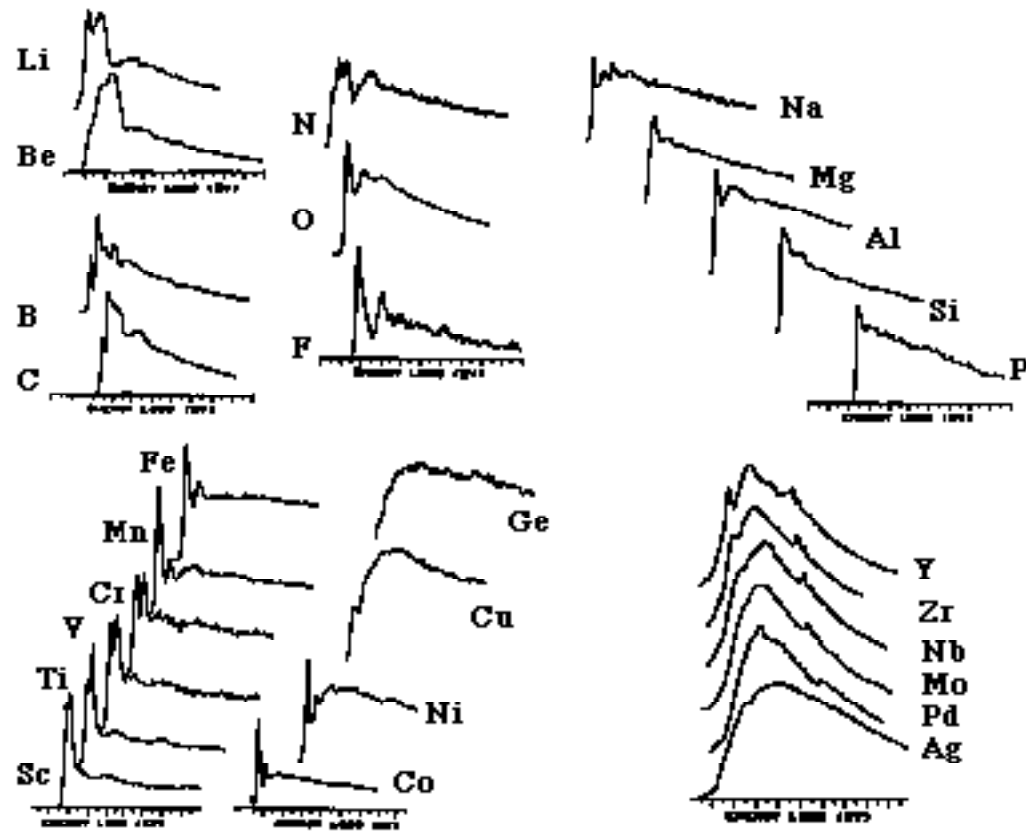
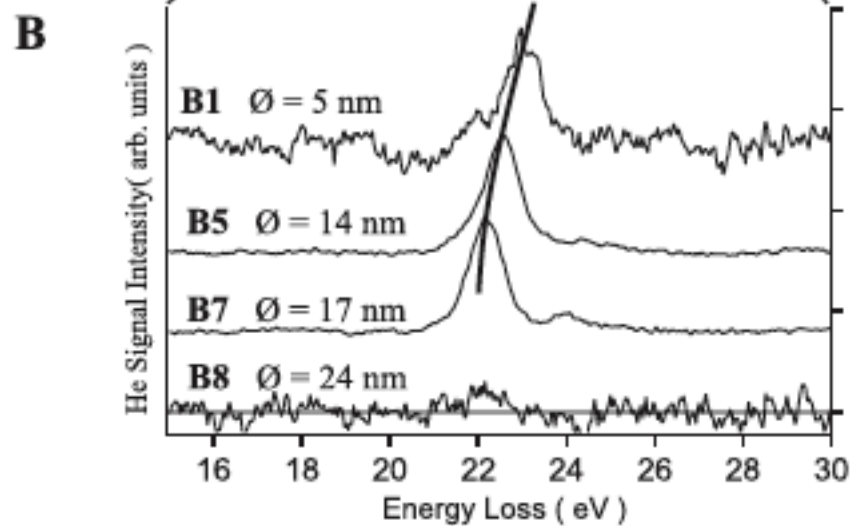
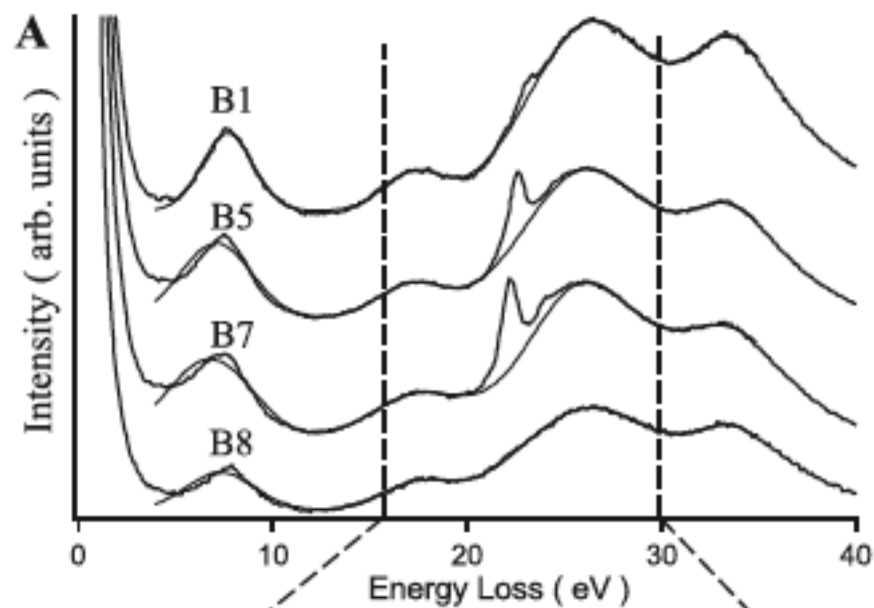


Figure 6. Selection of representative K-Shell [Li, Be, B, C, N, O, F, Na, Mg, Al, Si, P]; L-shell [Sc, Ti, V, Cr, Mn, Fe, Co, Ni, Cu, Ge]; and M-shell [Y, Zr, Nb, Mo, Pd, Ag] experimental spectral profiles (all background subtracted).



Helium
In Pd

D. Taverna et al
PRL 100, 035301 (2008)

Electron Scattering

Elastic Scattering

Single Atoms:

$$I(\theta) \sim |f(\theta)|^2 = |f_0|^2 \bullet \frac{1}{(\theta^2 + \theta_0^2)^2}$$

$$\theta_0 = \frac{1}{2\pi(0.885a_0Z^{-1/3})}$$

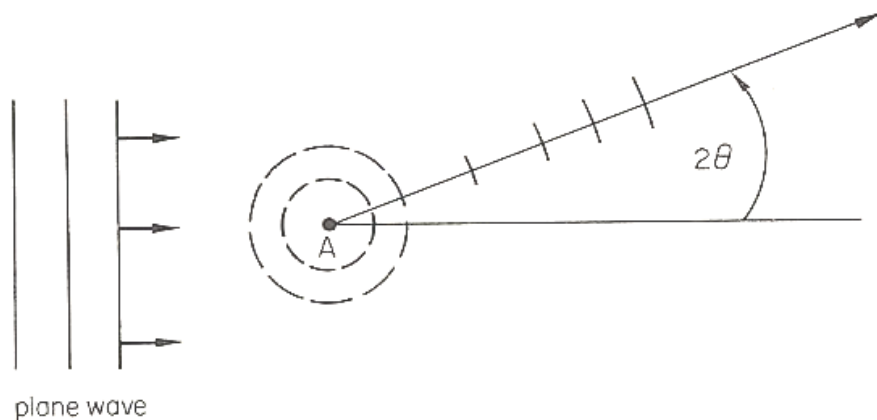


Figure 2.2 The scattering of a plane wave at an atom A through the formation of spherical wavelets travelling at an angle 2θ to the original direction of motion

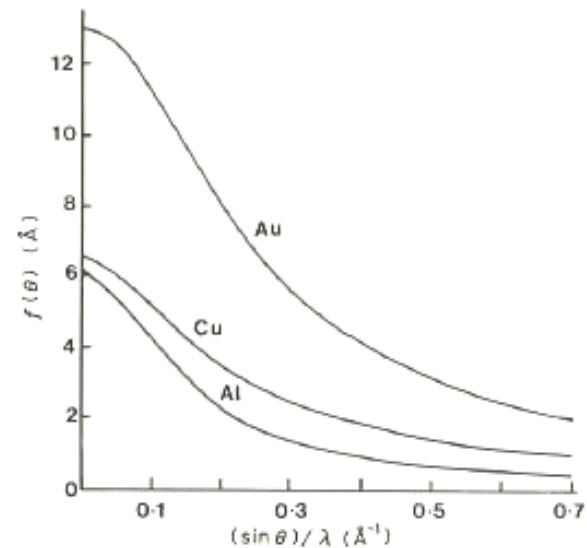


Fig. 2.2 Relationship between the atomic scattering factor $f(\theta)$ (in \AA) and the scattering angle $(\sin \theta) / \lambda$ (in \AA^{-1}) for aluminium, copper and gold calculated using equation (2.1).

Scattering from an isolated atom in free space

Elastic Scattering

Single Atoms:

$$I(\theta) \sim |\mathbf{f}(\theta)|^2 = |f_0|^2 \bullet \frac{1}{(\theta^2 + \theta_0^2)^2}$$

$$\theta_0 = \frac{1}{2\pi(0.885a_0Z^{-1/3})}$$



Amorphous Solids:

$$I(\theta) \sim |\mathbf{f}(\theta)|^2 \bullet \left\{ 1 + \frac{\sin(kR)}{kR} \right\}$$

$$k = \frac{4\pi}{\lambda} \sin(\theta)$$

Scattering from an collection of an amorphous collection of atoms
 - neighboring atoms give rise to interference

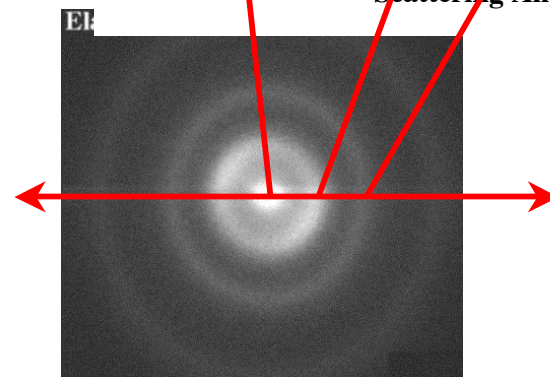
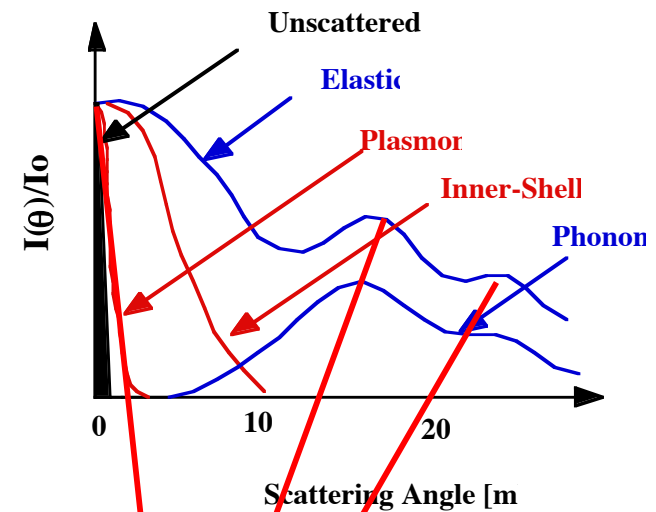
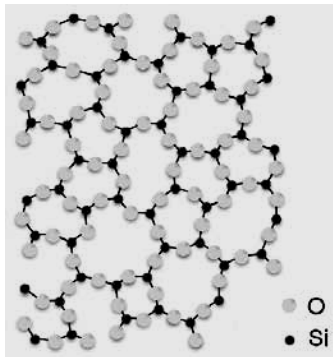
Amorphous Solids:

$$I(\theta) \sim |f(\theta)|^2 \cdot \left| 1 + \frac{\sin(kR)}{kR} \right|$$

$$k = \frac{4\pi}{\lambda} \sin(\theta)$$

R = Average Interatomic Spacing

Amorphous
Silica (SiO_2)



Phonons:

$$I(\theta) \sim |f(\theta)|^2 \cdot (1 - e^{-2M})$$

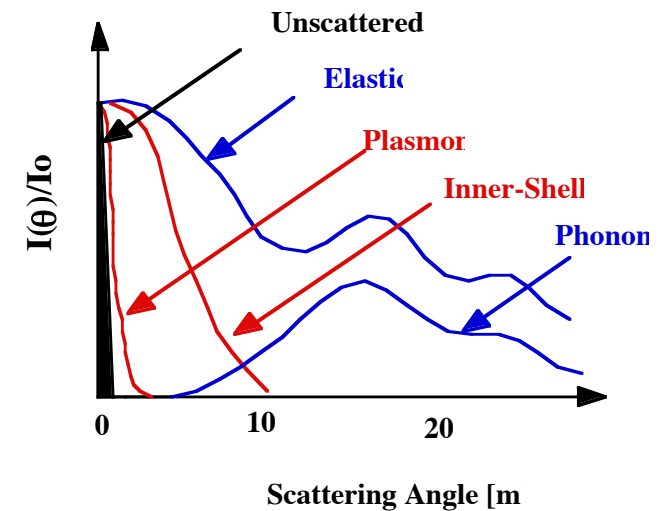
$$M = \frac{8\pi \langle u^2 \rangle \sin(\theta)}{\lambda}$$

Inelastic:

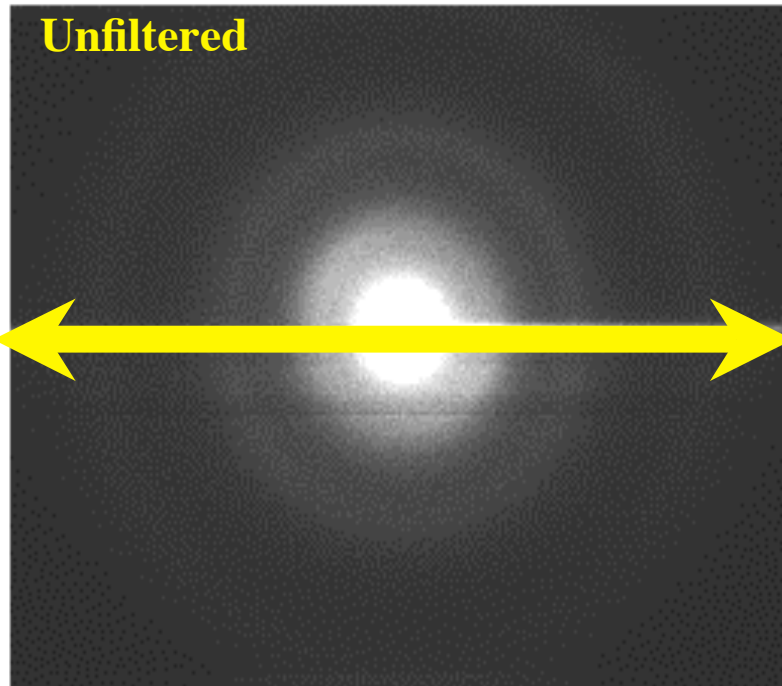
$$I(\theta) = \Gamma(\delta E, \theta) \cdot \frac{1}{\theta^2 + \theta_E^2}$$

$$\theta_E = \frac{\Delta E}{2\gamma_0 T_0} \quad \gamma_0 = \frac{1}{\sqrt{1 - \beta^2}}$$

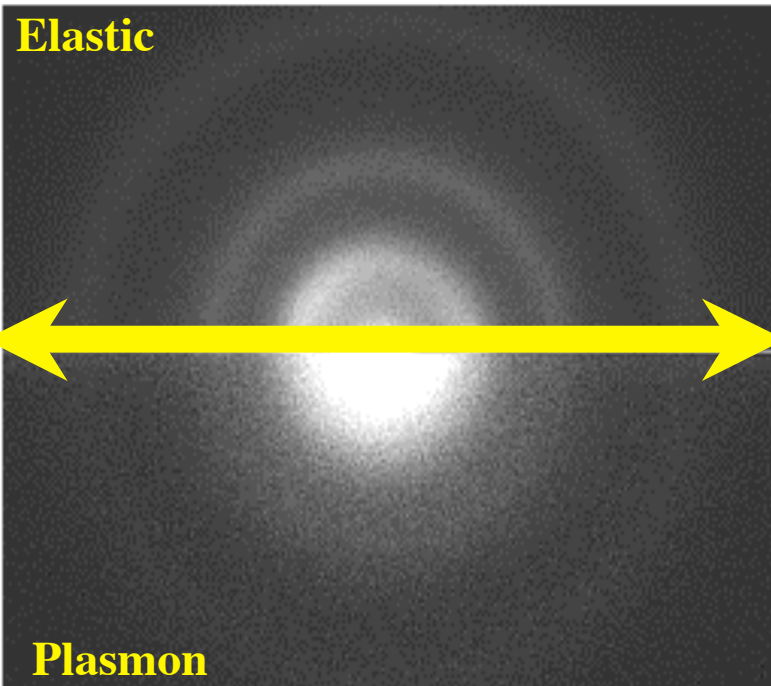
$\Gamma(\delta E, \theta)$: Imaginary Part of the Complex Dielectric constant(ϵ)
: Generalized Oscillator Strength



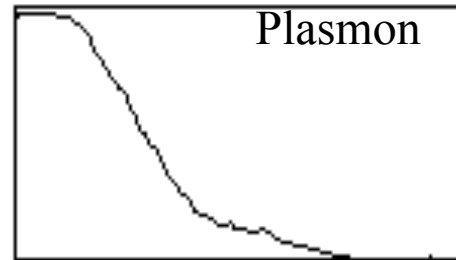
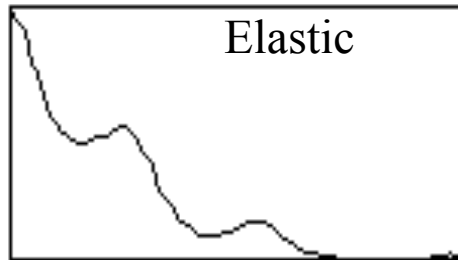
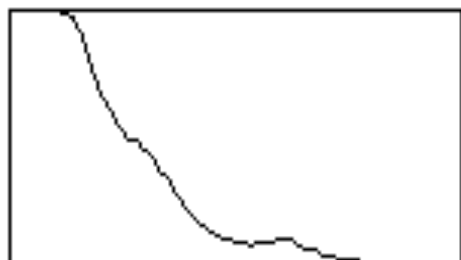
Unfiltered

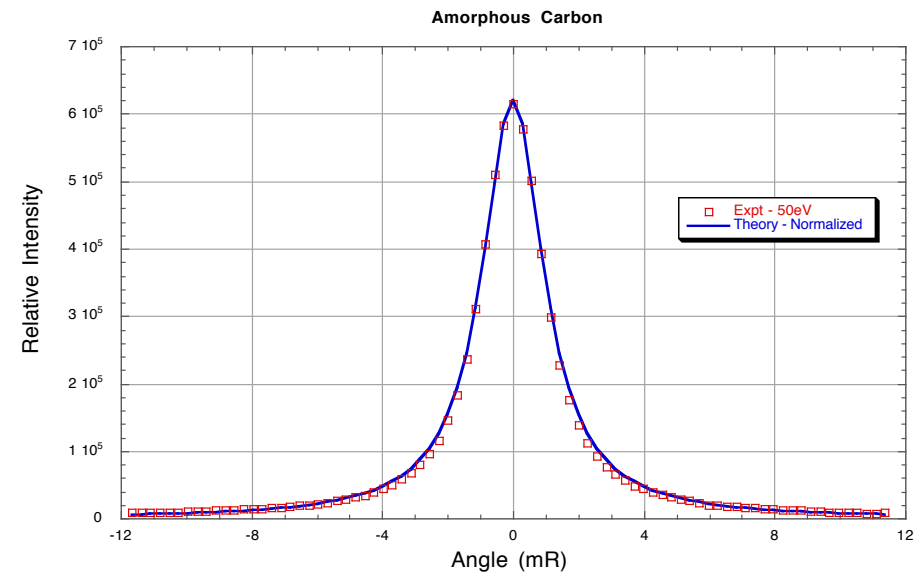
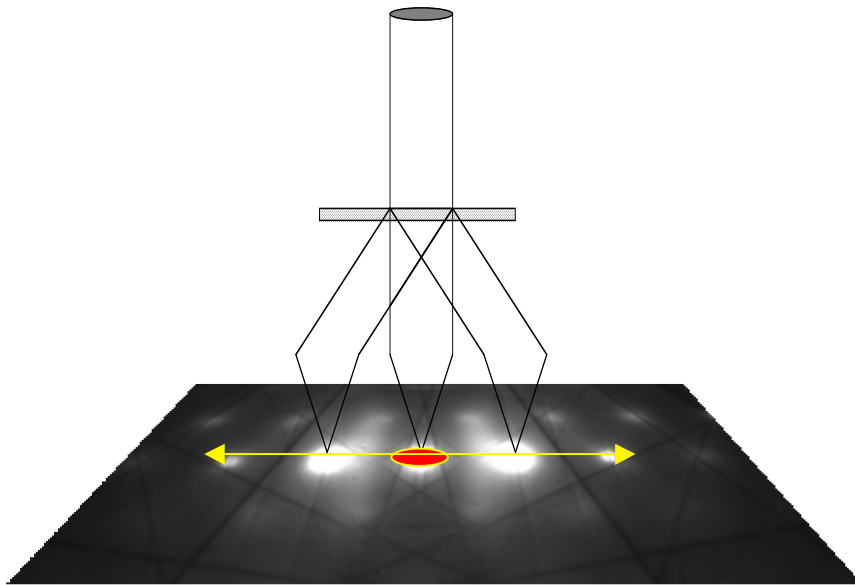


Elastic



Plasmon





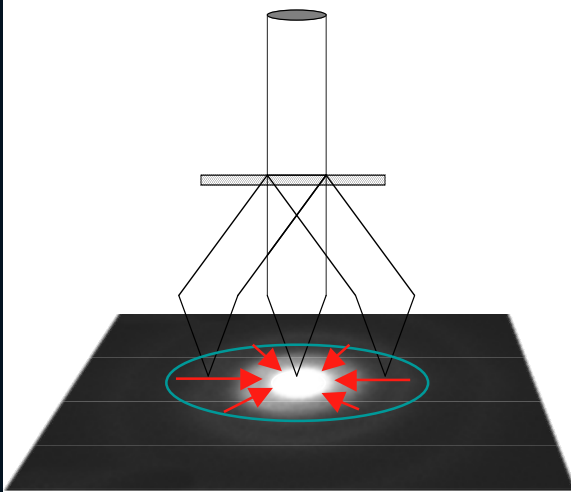
Inelastic:

$$I(\theta) = \Gamma(\delta E, \theta) \cdot \frac{1}{\theta^2 + \theta_E^2}$$

$$\theta_E = \frac{\Delta E}{2\gamma_0 T_0} \quad \gamma_0 = \frac{1}{\sqrt{1-\beta^2}}$$

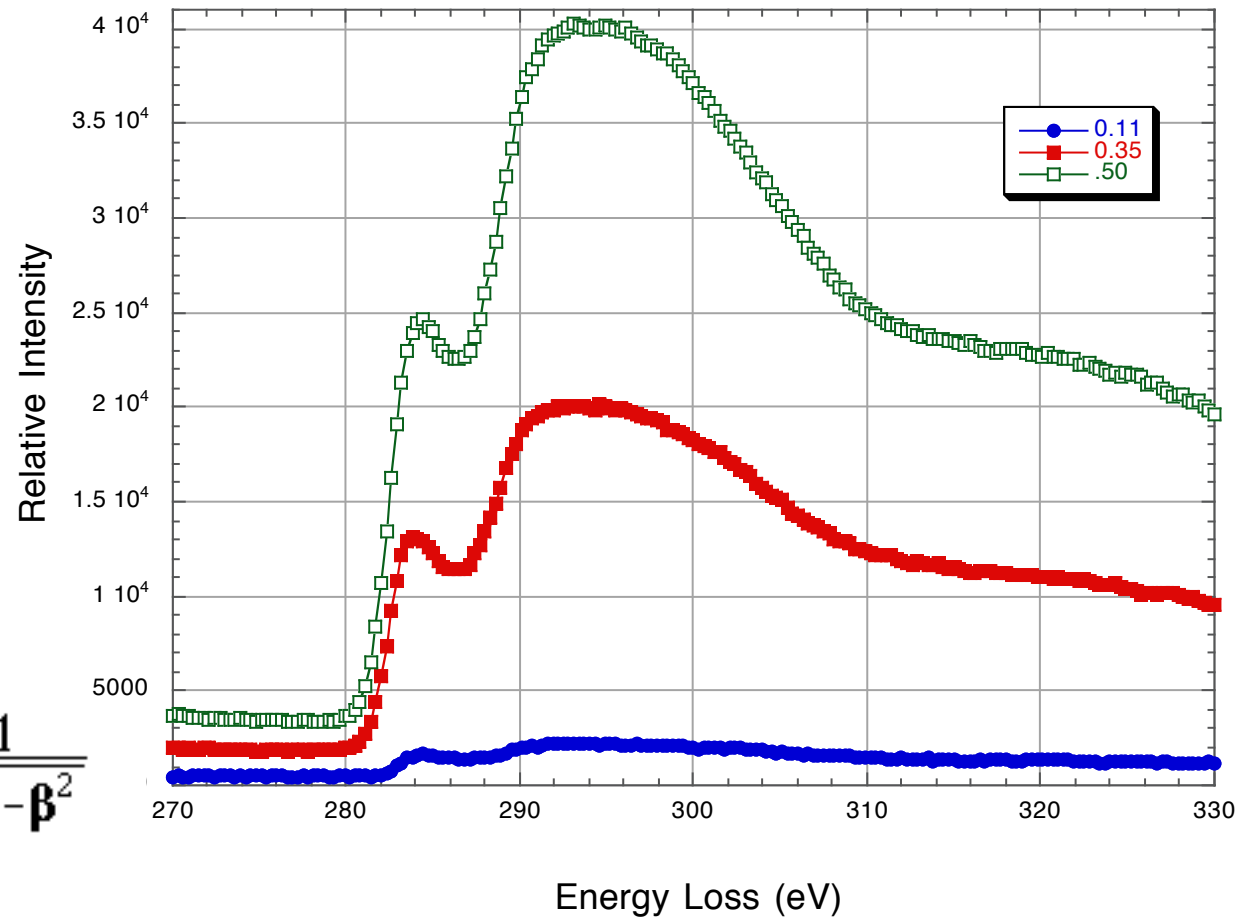
$\Gamma(\delta E, \theta)$: Imaginary Part of the Complex Dielectric constant(ϵ)
: Generalized Oscillator Strength

Intensity of Edges is Directly Related to Mean Scattering Angle Example: Amorphous Carbon



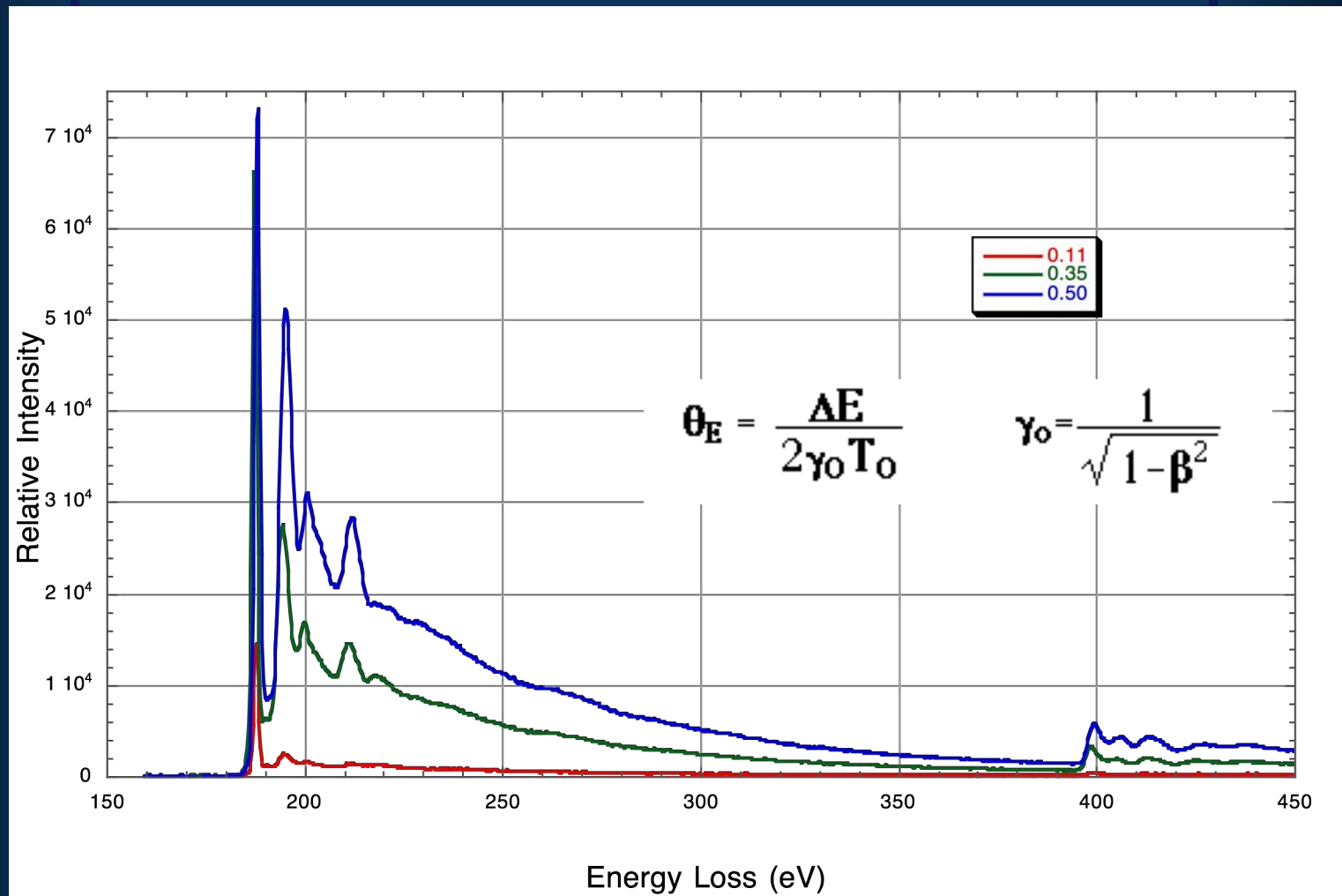
$$\theta_E = \frac{\Delta E}{2\gamma_0 T_0}$$

$$\gamma_0 = \frac{1}{\sqrt{1-\beta^2}}$$



$$\theta_E \sim 1.15 \text{ mR}$$

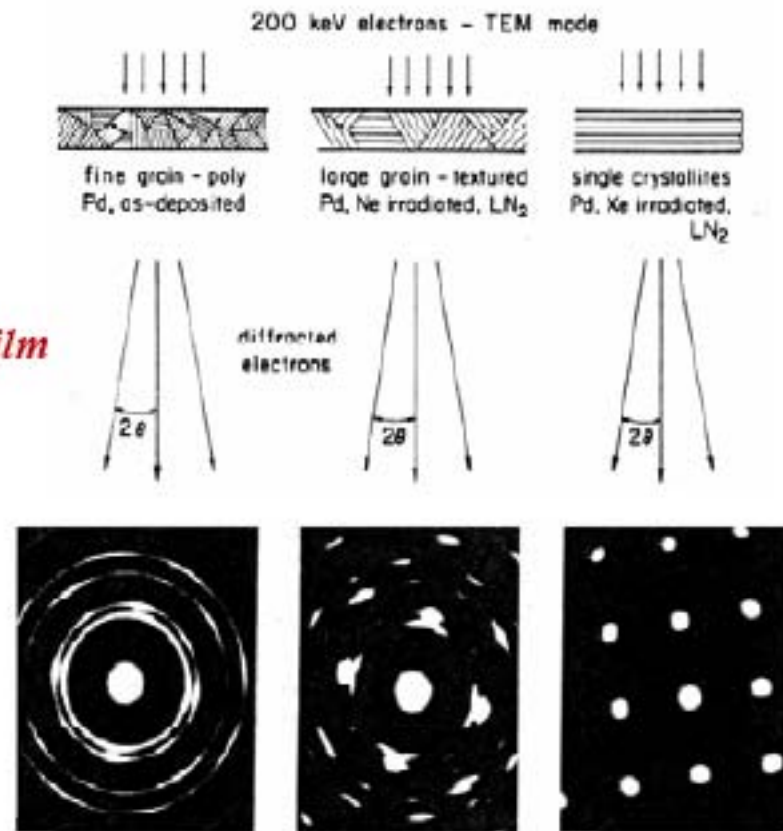
Intensity of Edges is Directly Related to Mean Scattering Angle Example: Boron - Nitride



$\theta_E \sim 0.777$ mR

$\theta_E \sim 1.62$ mR

*Electron Beam
Diffraction of a Pd film*



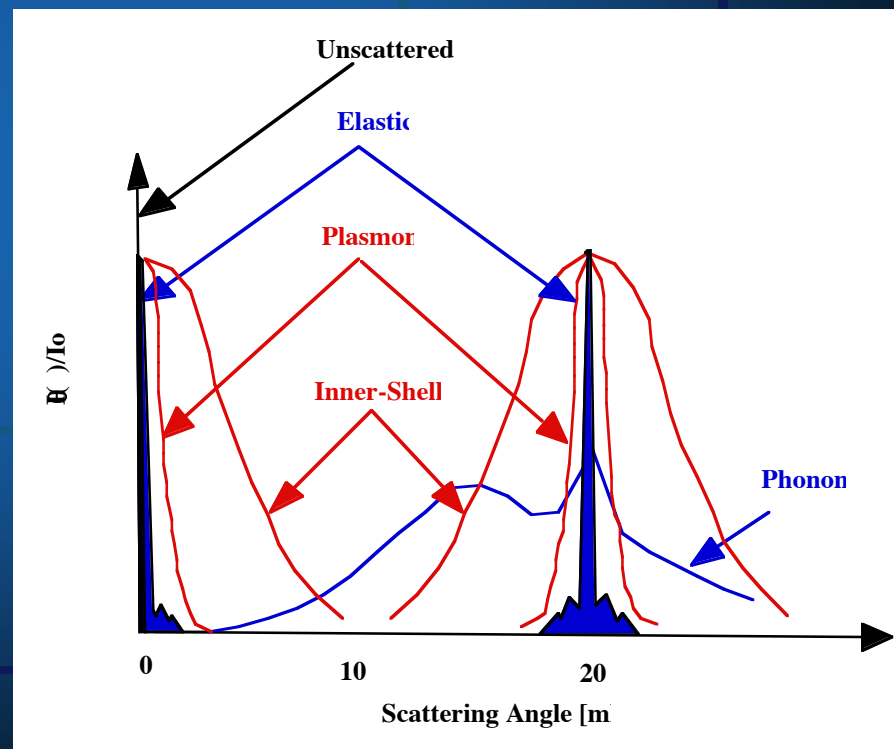
Type of Electron Scattering	Angular Range	Energy Loss
Unscattered	0	0
Elastic	10's-100's mR	~0
Phonon	10's-100's mR	<.025 eV
Inelastic	10's mR	everything else
Plasmon	< 1mr	10's of eV
Inner-Shell	~10's of mR	10's-1000's eV

Elastic Scattering

Crystalline Solids:

$$I(\theta) \sim |F(\mathbf{hk}l)|^2$$

$$F(\mathbf{hk}l) = \sum_j f_j(\theta) e^{(-2\pi i \mathbf{k} \cdot \vec{r}_j)}$$



Phonons:

$$I(\theta) \sim |f(\theta)|^2 \cdot (1 - e^{-2M})$$

$$M = \frac{8\pi \langle u^2 \rangle \sin(\theta)}{\lambda}$$

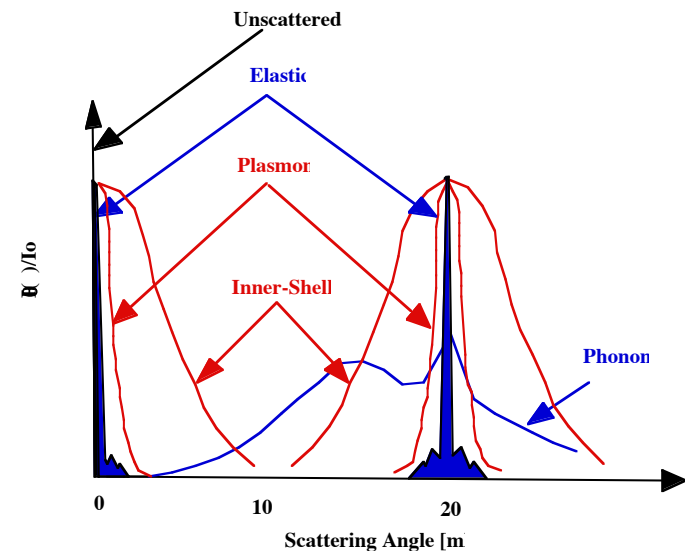
Inelastic:

$$I(\theta) = \Gamma(\delta E, \theta) \cdot \frac{1}{\theta^2 + \theta_E^2}$$

$$\theta_E = \frac{\Delta E}{2\gamma_0 T_0} \quad \gamma_0 = \frac{1}{\sqrt{1 - \beta^2}}$$

$\Gamma(\delta E, \theta)$: Imaginary Part of the Complex Dielectric constant(ϵ)

: Generalized Oscillator Strength

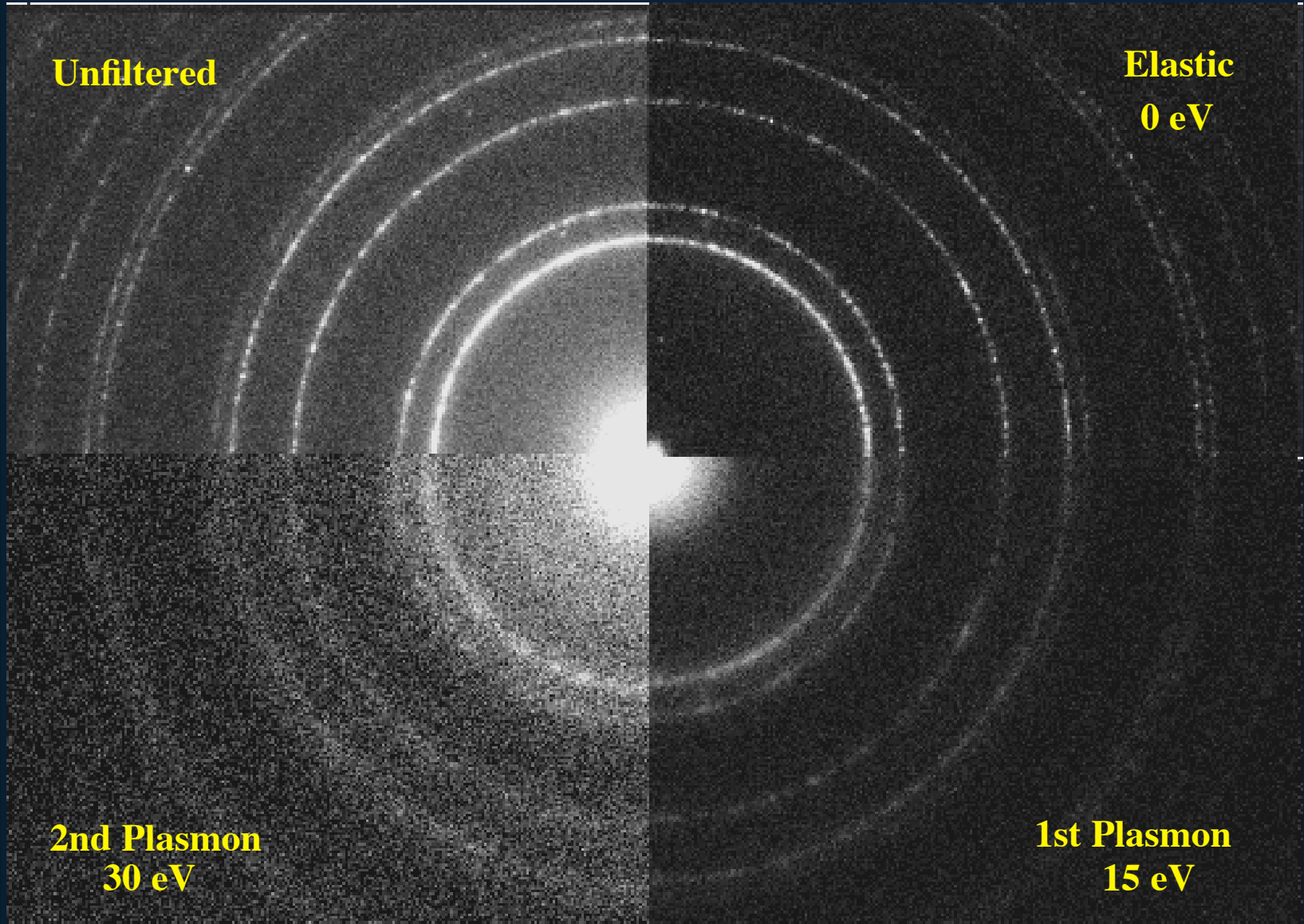


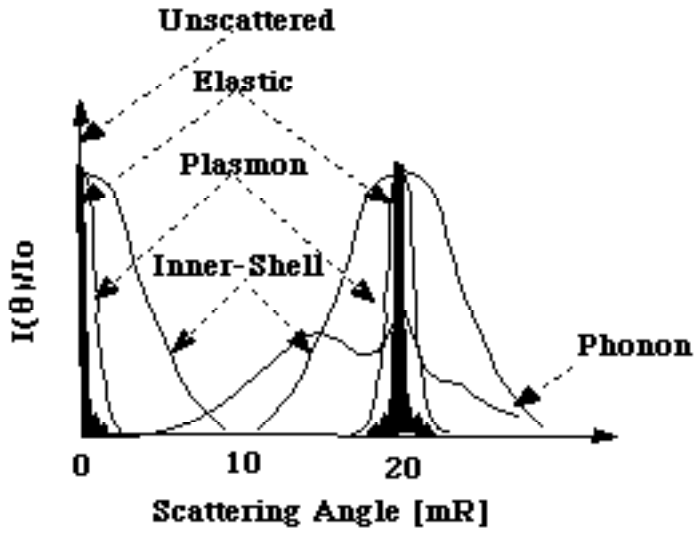
Unfiltered

**Elastic
0 eV**

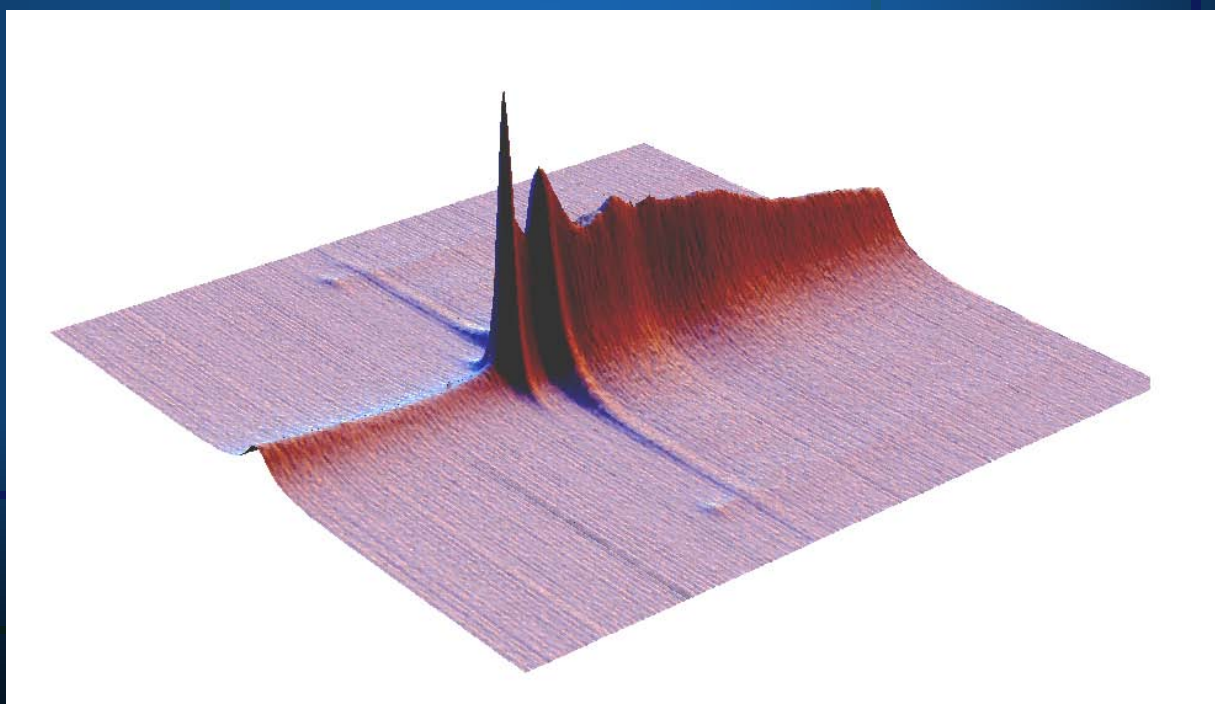
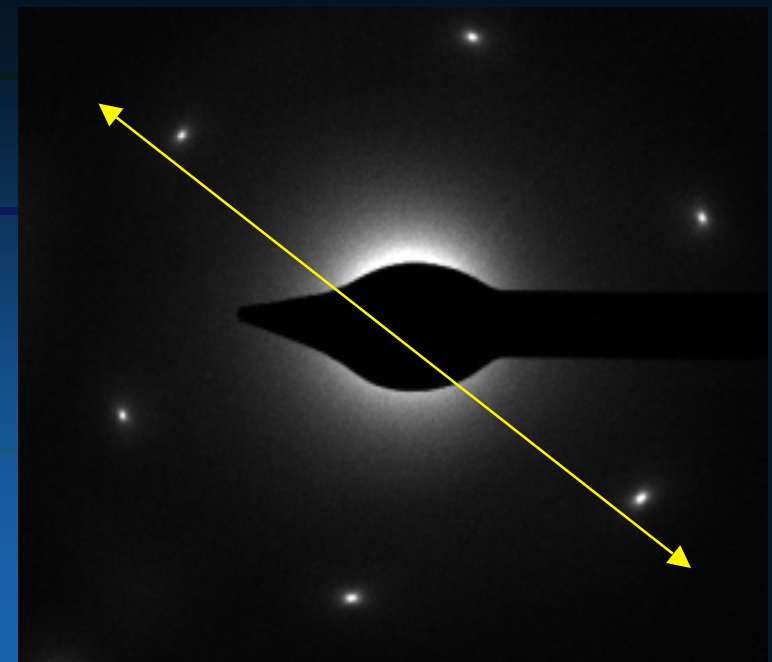
**2nd Plasmon
30 eV**

**1st Plasmon
15 eV**





Crystalline Solids



Instrumentation: Detector Systems

Energy Loss Spectrometers

Basic Principles

Electrostatic/Electromagnetic

Serial/Parallel Detector Systems

Spectral Artifacts

Multichannel Analyzers

Force (F) and displacements (X) on electrons by different types of fields yields a deflection in their trajectory. In a uniform field region the electrons drift at a characteristic radius (R).

Electrostatic

$$\vec{F}_E = q \vec{E}$$

$$X_E = \frac{1}{2} \frac{qEL^2}{m_0v^2}$$

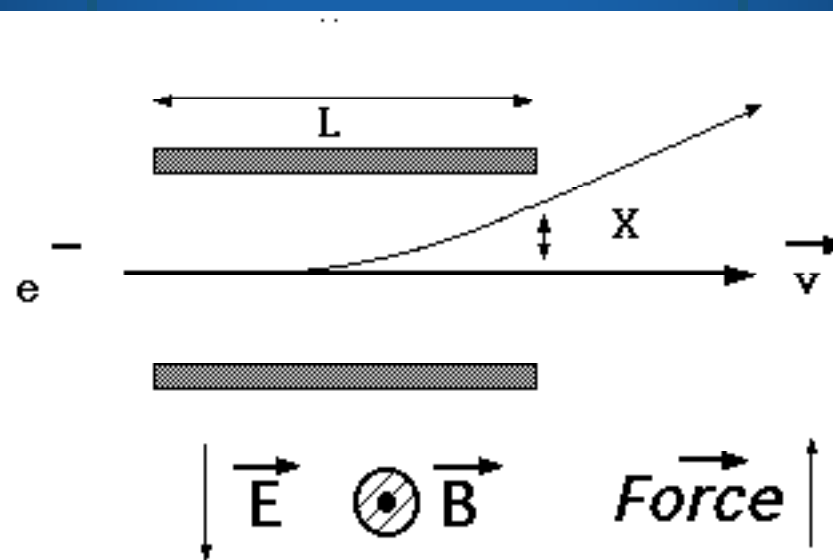
$$R_E = \frac{m_0v^2}{qE}$$

Electromagnetic

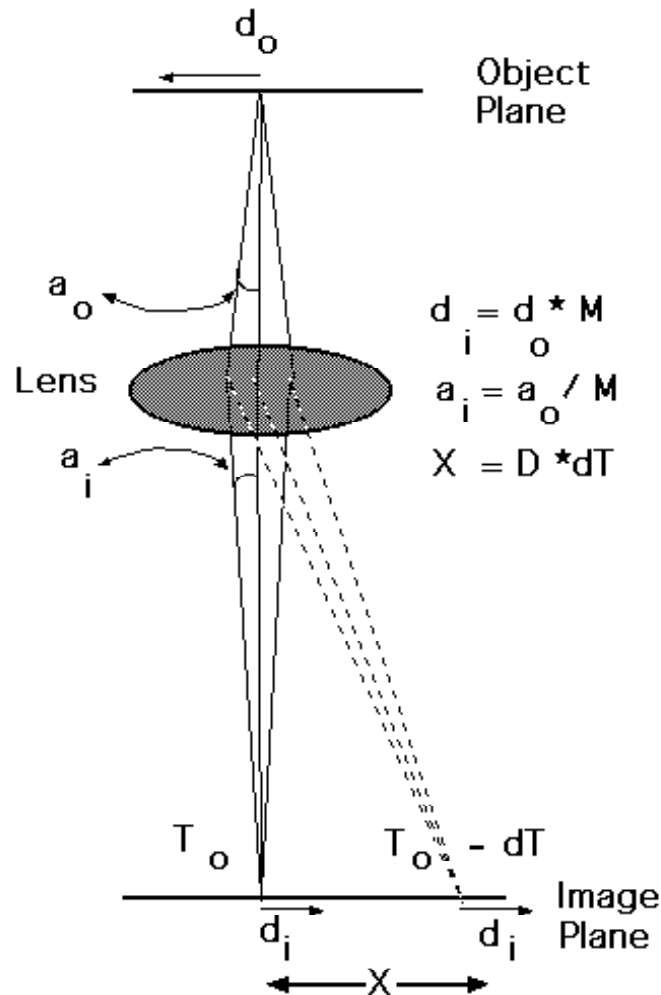
$$\vec{F}_B = q [\vec{v} \times \vec{B}]$$

$$X_B = \frac{1}{2} \frac{qBL^2}{m_0v}$$

$$R_B = \frac{m_0v}{qB}$$



Basic Spectrometer



Types of Electron Spectrometers:

Electrostatic:

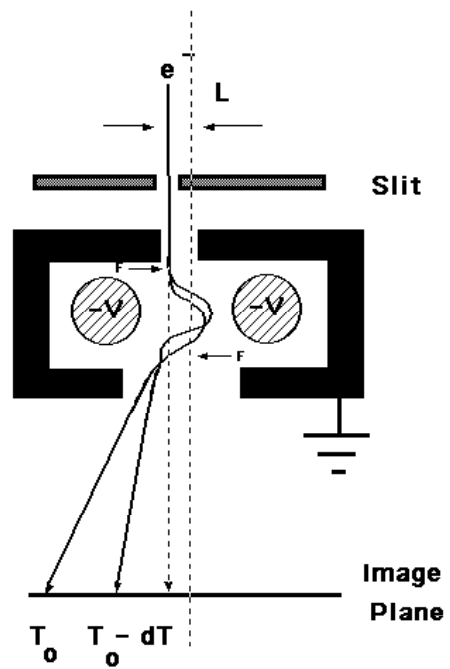
Electrostatic/magnetic:

Electromagnetic:

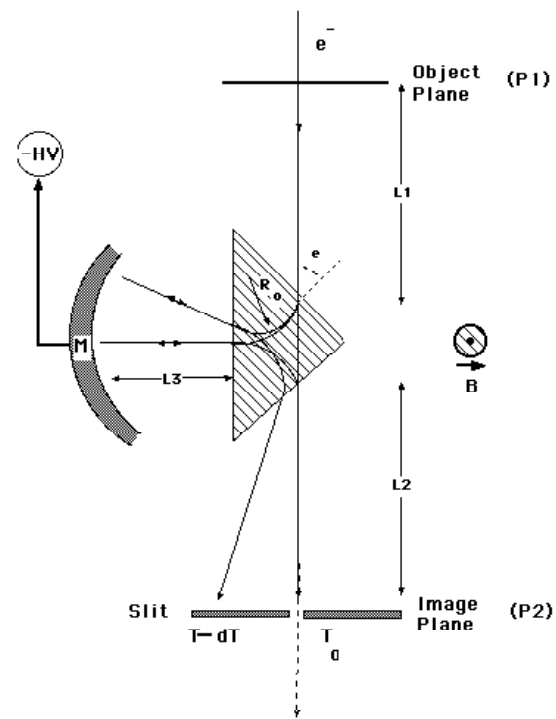
Mollenstedt

Wien, Castaing-Henry

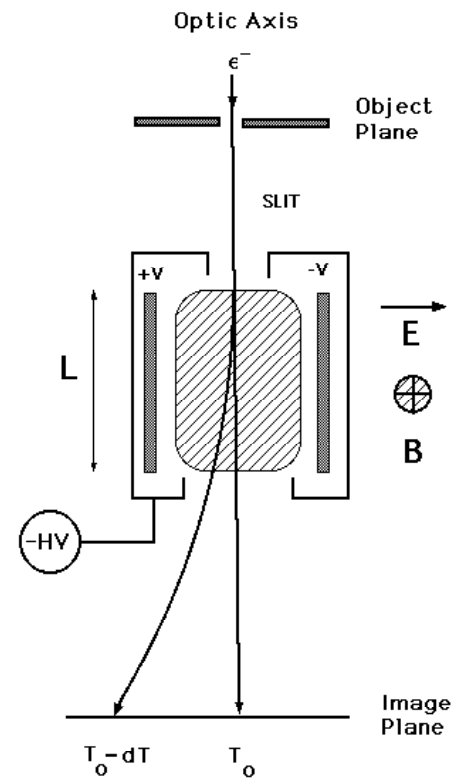
Cylindrical, Omega, Sector



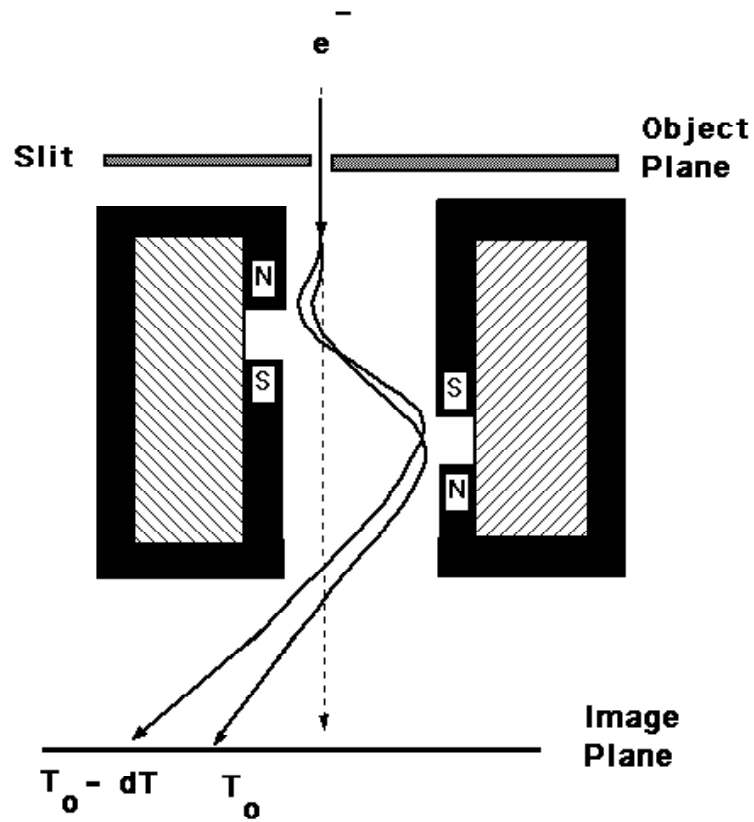
Mollenstedt Analyzer



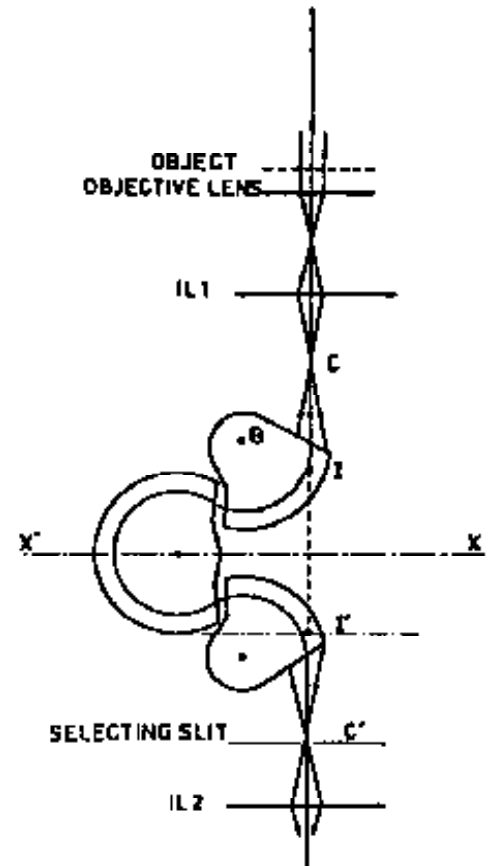
Castaing-Henry Filte



Wien Filter

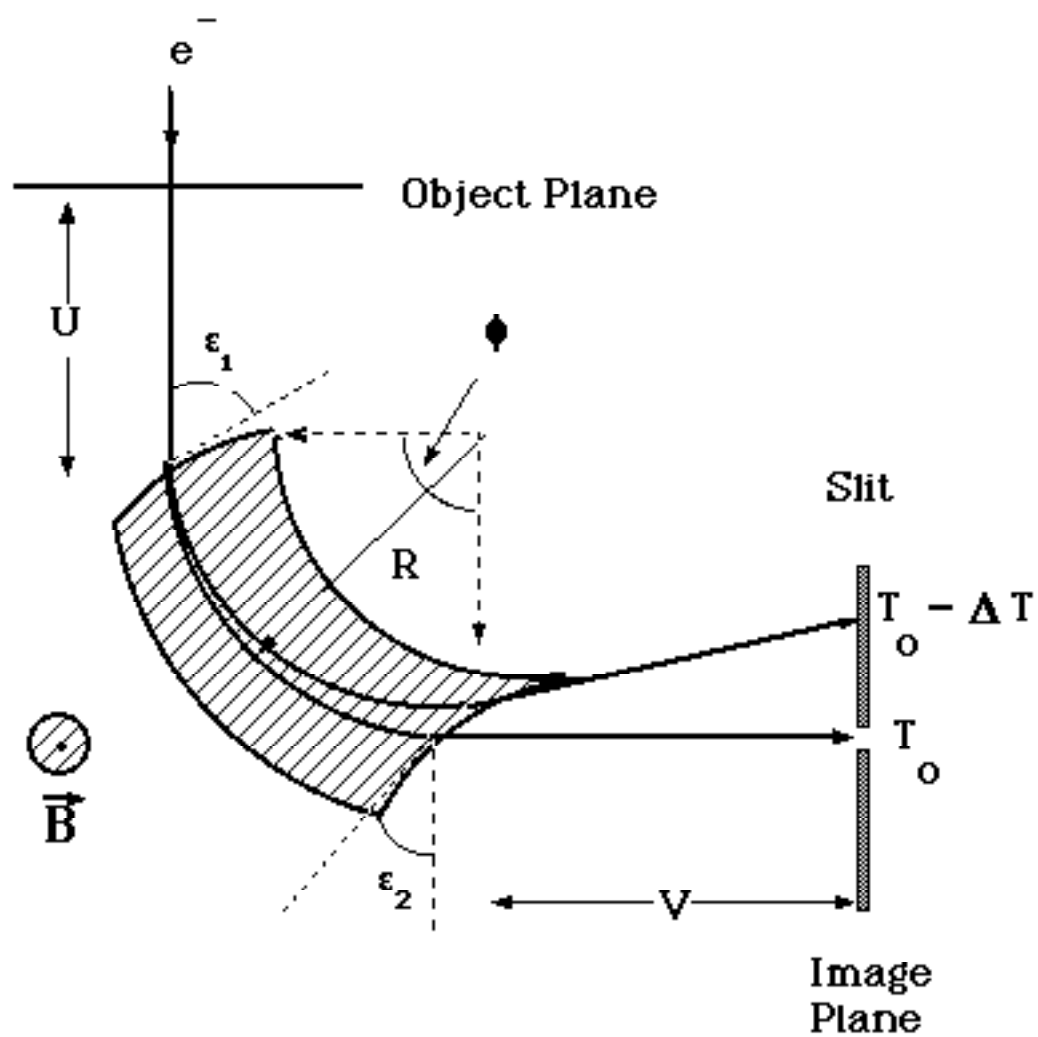


Cylindrical Magnetic Analyzer



Omega Filter

Magnet Sector Analyzer



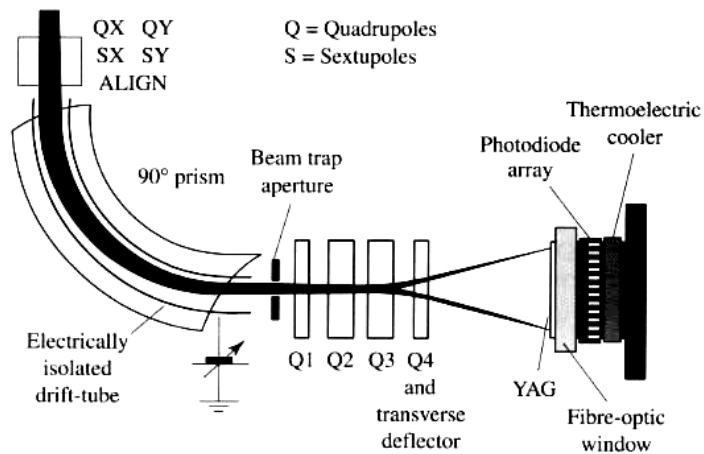


Figure 3.3. Schematic diagram of a Gatan PEELS system. Redrawn from Egerton (1996) *Electron Energy Loss Spectroscopy in the Electron Microscope*, 2nd Edn, with permission of Plenum Publishers.

Commercial Spectrometers Vs Imaging Filters

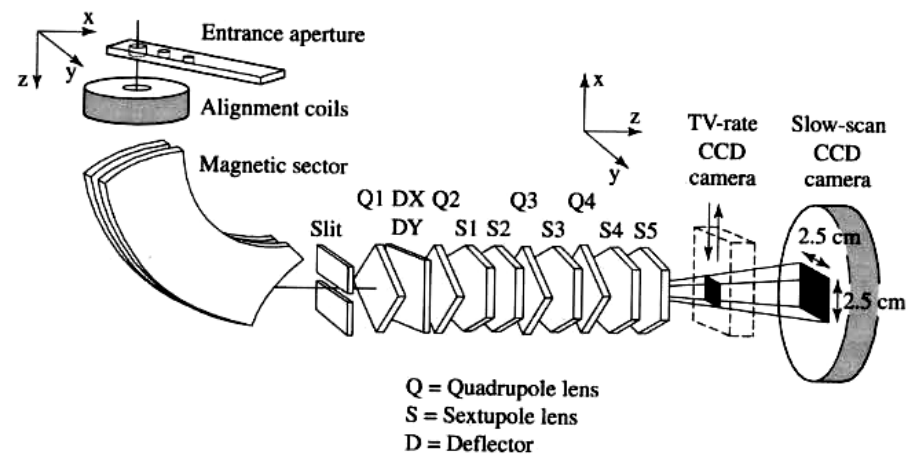
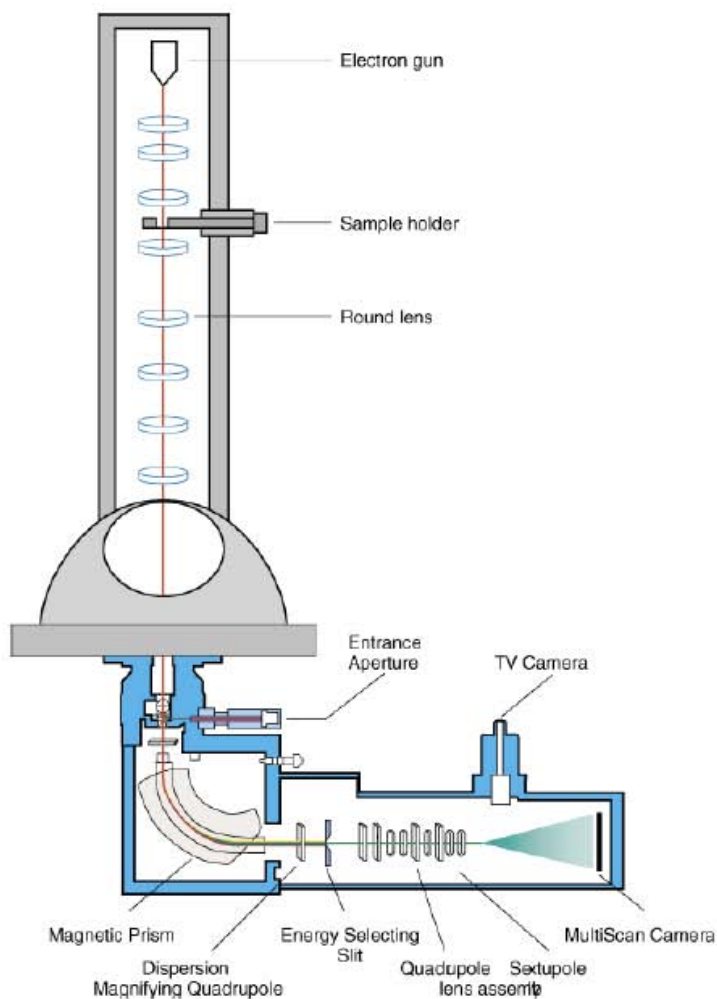


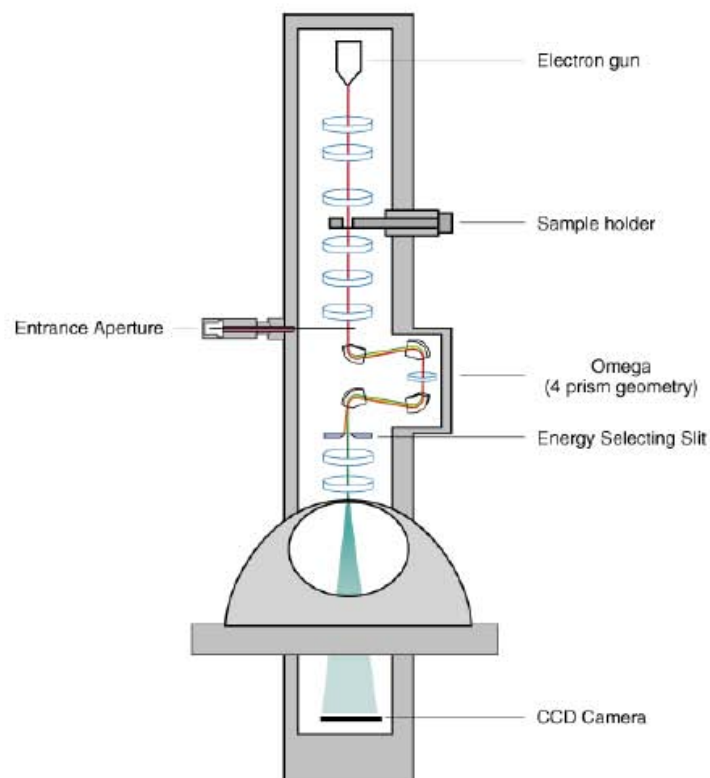
Figure 3.4. Schematic diagram of a Gatan imaging filter. Redrawn from Egerton (1996) *Electron Energy Loss Spectroscopy in the Electron Microscope*, 2nd Edn, with permission of Plenum Publishers.

Imaging Filters vs Spectrometers

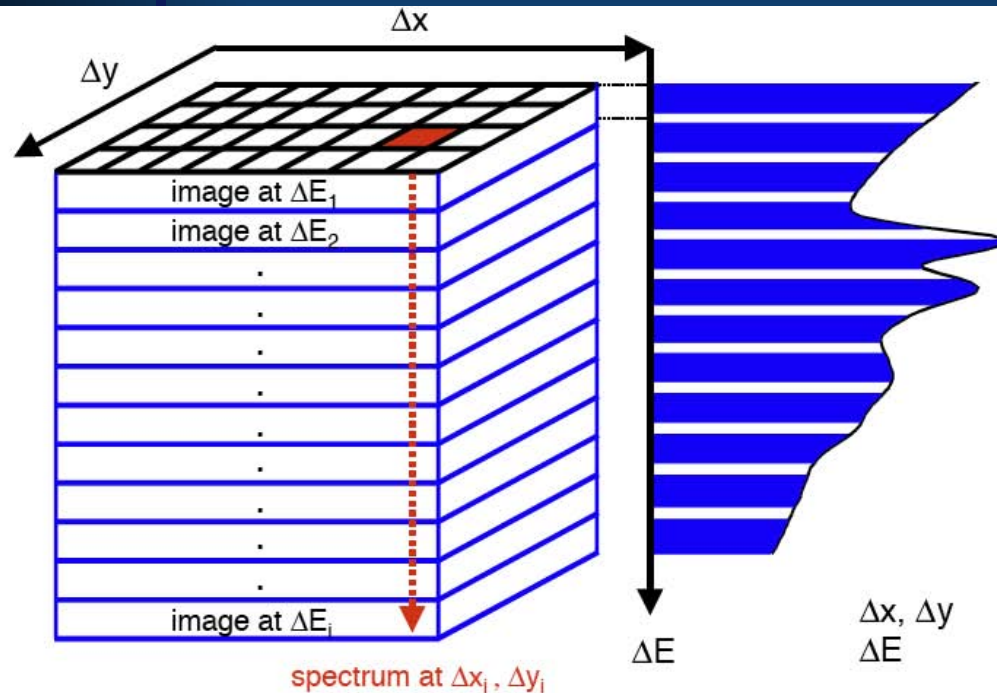
Post-column filter (Gatan)



In-column filter (LEO, JEOL)



Spectral Imaging Slice-by-Slice vs Point-by-Point



The technique of building up a more or less complete data cube is termed **Spectrum Imaging**

$\Delta x, \Delta y$ spatial dimensions
 ΔE energy-loss dimension

EFTEM Spectrum Imaging:

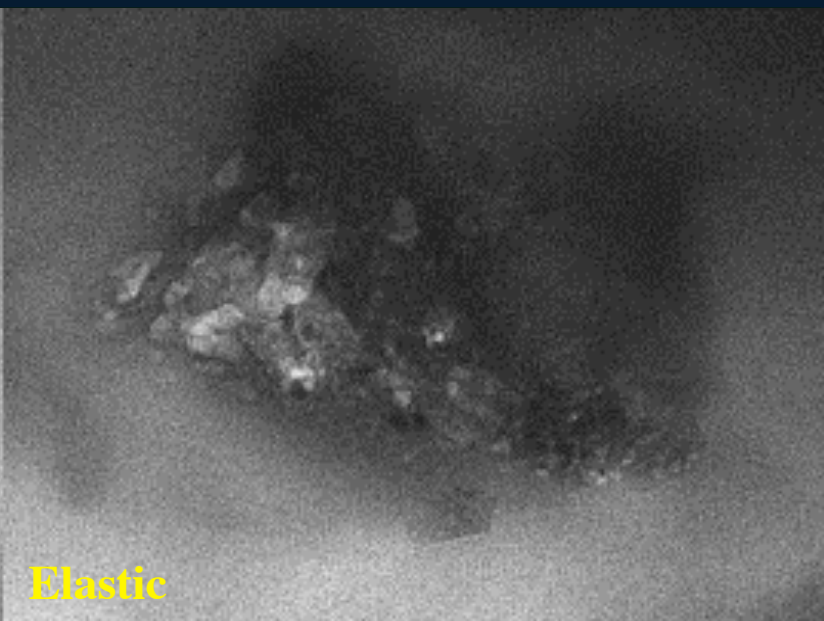
- Energy filtered broad beam technique
- fills data cube one image plane at a time
- less time

STEM Spectrum Imaging:

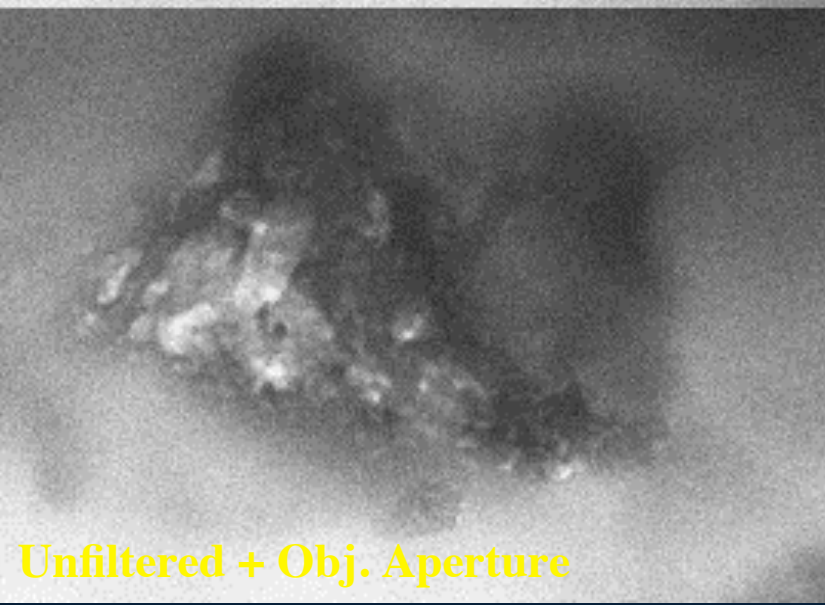
- Focused probe method
- fills data cube one spectrum at a time
- less dose



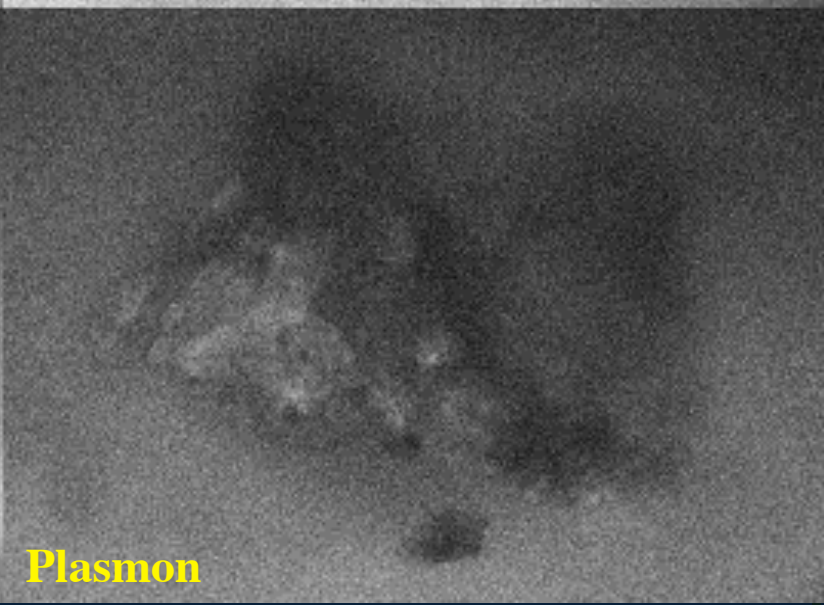
Unfiltered



Elastic



Unfiltered + Obj. Aperture



Plasmon

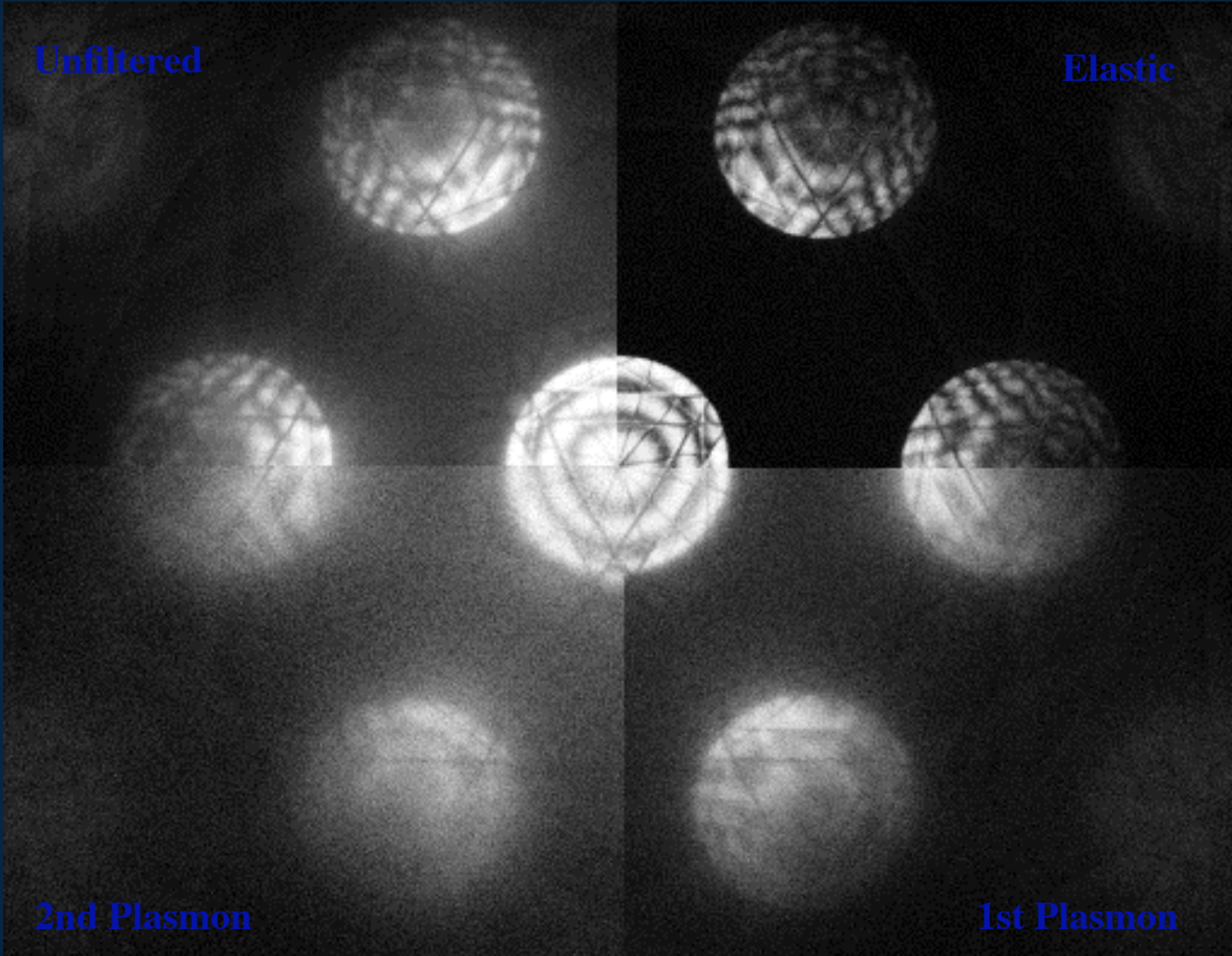
Silicon 111 ZAP- Gamma Corrected

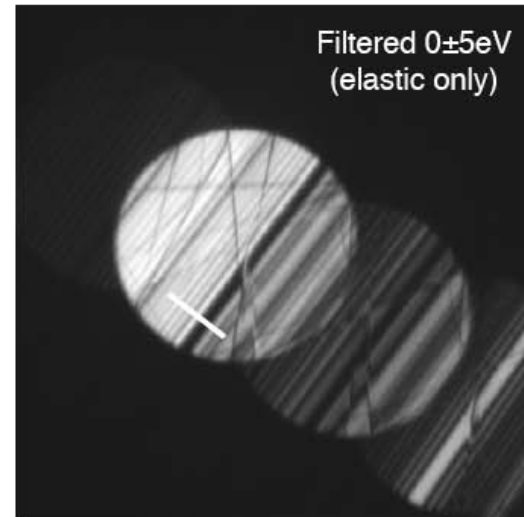
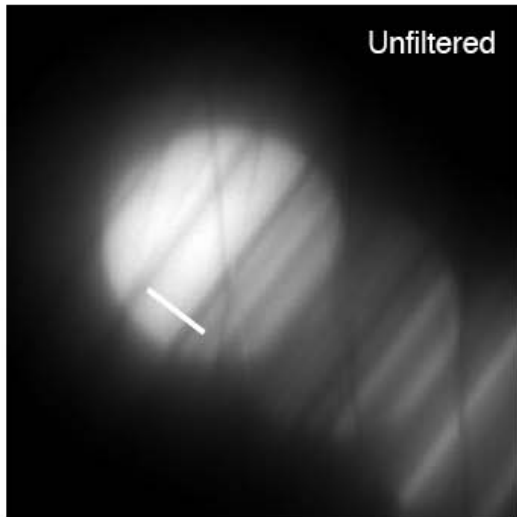
Unfiltered

Elastic

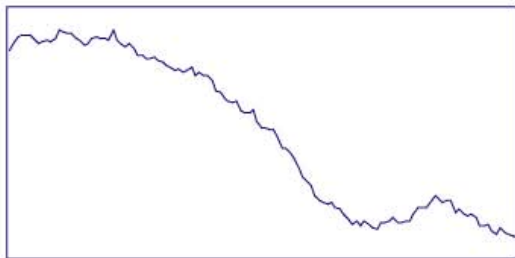
2nd Plasmon

1st Plasmon

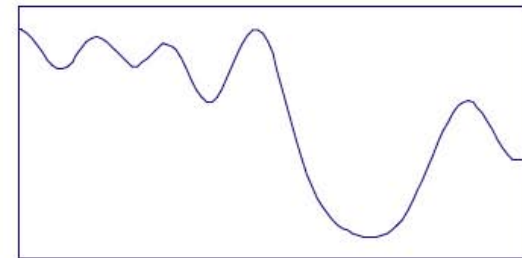




Silicon [110]

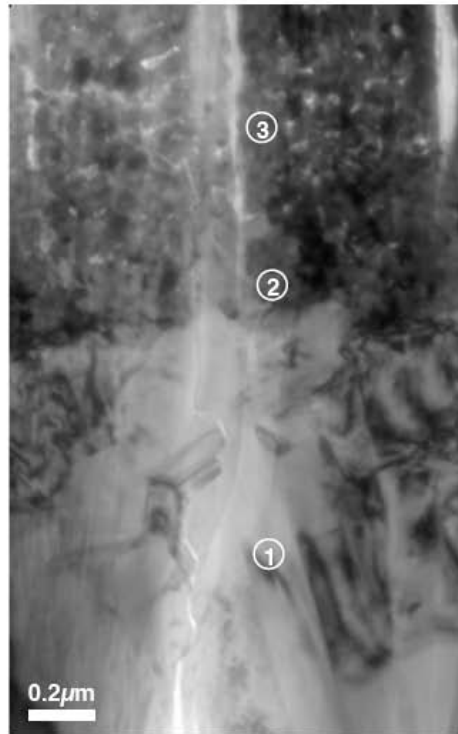


essential for
quantitative CBED



Spectroscopy vs Filtered Imaging

Information without EFTEM

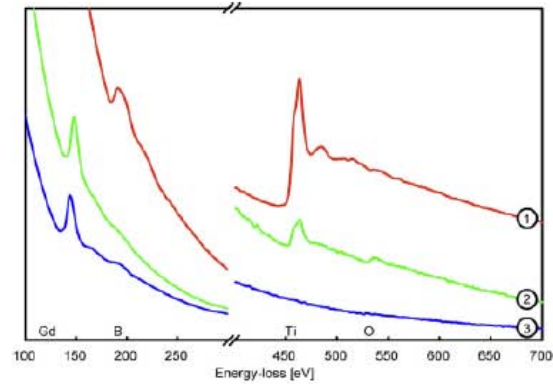


Unfiltered bright field image - structural contrast only

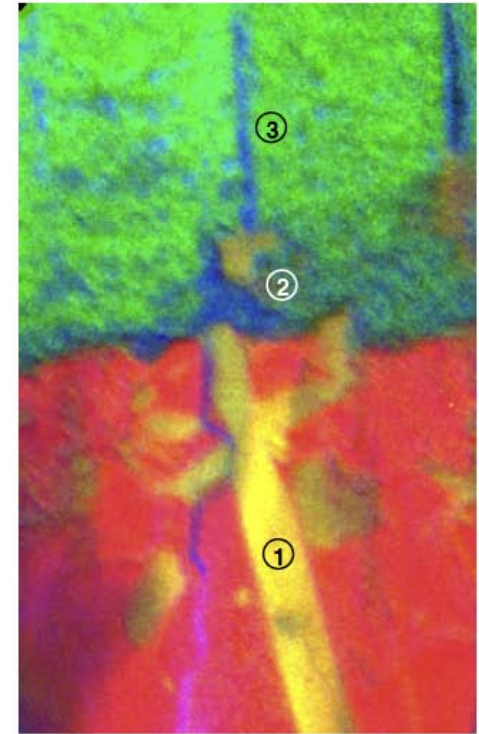
Information gain with EELS + EFTEM

Interface Titanium alloy and PVD-grown Gadoliniumboride

EELS spectra



from conventional TEM images
via EEL-spectra
to energy-filtered images
showing elemental distributions



EFTEM - Elemental contrast
Titanium Boron Oxygen

- What are the goals of the experiment?
 - Detection or quantification
 - Detection
 - * What threshold is of interest?
 - Quantification
 - * What threshold is of interest?
 - * What accuracy & precision needed
 - What kind of data is requested: point analysis, line scans, maps

- Choose analysis technique

- Select spectrum features to analyze
 - Predict feature overlaps in advance
- Estimate required S/N for desired detection threshold or quantification precision
 - How long will this take? Are line scans and maps still practical?
 - Determine if unusual techniques or effort is required
- Determine needed equipment parameters
 - What energy and spatial resolution is required?
 - What equipment configuration allows this?

- Other questions

- Would another spectroscopy work better for this application?

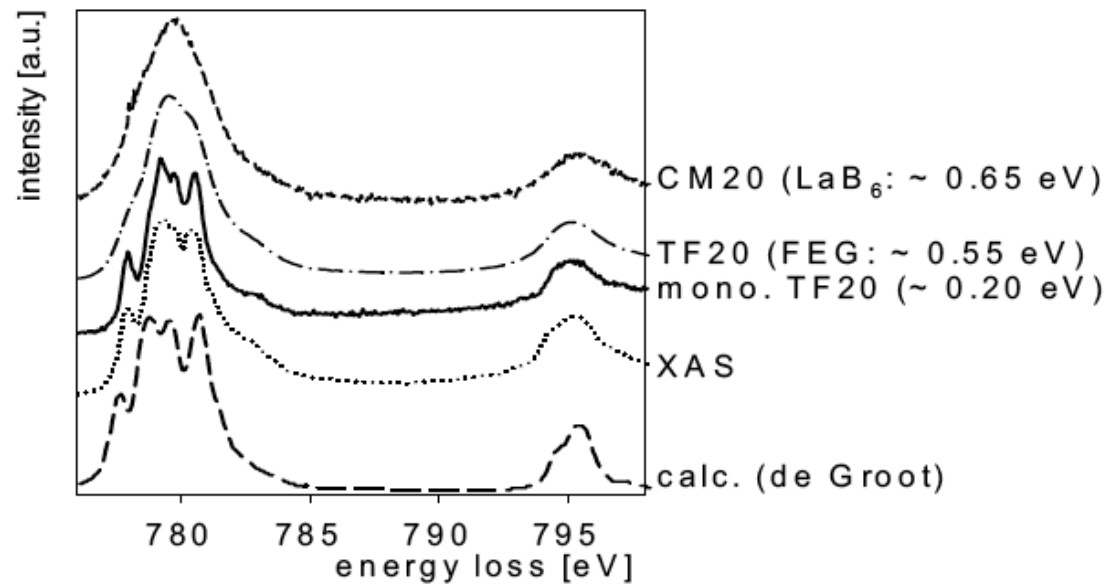


Fig. 2: Comparison of the Co L₂₃ ELNES of CoO measured on different microscopes with X-ray absorption data and calculated values. The energy resolution values given are FWHM values of the zero-loss peak.

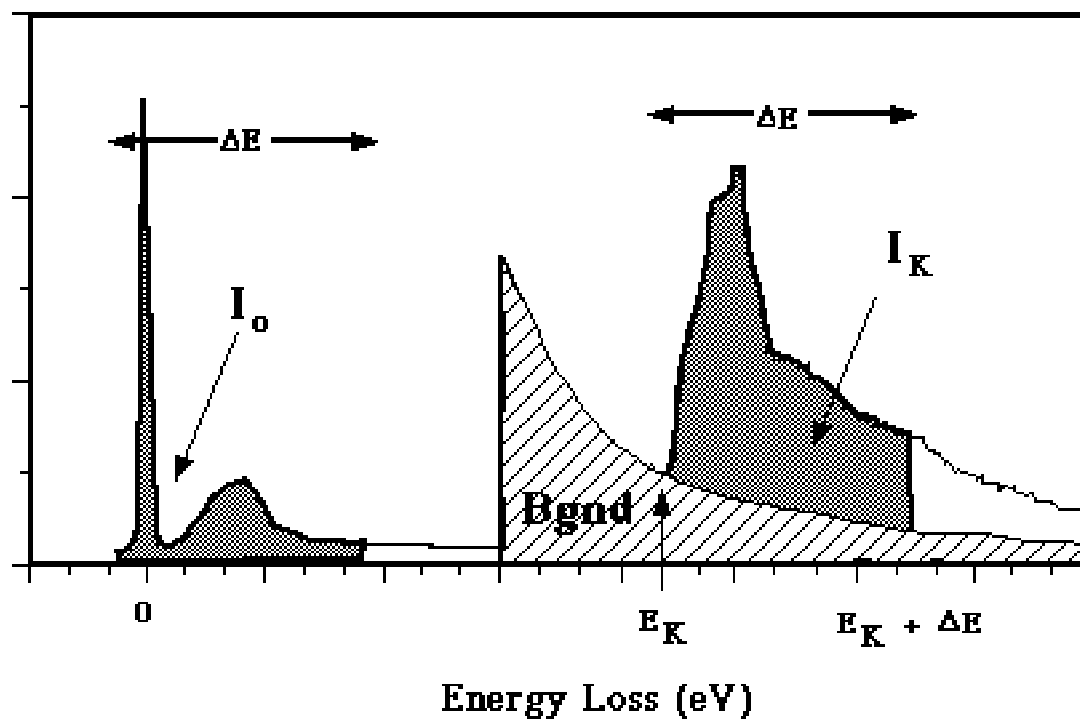
Data Analysis and Quantification:

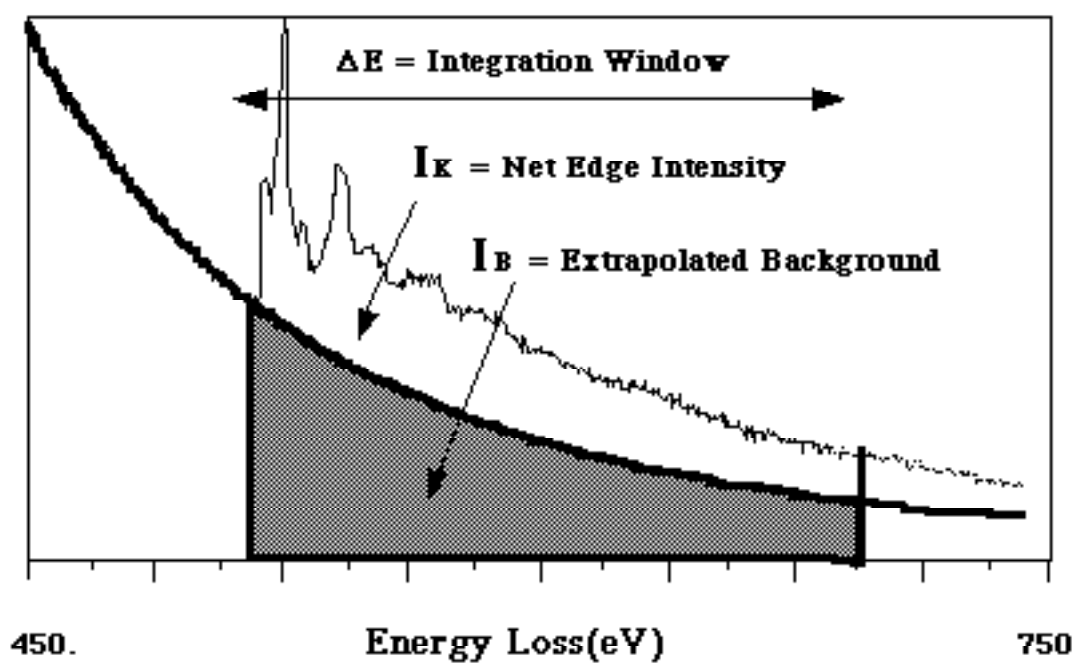
Spectral Processing

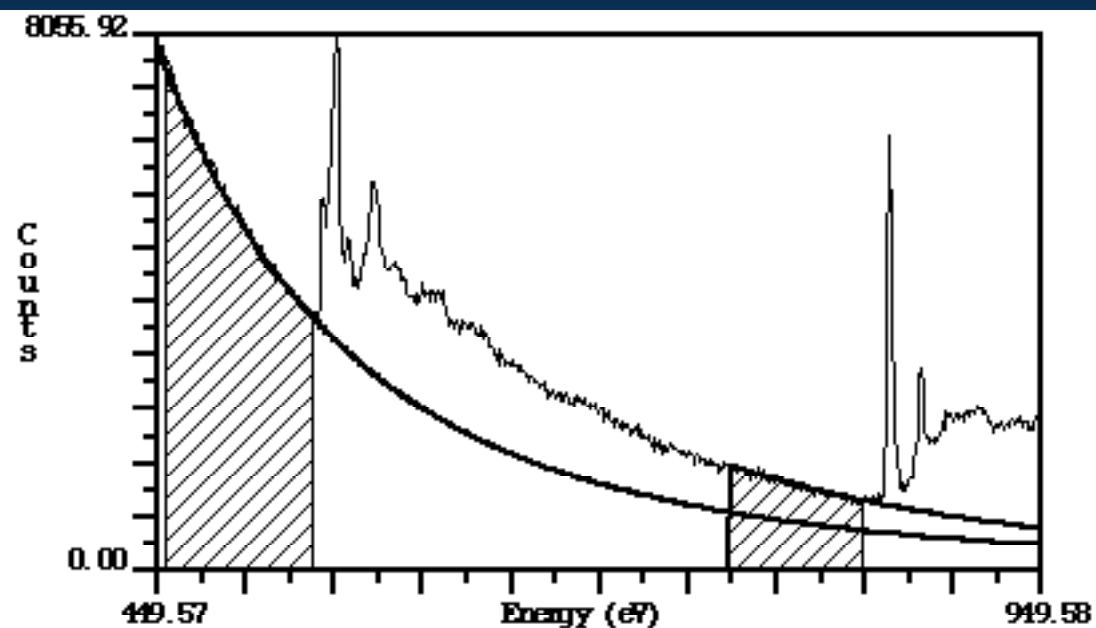
Thin Film Quantification Methods

Specimen Thickness Effects

Measurement of Parameters required for EELS Quantification







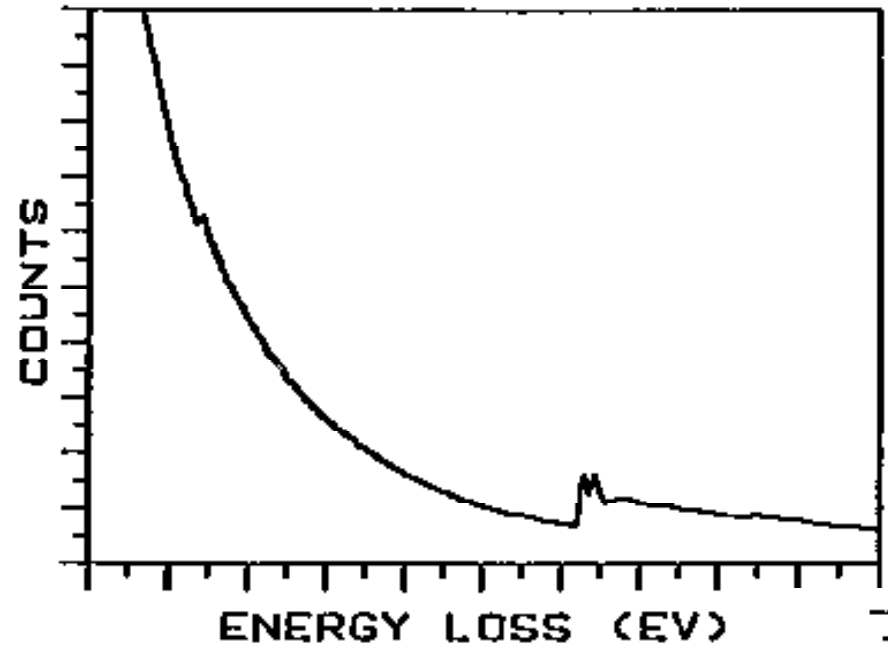
Most Frequently Used Model in the Medium Loss Regime

$$I_{\text{Bgnd}} = A E^{-R}$$

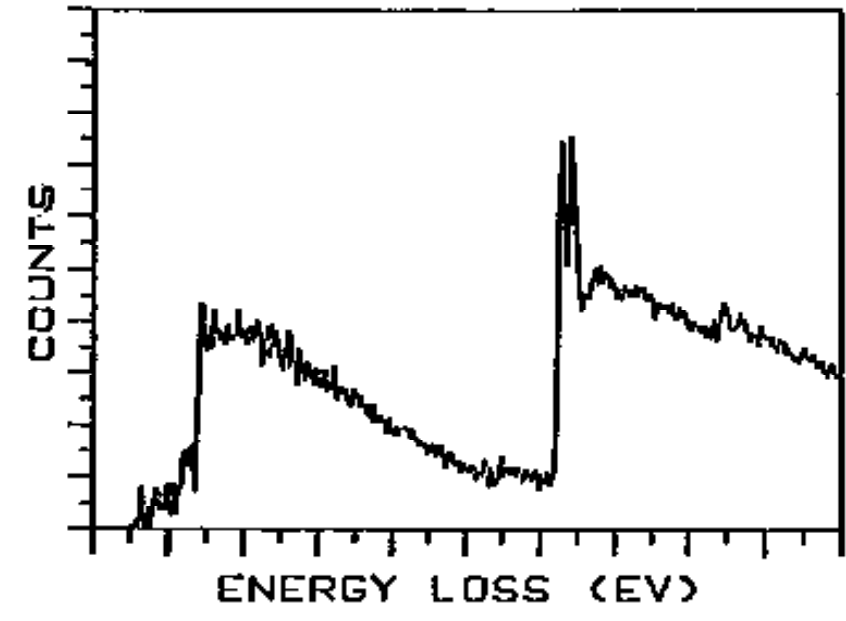
$2 \leq R \leq 7$ typical values for $200 \text{ eV} < E < 1500 \text{ eV}$

Other Background Models Used are Phenomenological
 N^{th} Order Polynomial & Log-Polynomial mainly used $< 200 \text{ eV}$ Loss

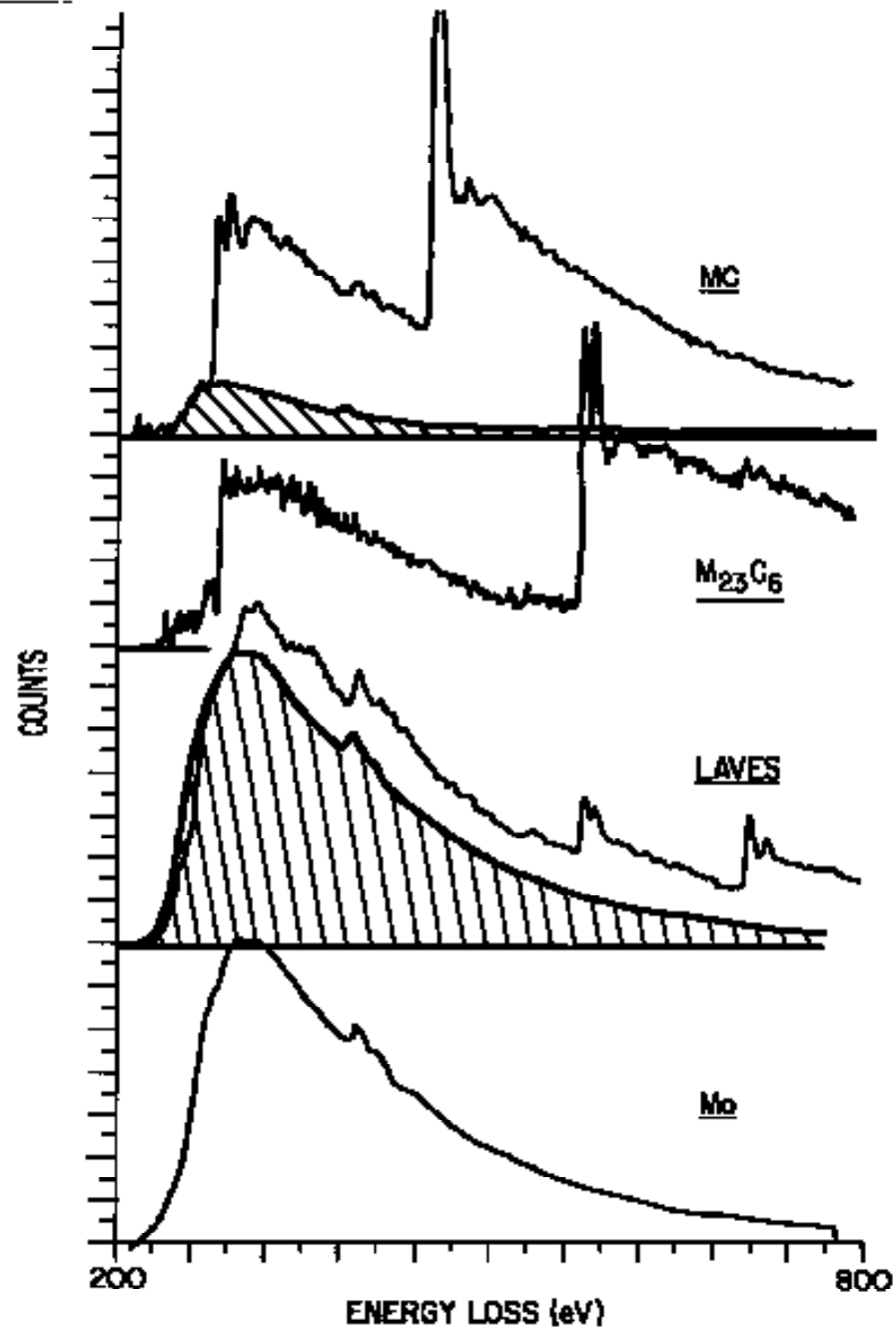
YMIN:YMAX:DIV= 0.000 5.500E-04 2750.000
XMIN:XMAX:DIV= 200.000 800.000 30.000

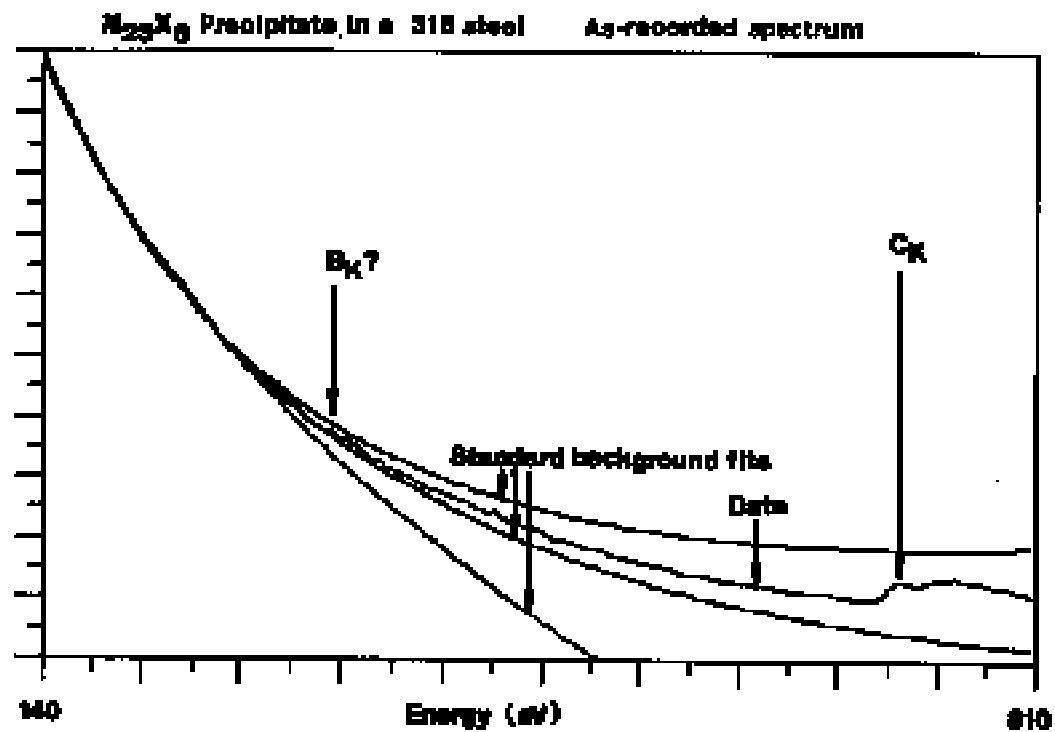


$M_{23}C_6$ in Steel :
Spectral Overlap



**Spectral
OverLap
Problems also
exist in EELS**





Conventional Background Fitting does not always allow the user to find small peaks in high background areas.

Two Related Methods are sometimes used:

Second Difference Filtering (Shuman et al MAS, 1983)

Record 3 Energy Loss Spectra which are displaced in energy by dE
Mathematically combine in computer to form the Second Difference
(SD) Spectrum

$$SD(E) = I_1(E-dE) - 2 I_2(E) + I_3(E+dE)$$

Spectrum has the appearance of a derivative, removes channel to channel gain variation in parallel EELS and slowly varying backgrounds. Sharp features are enhanced in visibility.

Digital Filtering

This is related to a simple numerical differentiation of a single spectrum

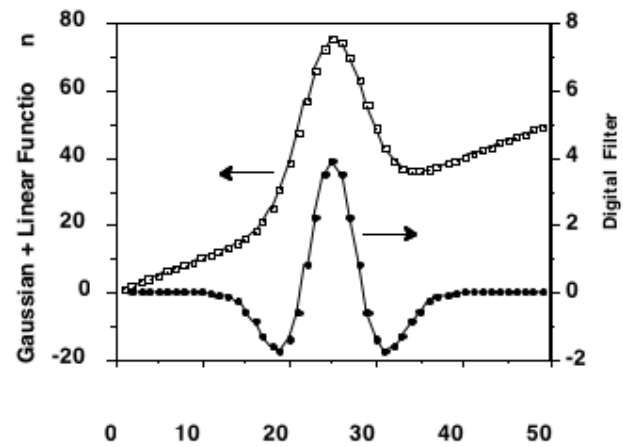
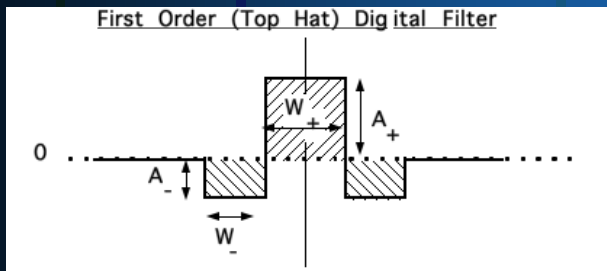


Fig 1.6 Application of a tophat digital filter to a spectral function composed of a linear + Gaussian distribution. Note removal of linear component and distortion of the Gaussian.

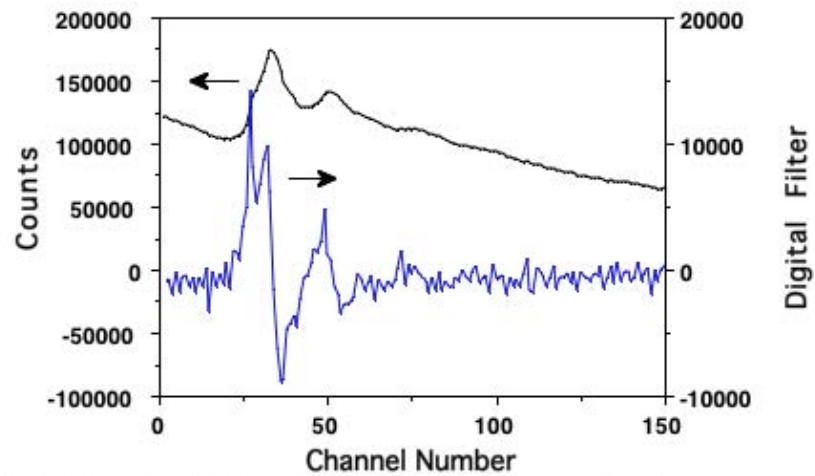
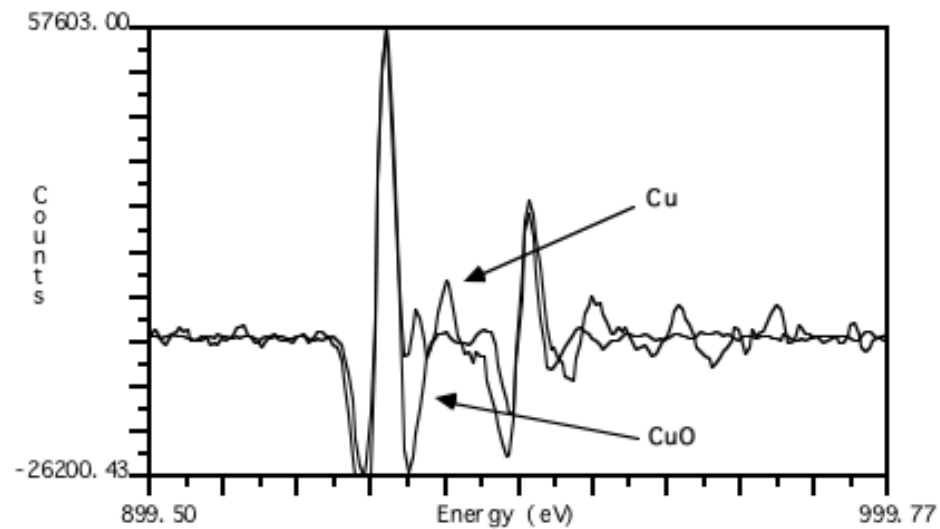
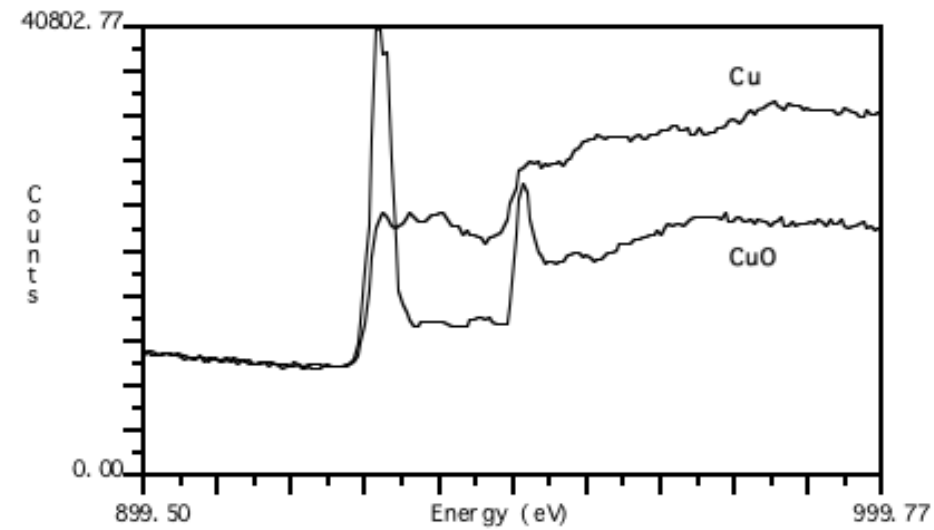
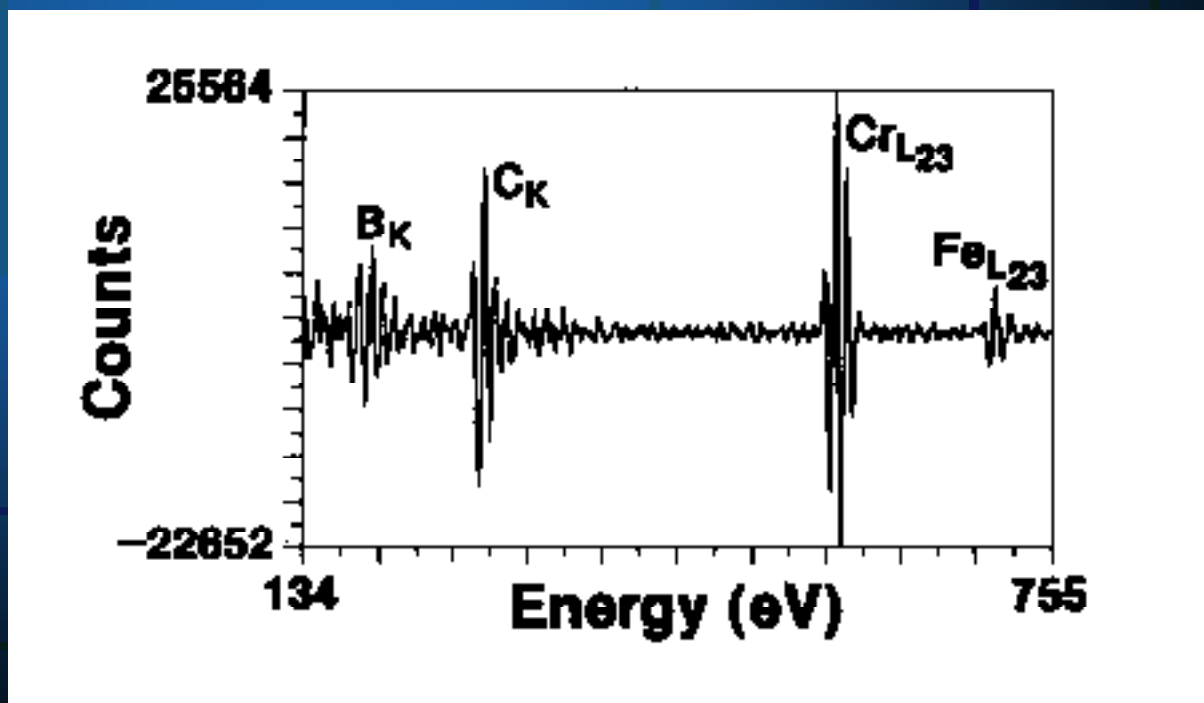
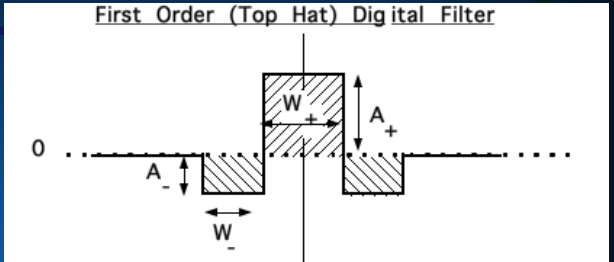
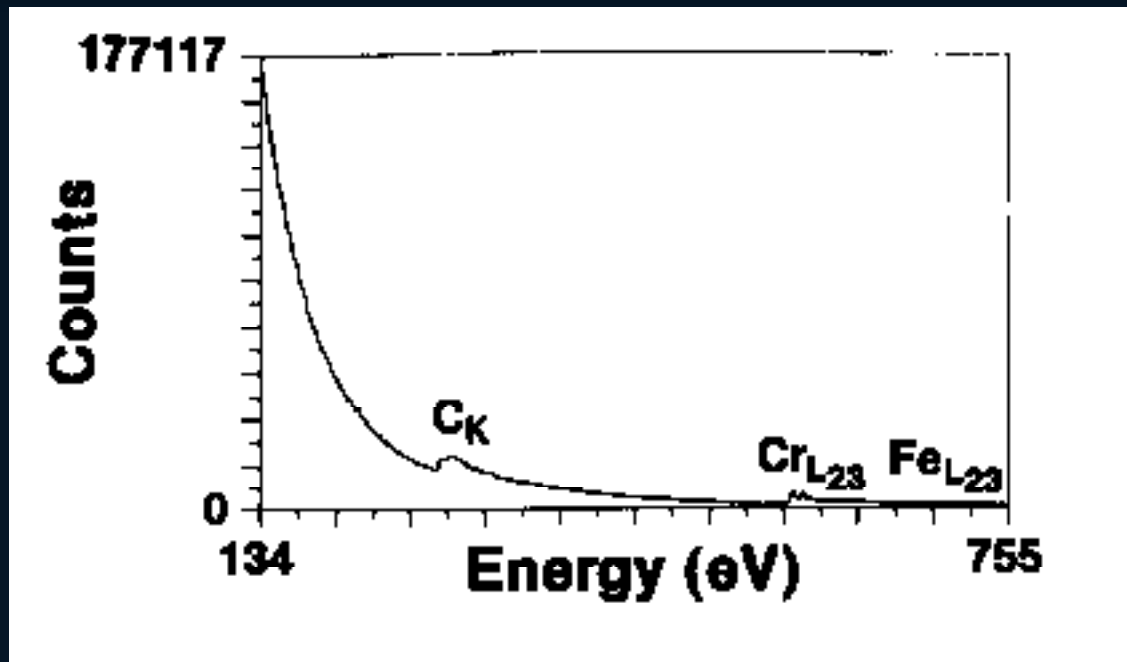
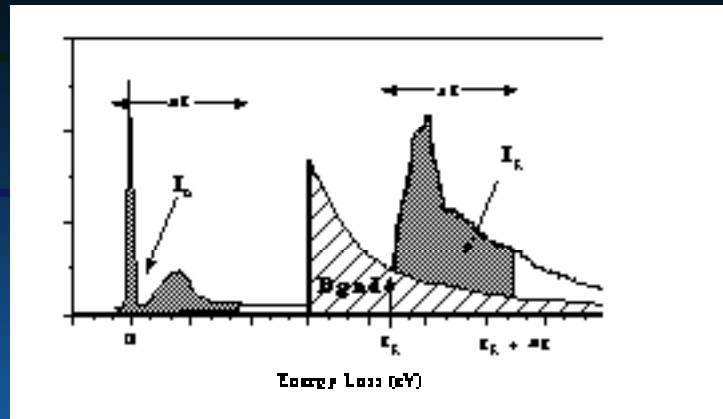


Fig 1.7 Example of digital filter of EELS data. Note complete background suppression, but severe spectral distortion.

Filtering of EELS Spectra







$$I_k = P_k * I_0$$

I_k = Number of electron having excited a kth inner shell

P_k = Probability of excitation of the kth shell

I_0 = Incident electron current

$$P_k = N \sigma_k$$

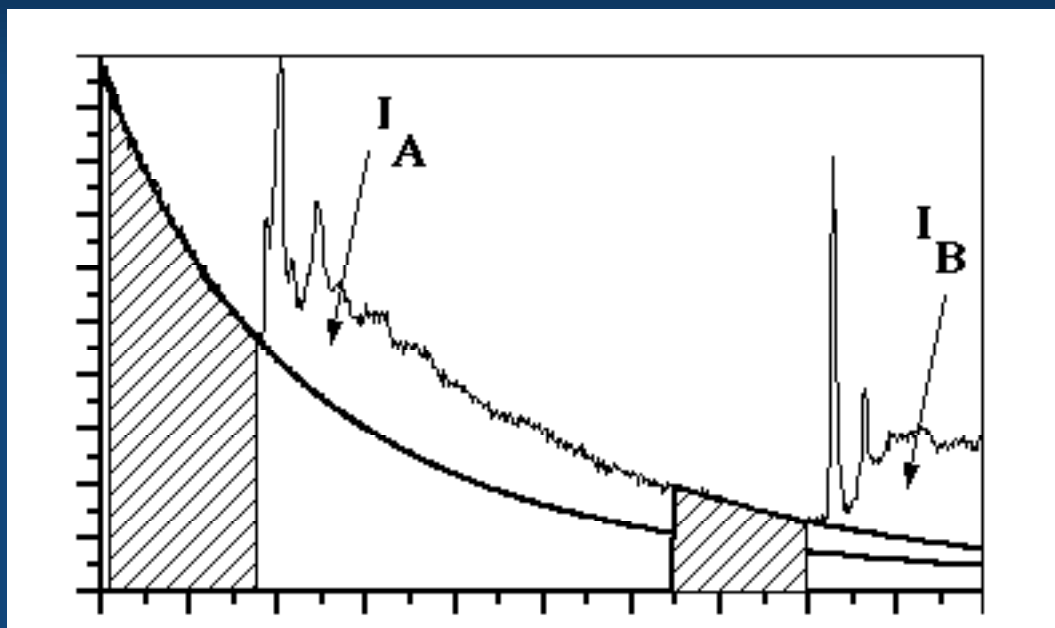
N = Number of atoms of the element analyzed

σ_k = Ionization cross-section for the kth shell

$$N = \frac{I_k}{\sigma_k I_0}$$

Alternatively;

Consider the ratio of Intensities of any two Edges in the same spectrum I_A and I_B



Invoke the Ratio Method and obtain the exact equation:

$$\frac{I_A}{I_B} = \frac{\sigma_A N_A}{\sigma_B N_B}$$

Note the similarity of this equation with that of Thin Film XEDS

But in the real world the assumptions used in the above simple arguments are never realized:

- Measure all scattered electrons ($\beta = \pi = 180^\circ$)
- Integration over all energy Losses

Because we must measure over a finite energy window (δE) we modify the expression to:

$$N_A = \frac{I_A(\delta E)}{\sigma_A(\delta E) * I_0}$$

we also measure over a finite angular window (β) and therefore, we modify the expression to:

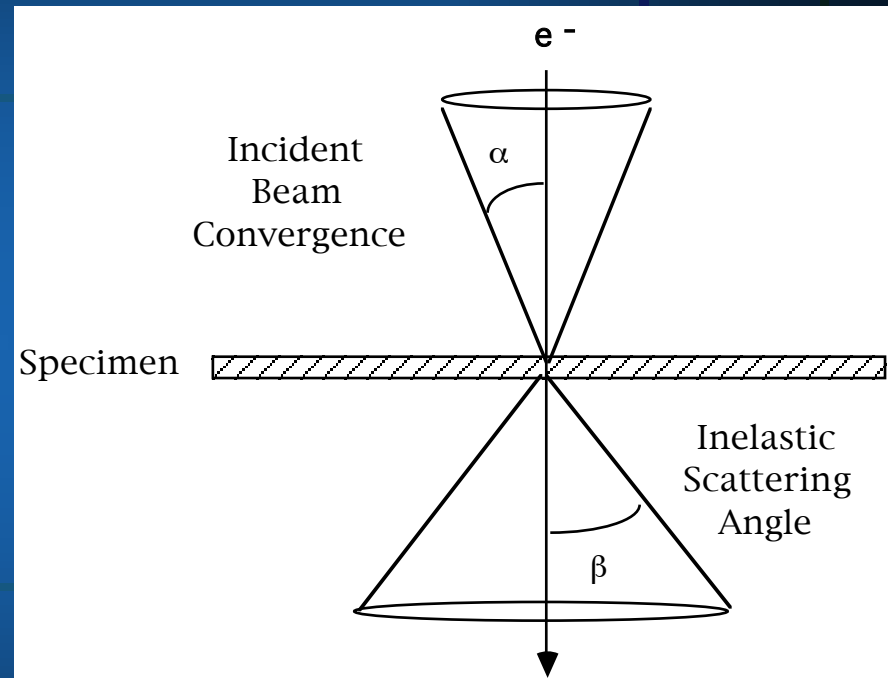
$$N_A = \frac{I_A(\delta E, \beta)}{\sigma_A(\delta E, \beta) * I_0}$$

and the ratio equation becomes:

$$\frac{N_A}{N_B} = k_{AB} \frac{I_A(\delta E, \beta)}{I_B(\delta E, \beta)}$$

with

$$k_{AB} = \frac{\sigma_B(\delta E, \beta)}{\sigma_A(\delta E, \beta)}$$



By measuring \mathcal{X} edges we have $\mathcal{X}-1$ equations, if we invoke the argument that the compositions must sum to unity

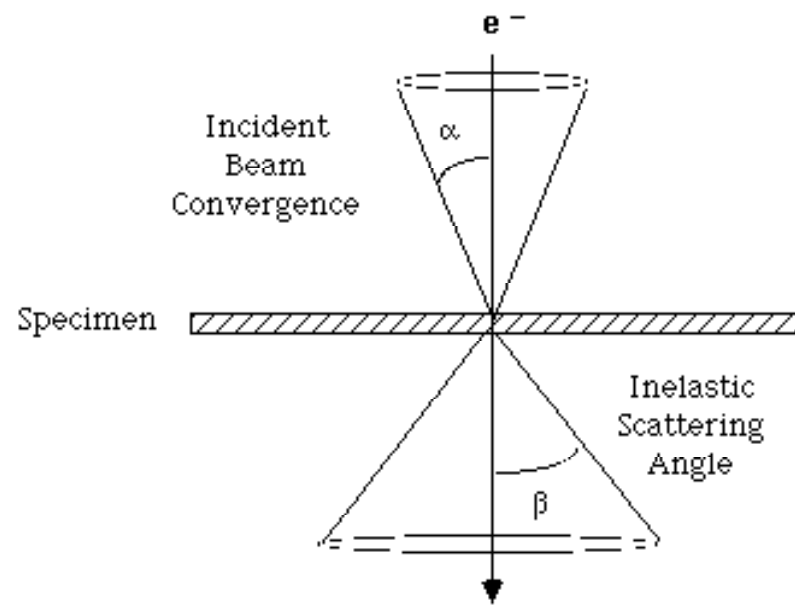
$$\sum_{i=1}^{\mathcal{X}} C_i = 1$$

we arrive at a set of \mathcal{X} equations and \mathcal{X} unknowns which can be solved by simple algebra.

For example:

- if $N_A/N_B = 2$; then $N_A = 2 N_B$
- if $N_A + N_B = 1$; then $3N_B = 1$ or $N_B = 0.33$
- and $N_A = 1 - N_B = 0.67$

Measuring Incident and Scattering Solid Angles



Definitions of electron beam incidence (α) and scattering (β) angles

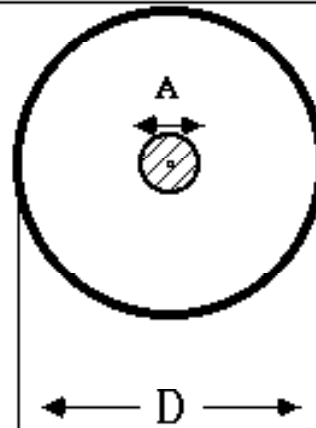
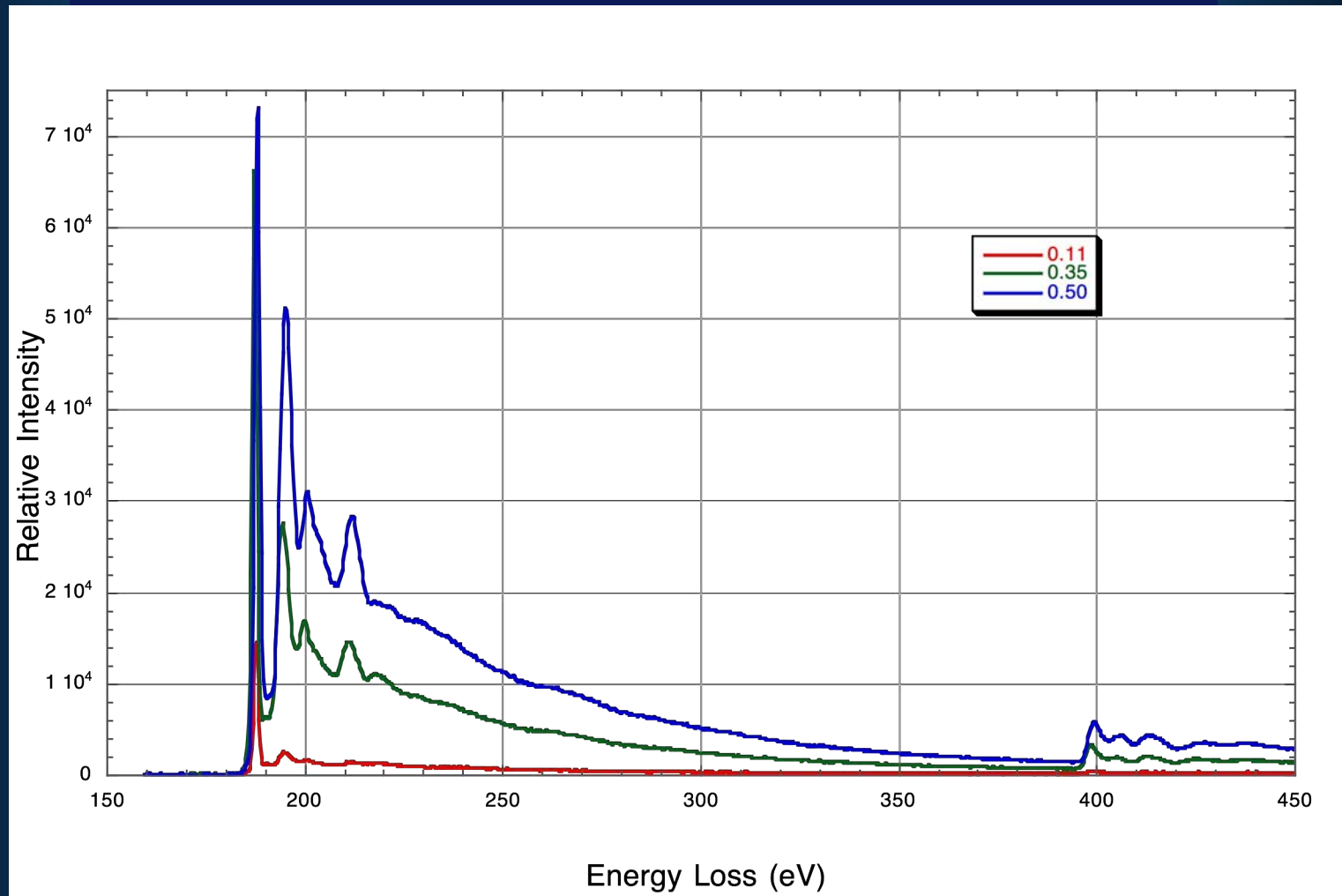


Figure 1.4 Measurement of convergence or scattering angles by comparison to a polycrystalline diffraction pattern of a standard.

$$\alpha \text{ or } \beta = \frac{A}{D} * 2 \text{ Arcsin} \left(\frac{\lambda}{2d} \right) \quad \lambda = \frac{12.27}{\sqrt{V_0(1+0.978 \times 10^{-6} V_0)}}$$

Hexagonal Boron- Nitride



$\theta_E \sim 0.777$ mR

$\theta_E \sim 1.62$ mR

Problems in EELS Quantification

Cross-section Calculations

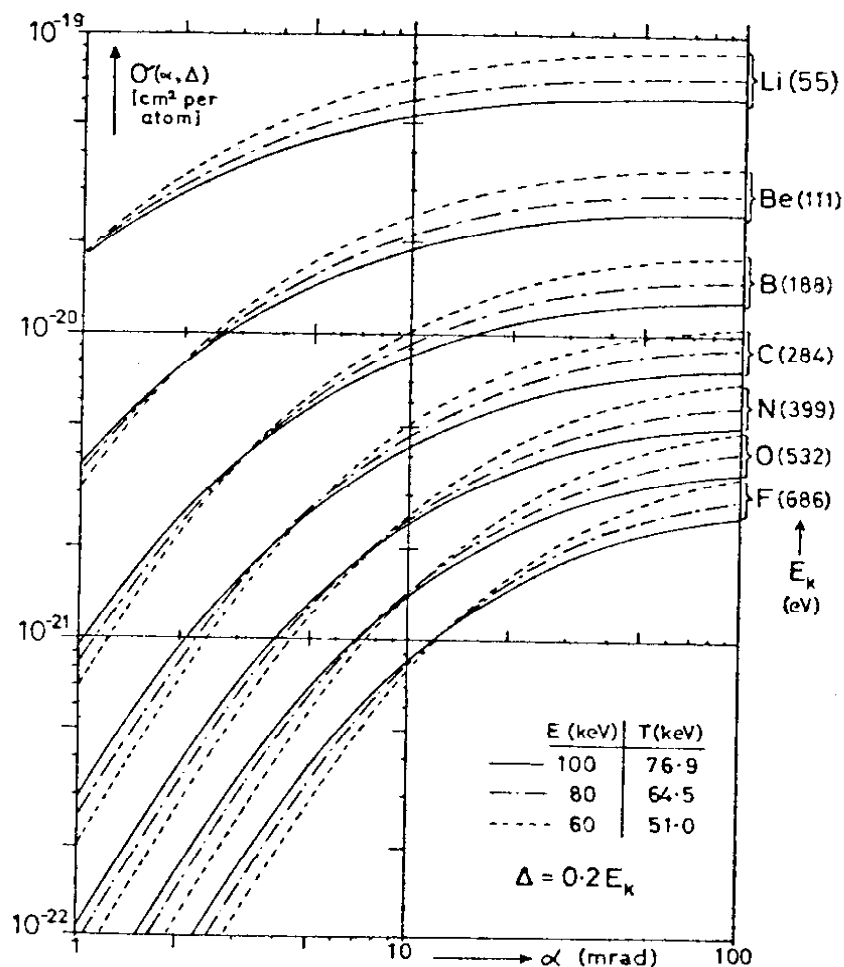


Fig. 3. K-shell partial cross-sections for first-row elements with $\Delta = 0.2 E_K$ and incident electron energies of 60, 80 and 100 keV.

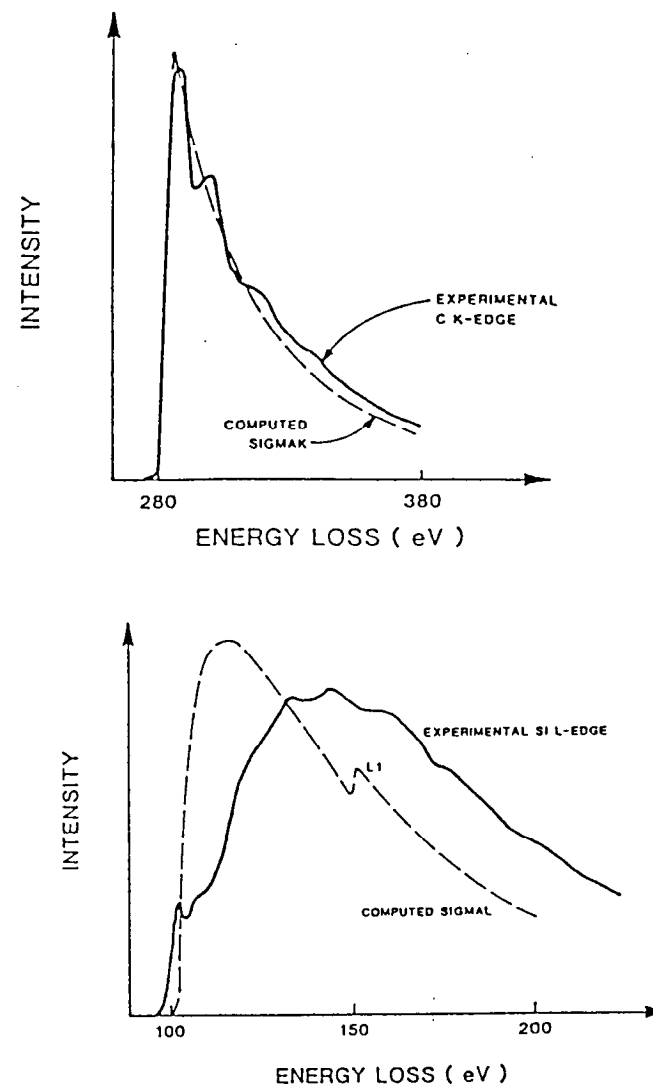
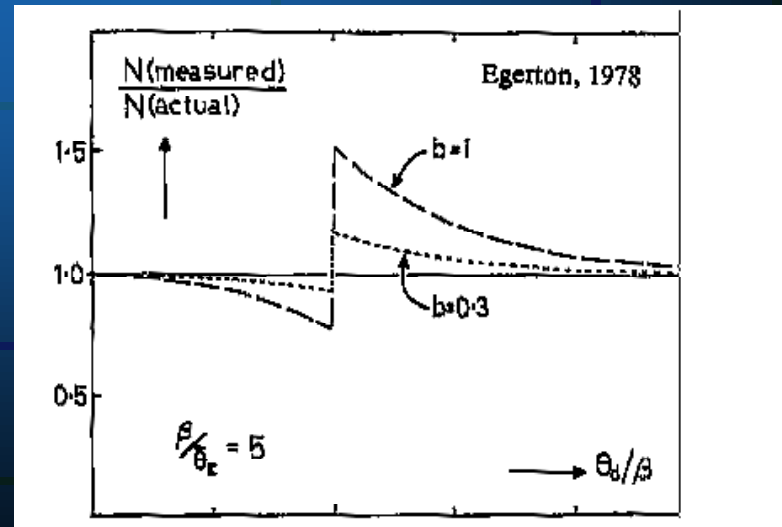
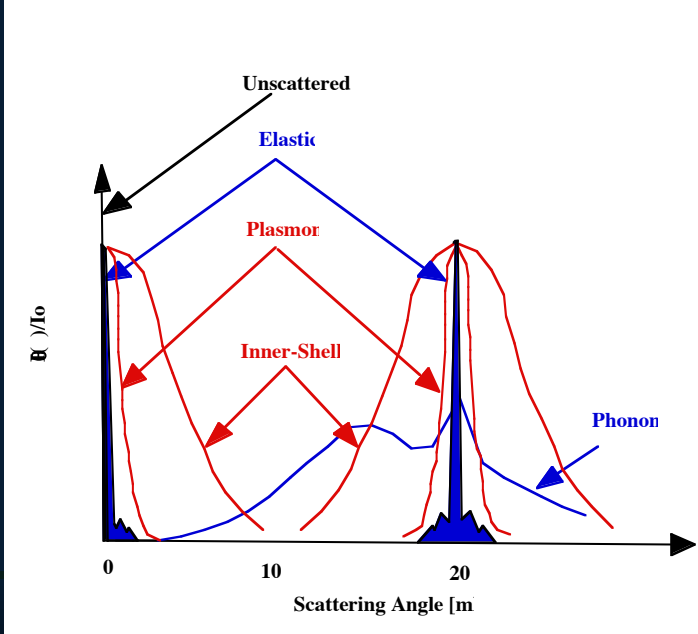
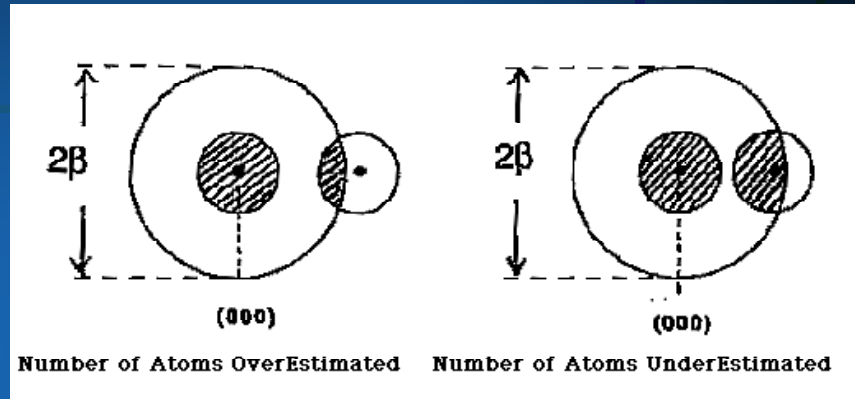
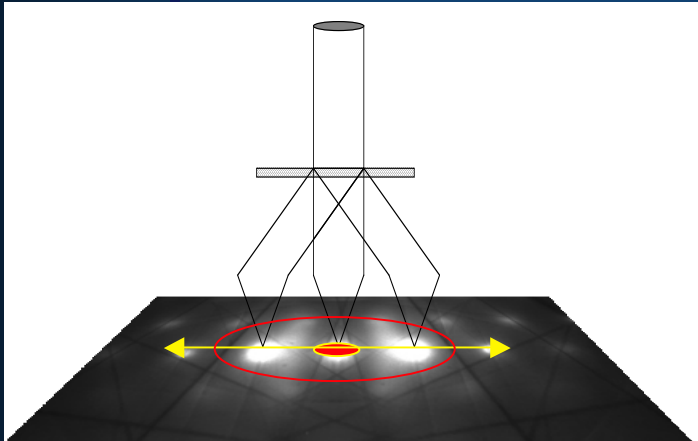


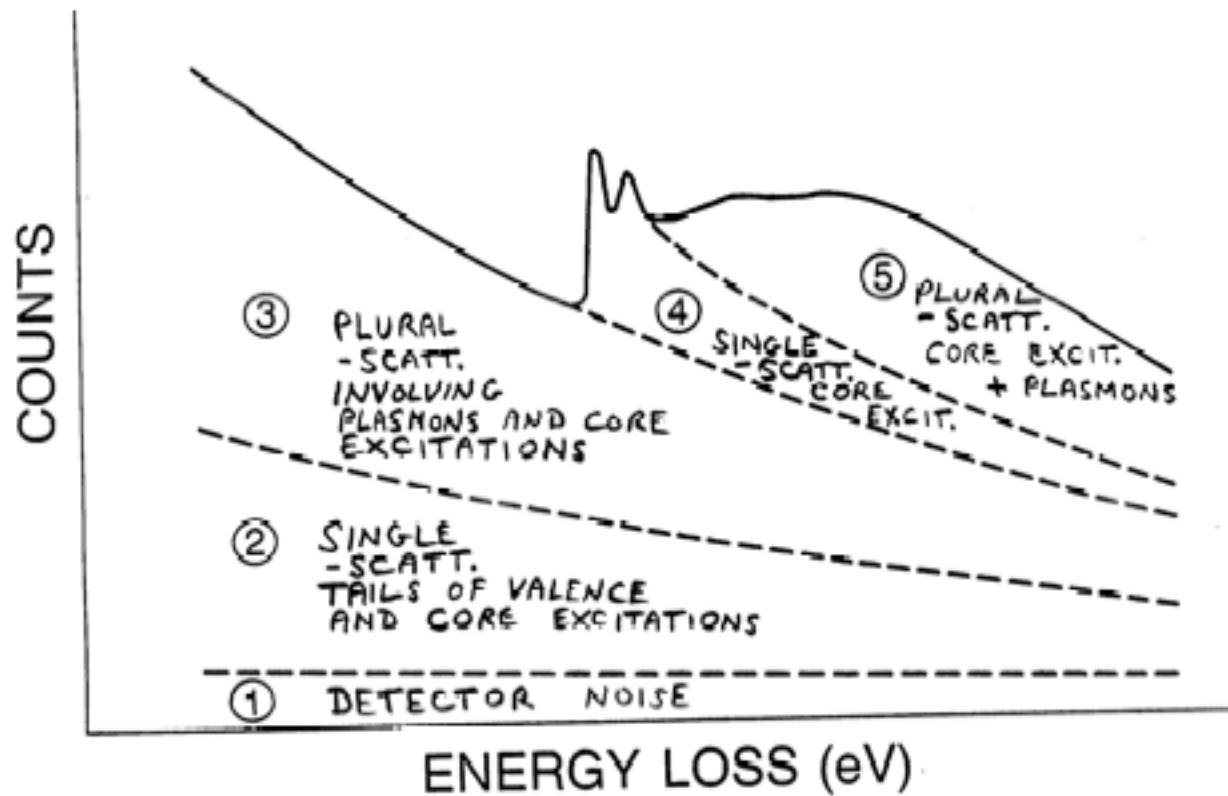
Figure 5 Comparison of an experimental L edge profile with the equivalent profile calculated by using the SIGMAK model.

Problems In EELS Quantification

Collection Angle Errors



Problems In EELS Quantification Multiple Scattering



Leapman, 1991

Effects of Specimen Thickness

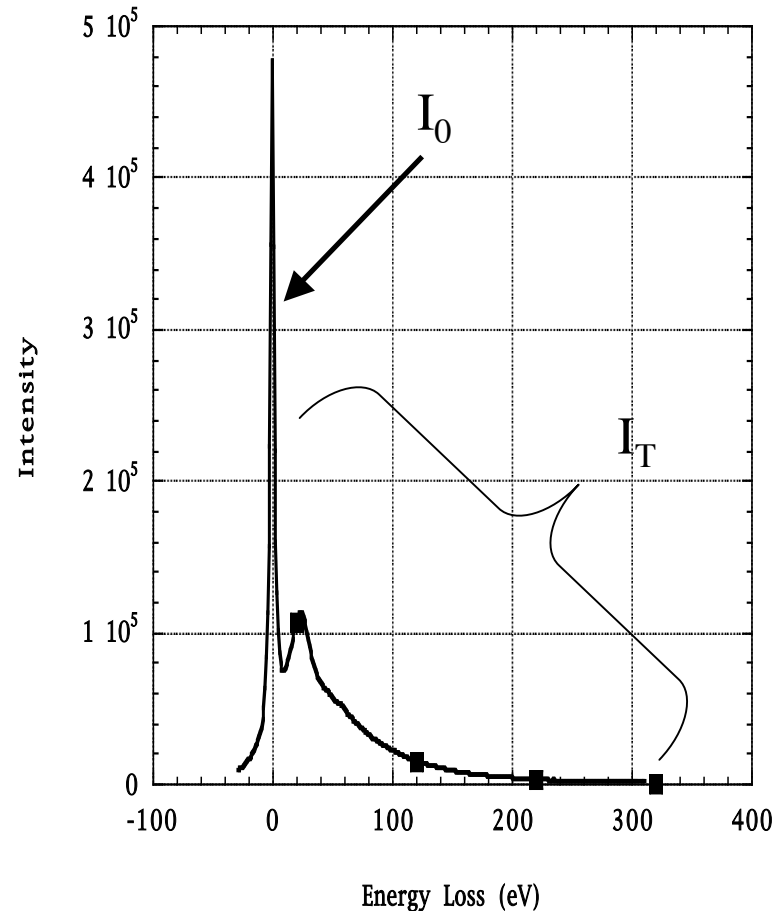
- **Multiple Scattering**
 - **Low Loss**
 - **Core Loss - Visibility**
- **Quantification Effects**

- To measure the thickness of compare the intensity of the zero loss (I_0) to the total integrated intensity in the spectrum (I_T).

- This ratio is directly proportional to the local thickness of the specimen.

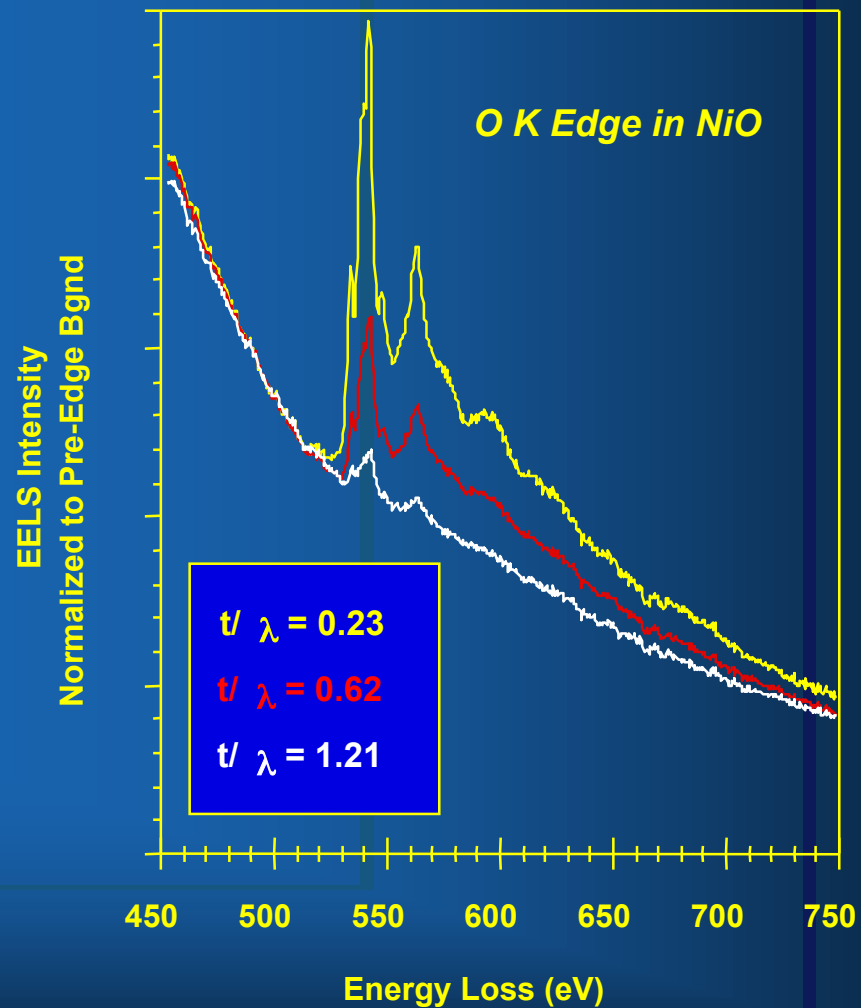
$$t = \lambda * \ln (I_0 / I_T)$$

λ = mean free path



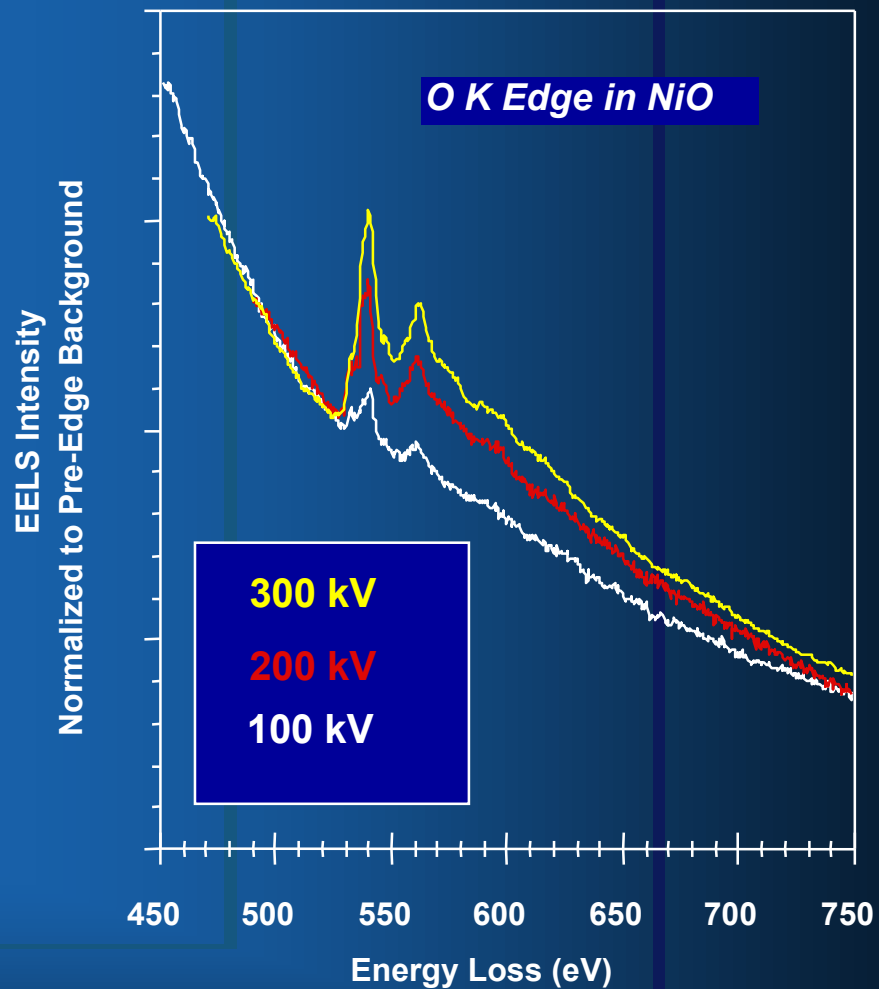
Variation
in EELS
Edge P/B
with
Thickness

Experimental EELS Edge/Background Ratio
as a Function of Specimen Thickness
at Constant Accelerating Voltage

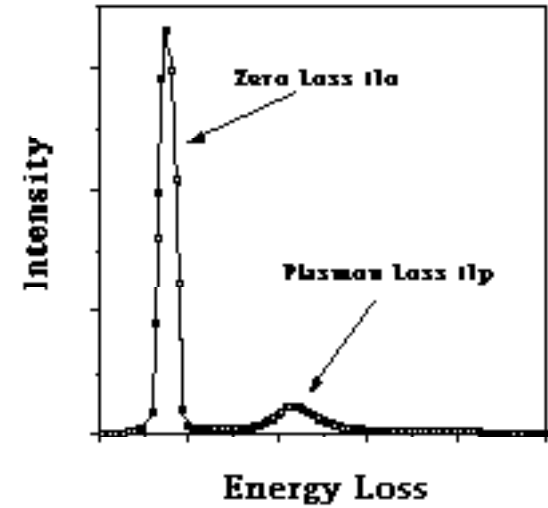
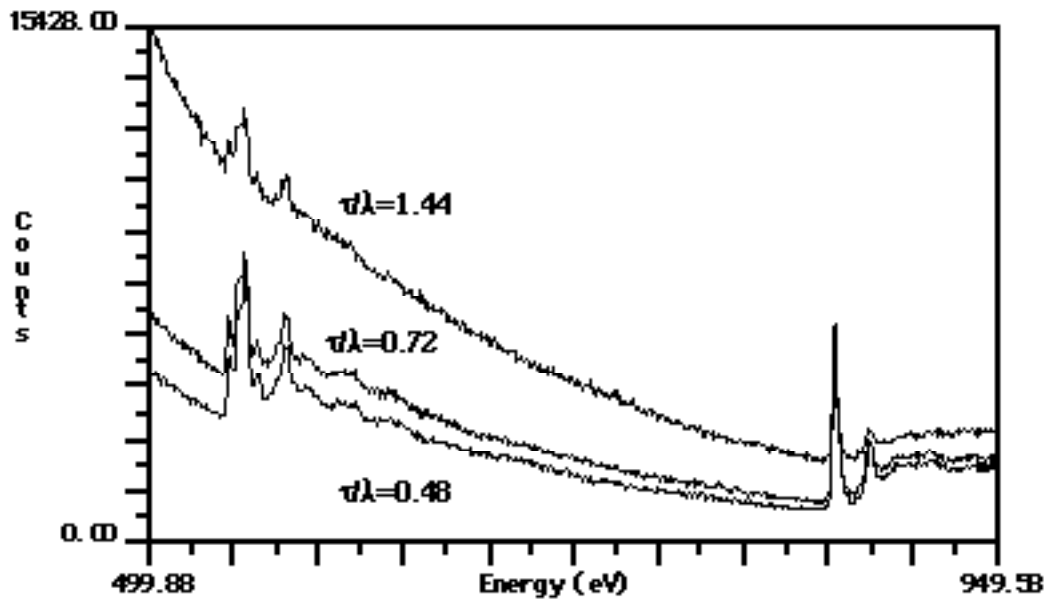


Variation
in EELS
Edge P/B
with
kV

Experimental EELS Edge/Background Ratio
as a Function of Accelerating Voltage
at Constant Specimen Thickness

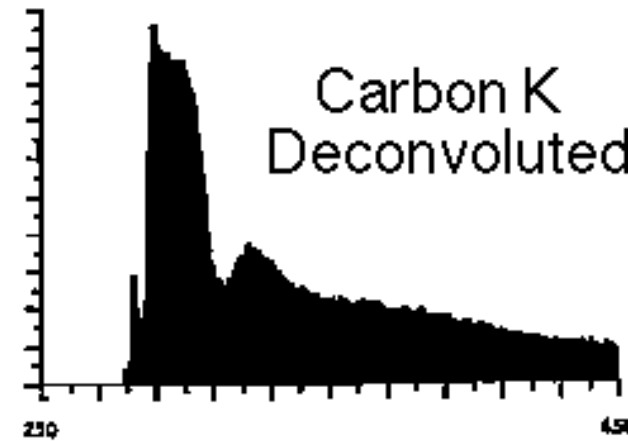
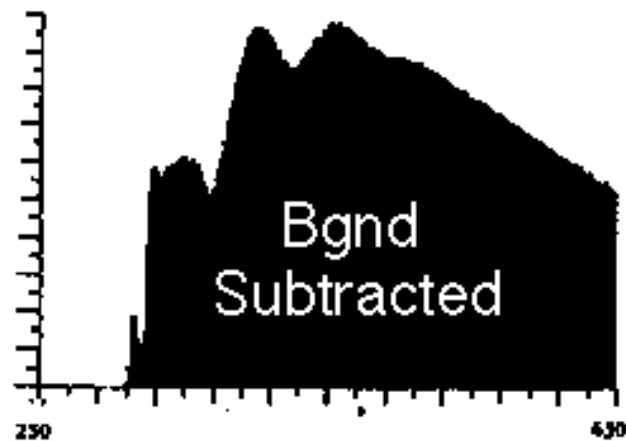
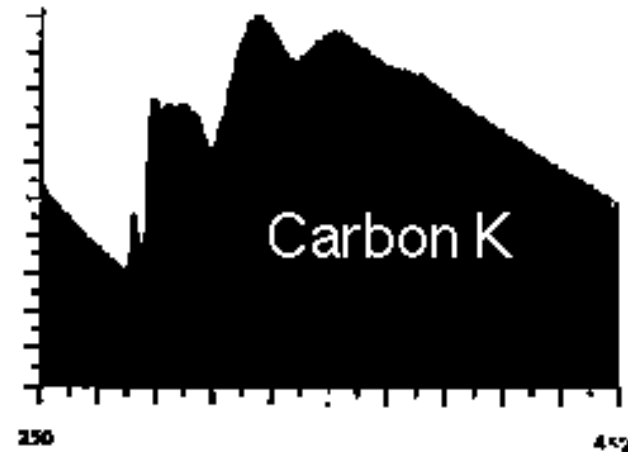
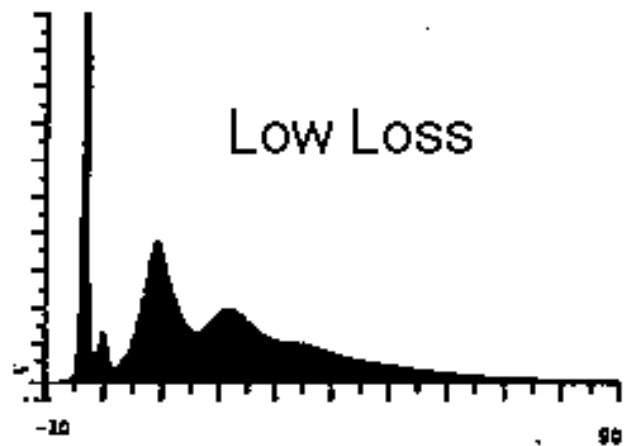


Specimen Thickness Effects on EELS



$$\frac{I_p}{I_0} = \frac{t}{\lambda} \leq 0.1$$
$$\ln\left(\frac{I_T}{I_0}\right) = \frac{t}{\lambda} \leq 1.0$$

Deconvolution of Multiple Scattering using Leapman/Swyt Method



$$MS = SS * LL$$

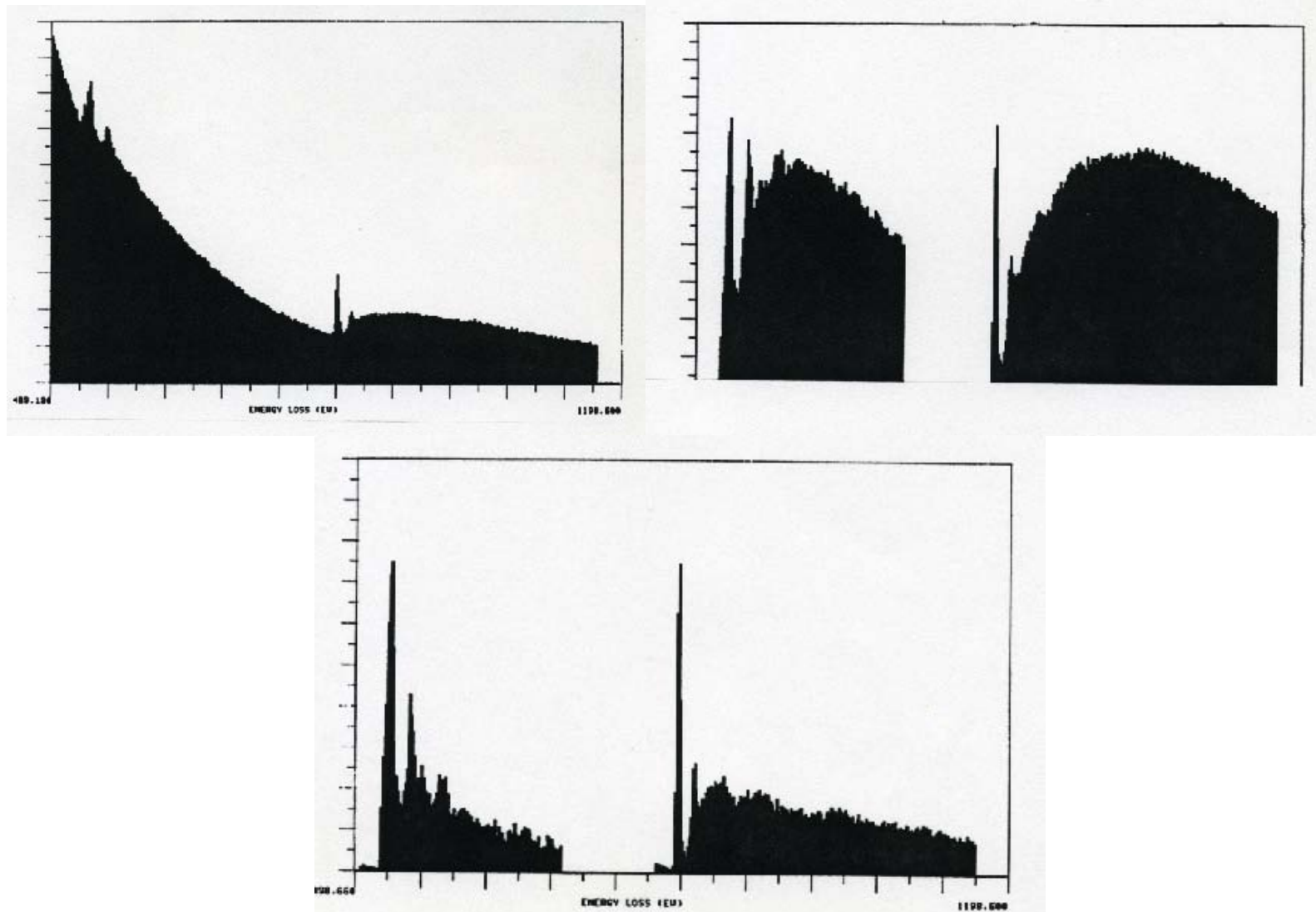
$\mathcal{F} = \text{Fourier Transform}$

$$SS = \mathcal{F}^{-1} \left\{ \frac{\mathcal{F}(MS)}{\mathcal{F}(LL)} \right\}$$

$\mathcal{F}^{-1} = \text{Inverse Fourier Transform}$

Does Deconvolution Help Quantification?

$$\frac{I_A}{I_B} = \frac{\sigma_A N_A}{\sigma_B N_B}$$



Does Deconvolution Help Quantification?

$$\frac{I_A}{I_B} = \frac{\sigma_A N_A}{\sigma_B N_B}$$

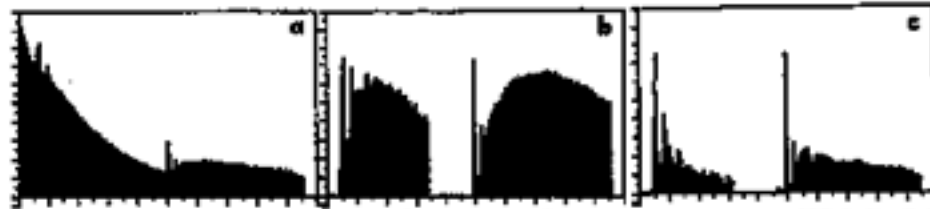
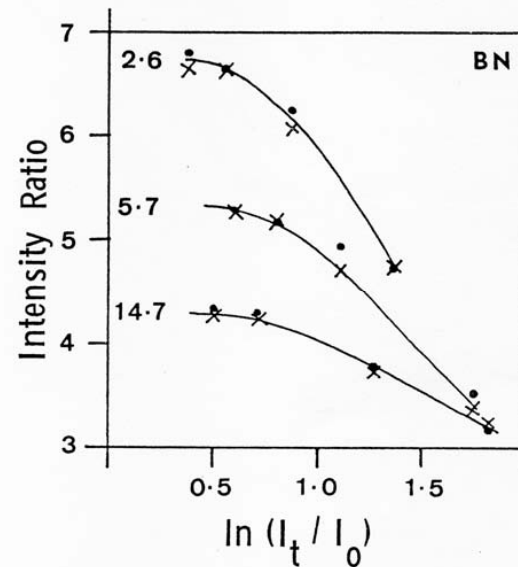
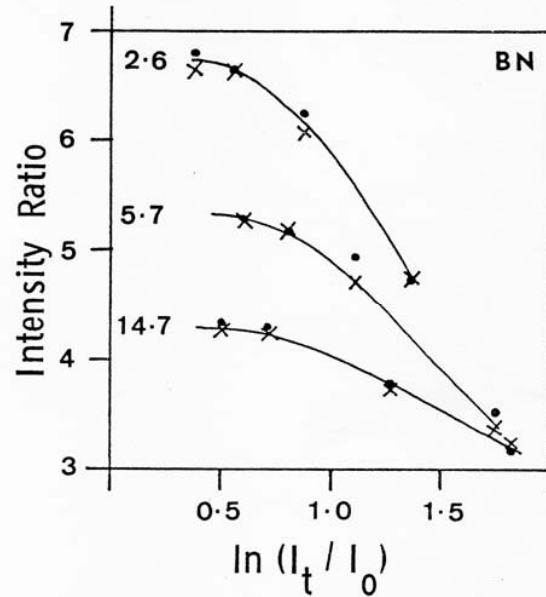
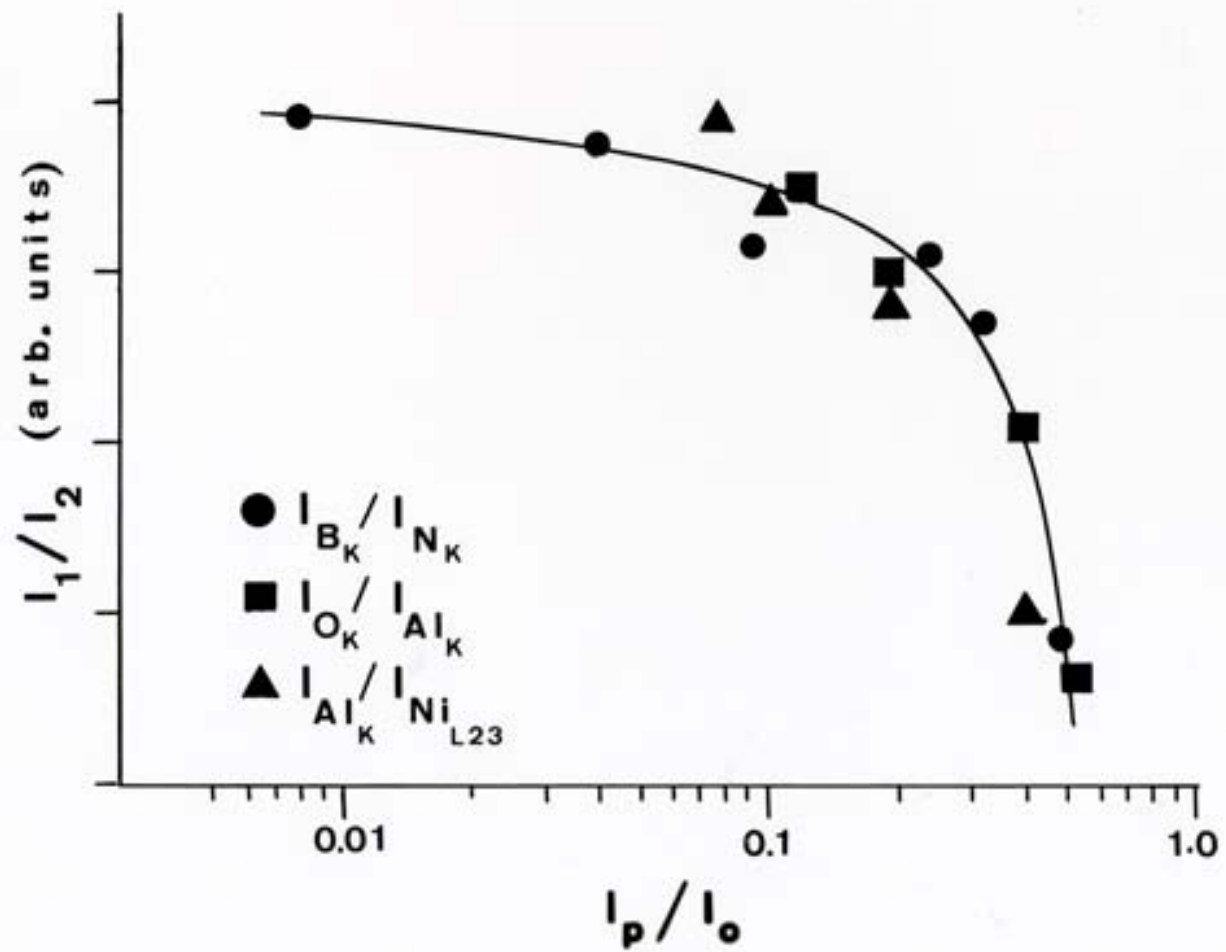


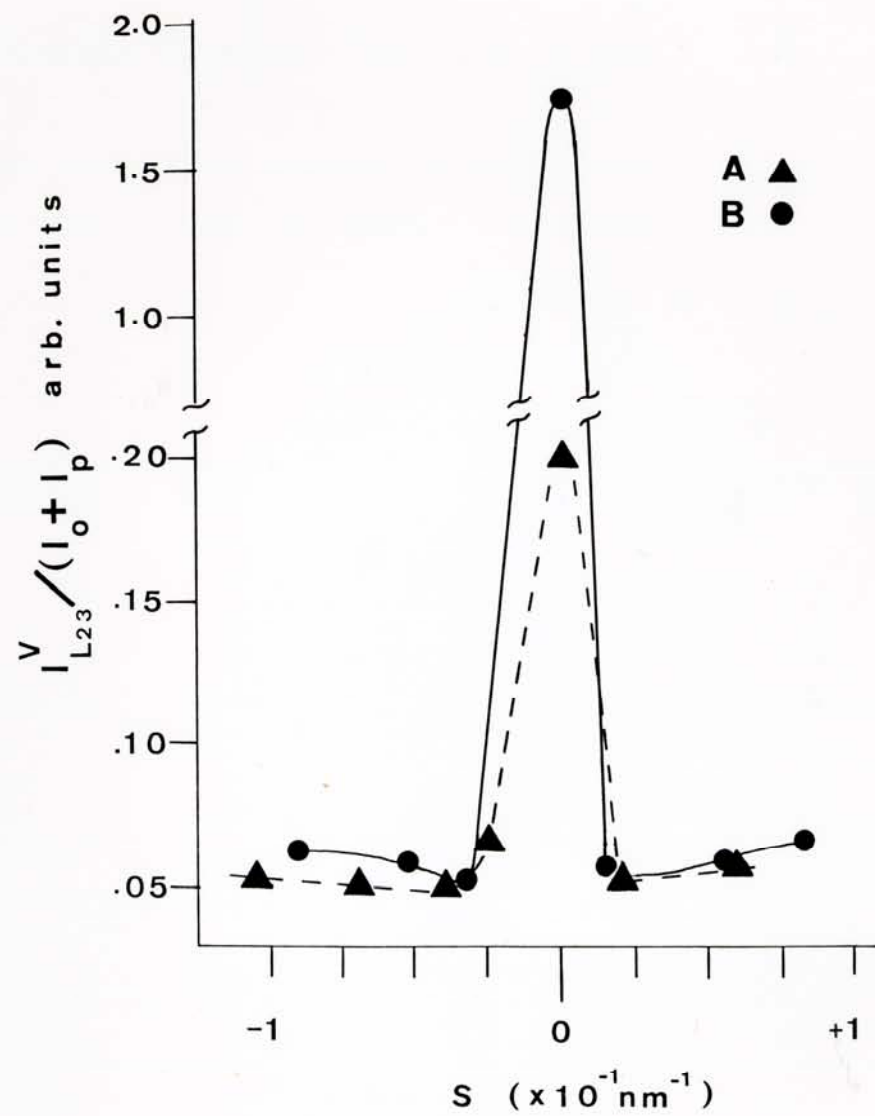
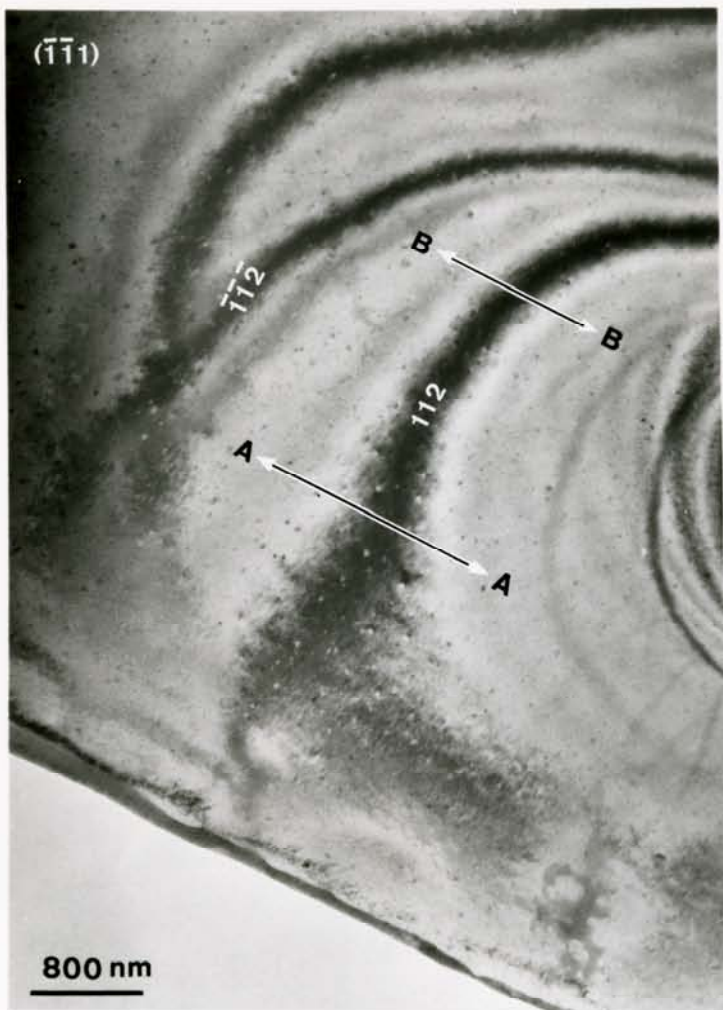
FIG. 1.—Partial EELS Spectrum (500–1200 eV) from NiO specimen: 100 keV, 5.7 mrad scattering angle, a) unprocessed data b) background stripped, c) deconvoluted.



This defines a "Thin Film Approximation" for EELS i.e. $\frac{t}{\lambda} < 1.0$

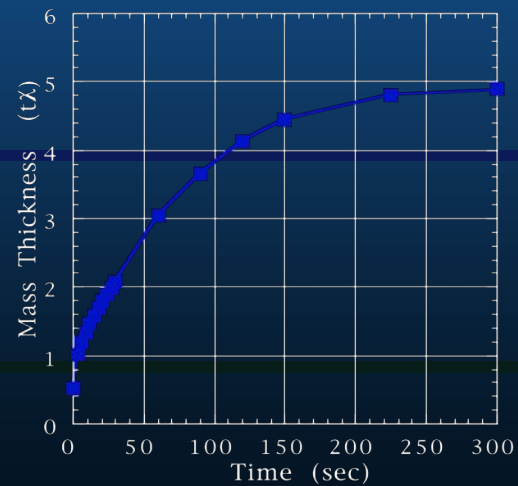
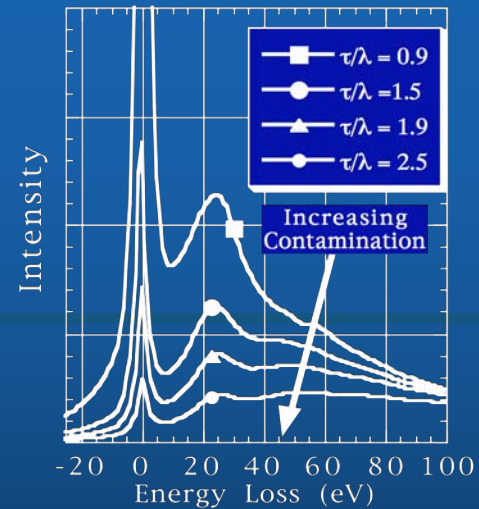
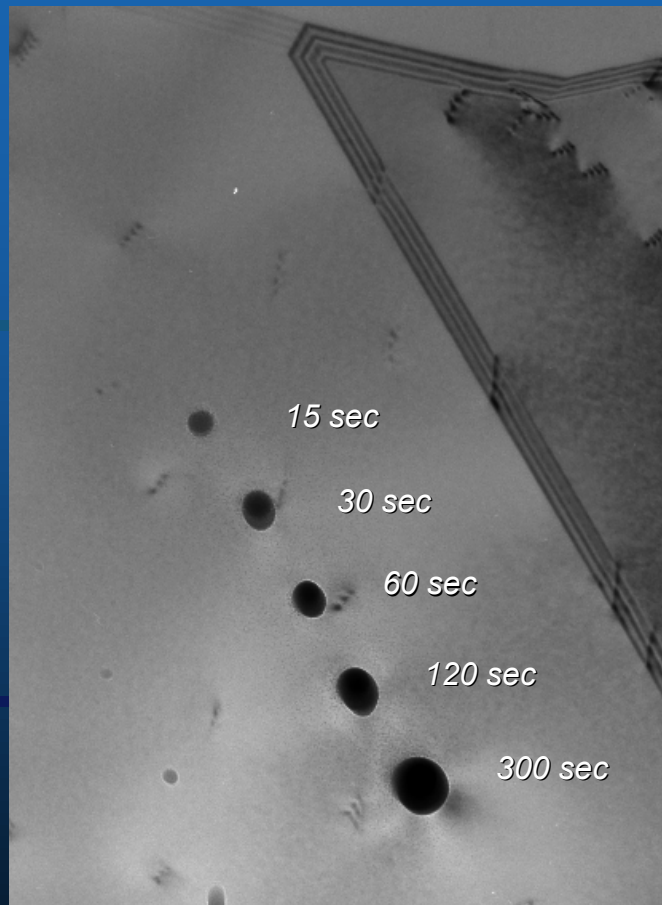


Orientation & Thickness Effects on EELS Signals

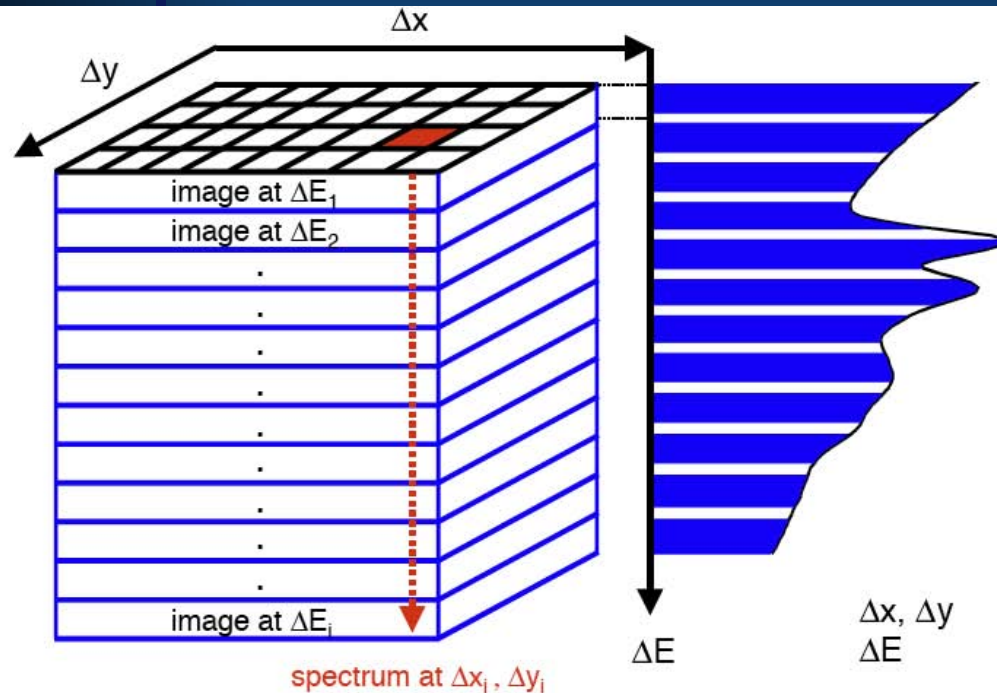


Specimen Contamination

The Microscopists Bane



Spectral Imaging Slice-by-Slice vs Point-by-Point



The technique of building up a more or less complete data cube is termed **Spectrum Imaging**

$\Delta x, \Delta y$ spatial dimensions
 ΔE energy-loss dimension

EFTEM Spectrum Imaging:

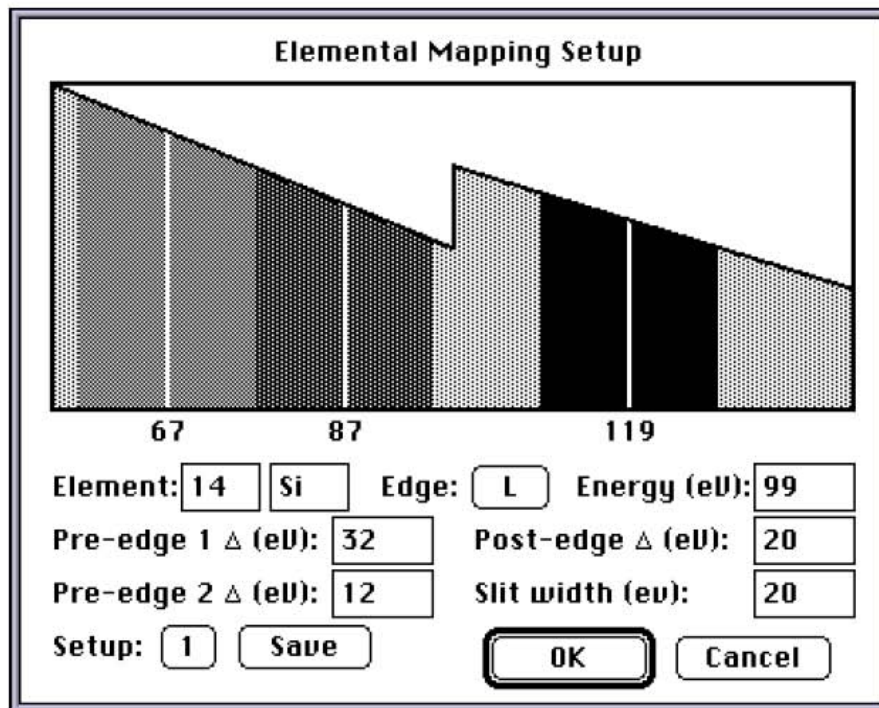
- Energy filtered broad beam technique
- fills data cube one image plane at a time
- less time

STEM Spectrum Imaging:

- Focused probe method
- fills data cube one spectrum at a time
- less dose

Elemental Mapping

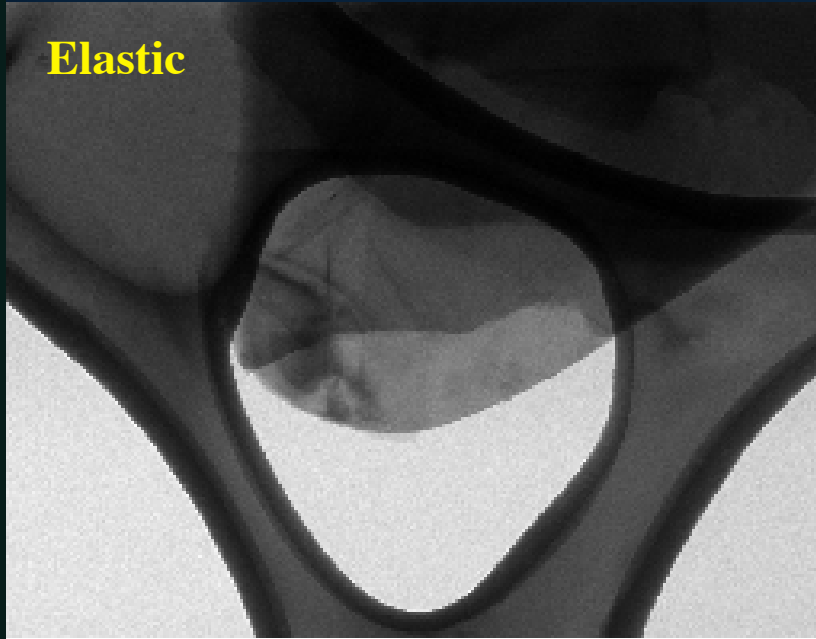
Determine and subtract edge background using two pre-edge images to obtain the true edge signal



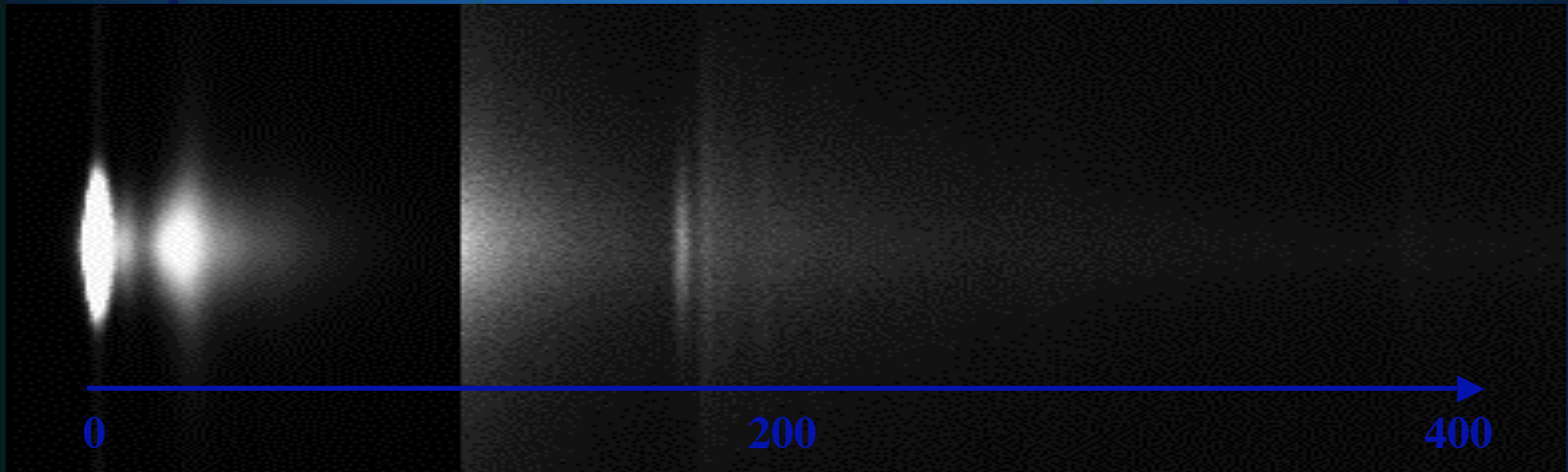
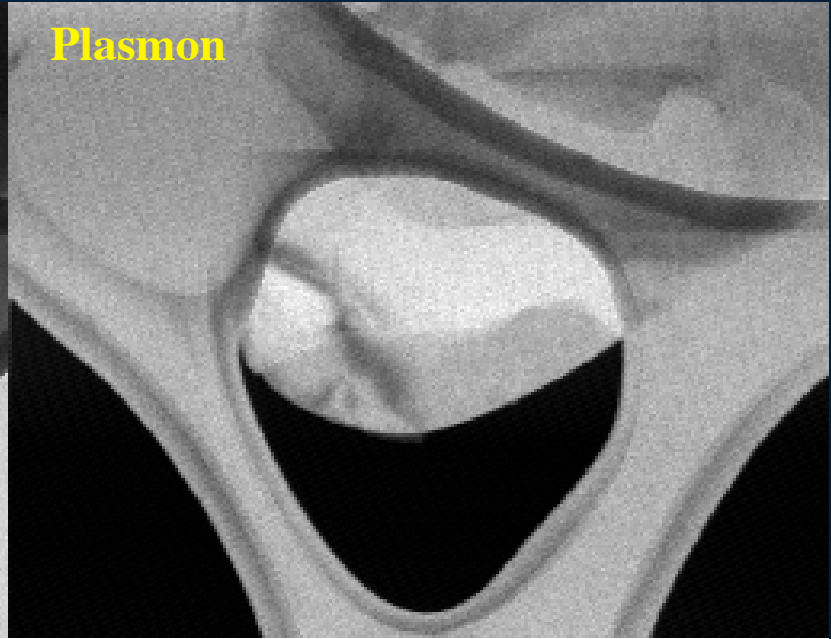
- Minimum of two background windows are necessary
- Map intensity is directly proportional to projected concentration
- Map-intensity can be related to absolute concentration if thickness and elemental cross-sections are known

Boron Nitride on Holey Carbon

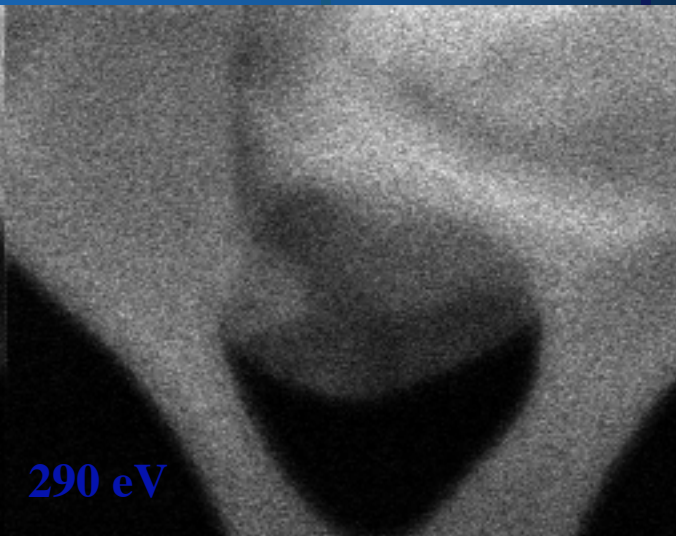
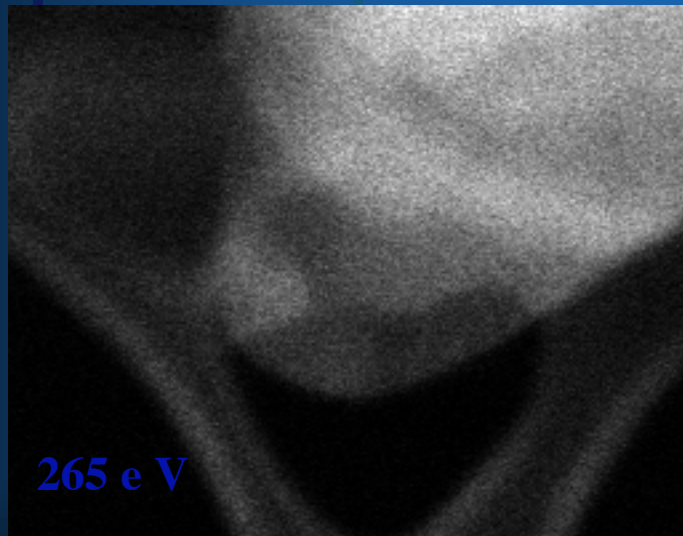
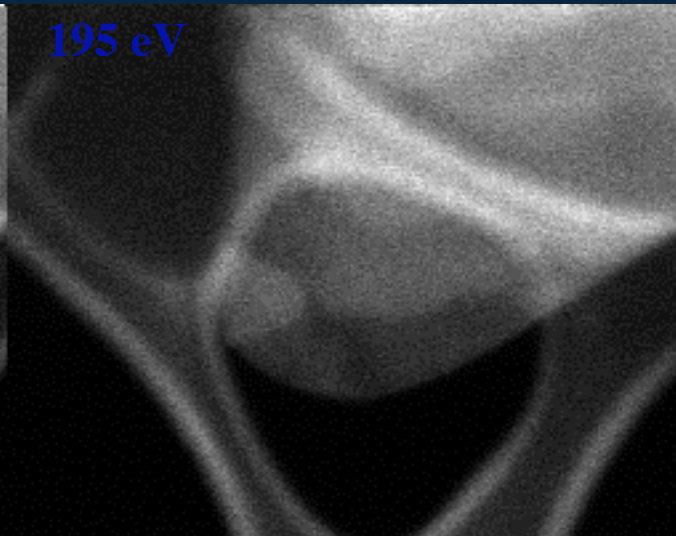
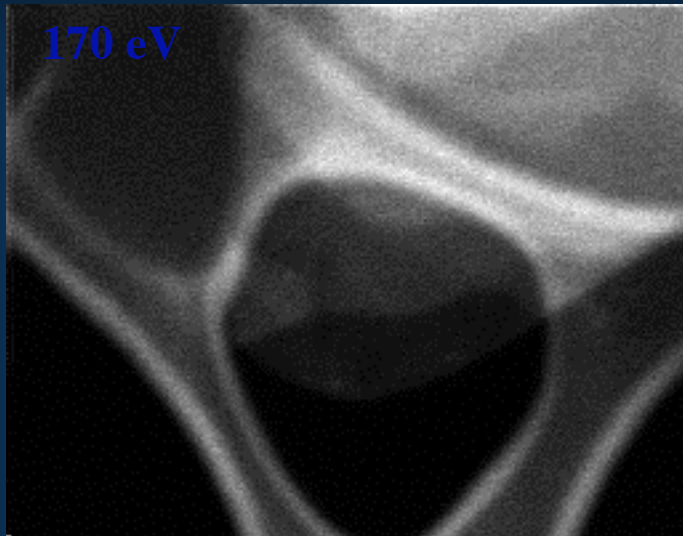
Elastic



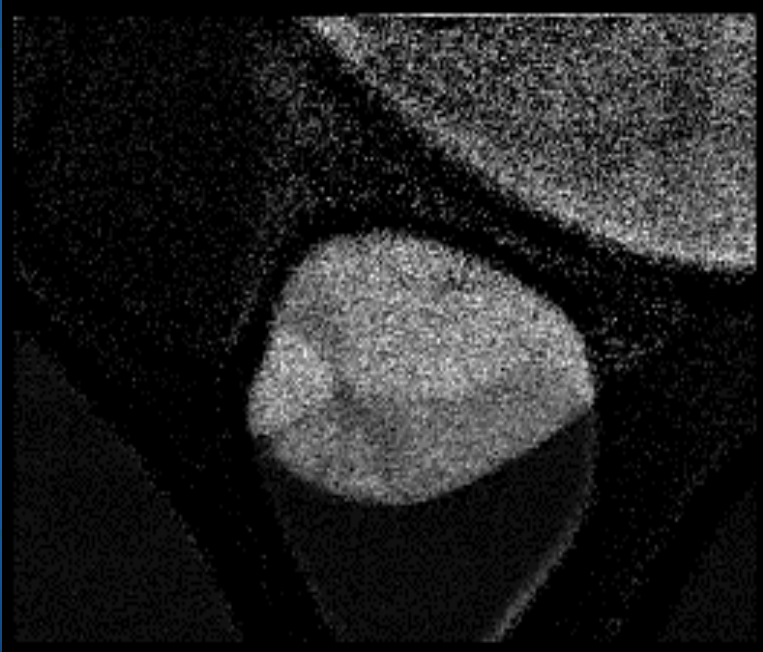
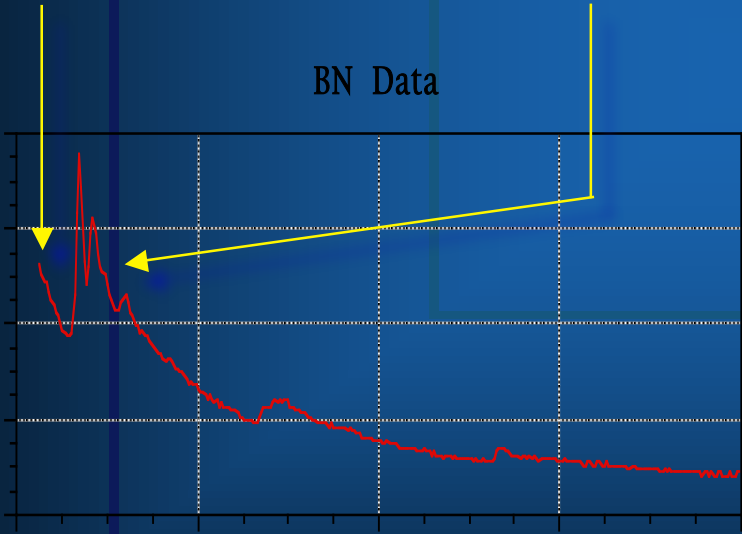
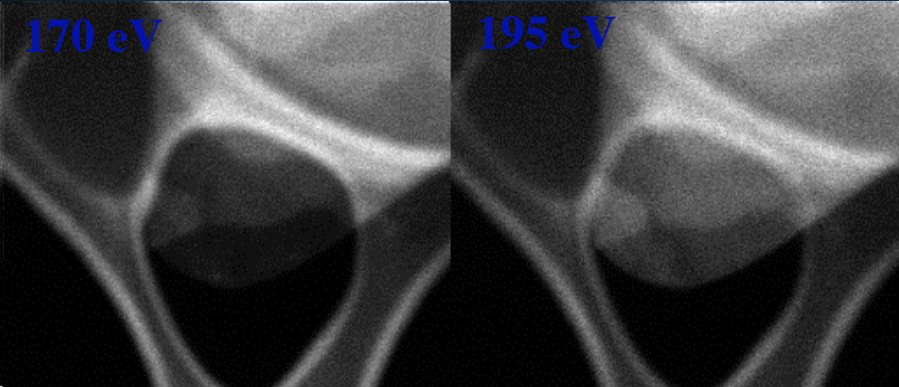
Plasmon



Energy Loss

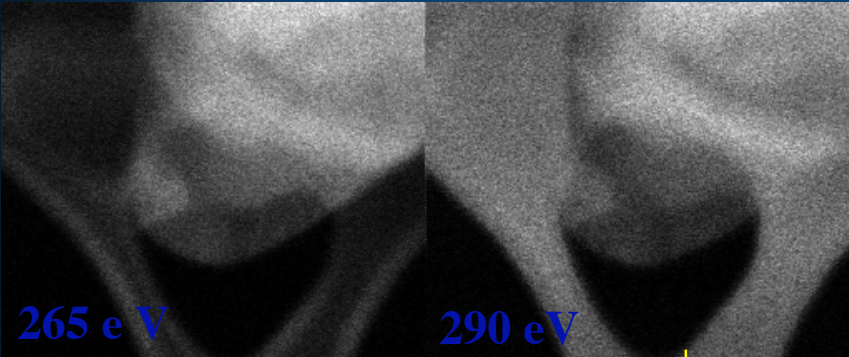


Filtered Elemental Imaging

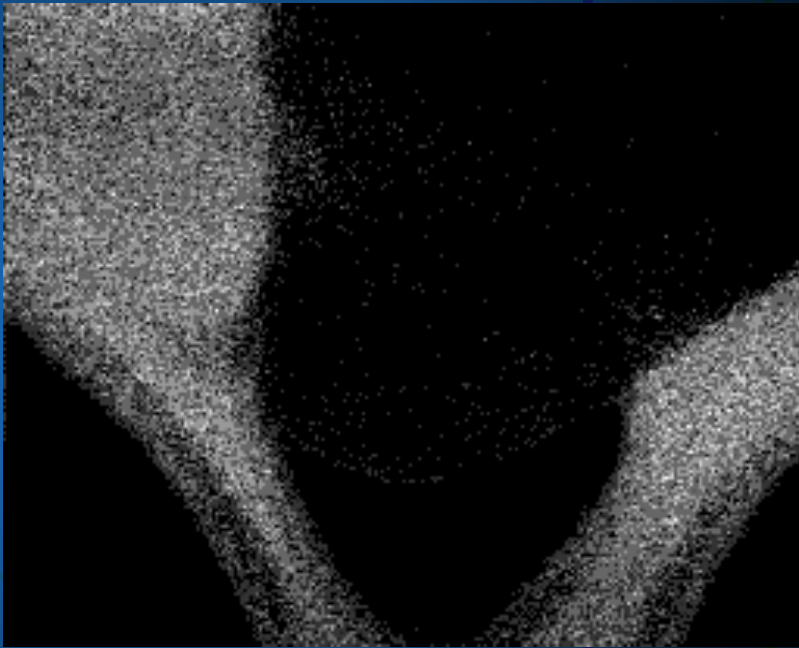
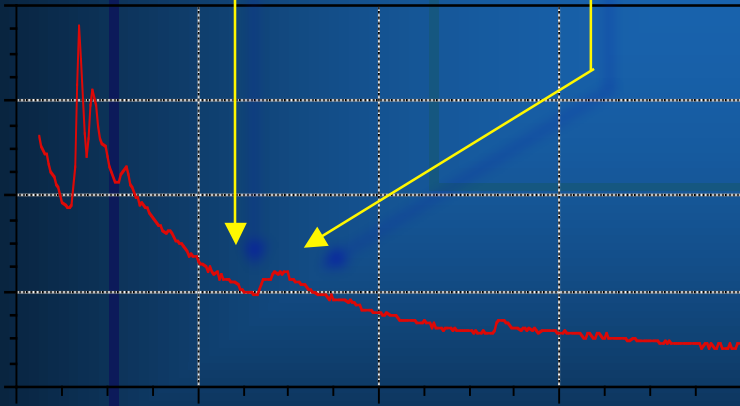


Net Boron K Image

Filtered Elemental Imaging



BN Data

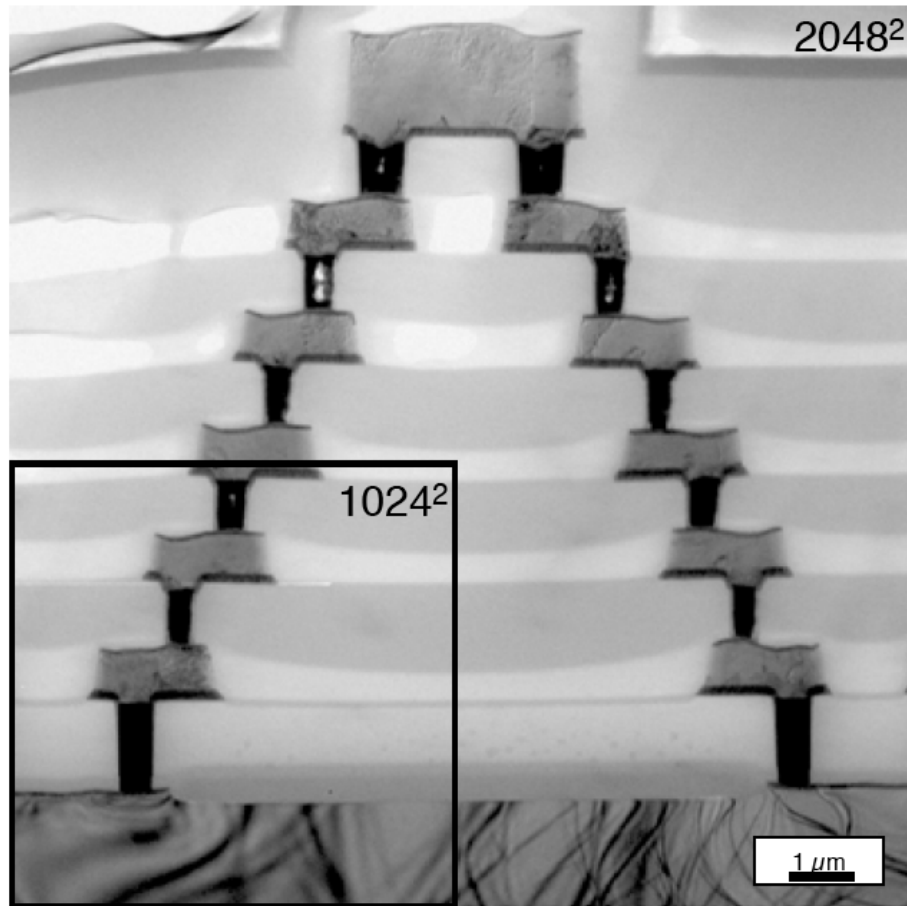


Elemental Mapping

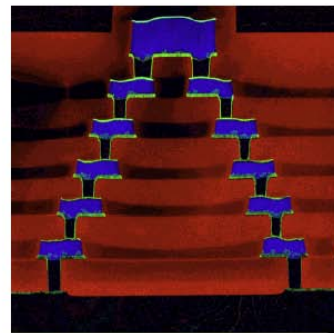
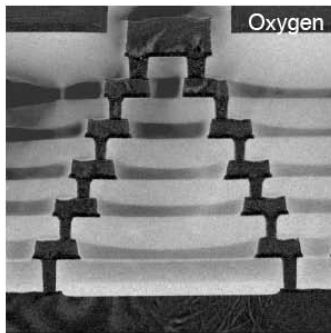
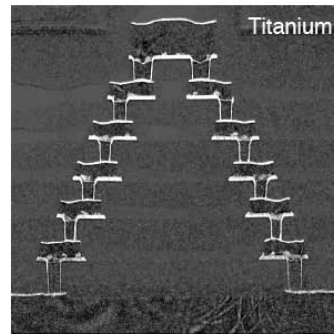
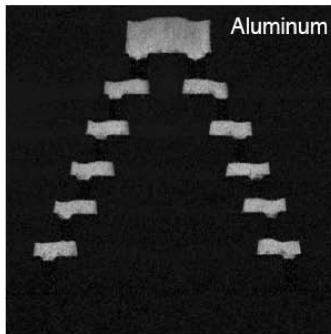
6 layer metallization
test structure

recorded on a CM200, LaB6
with a GIF2002 (2K CCD)

field of view: $12\ \mu\text{m}$
number of pixels: 4.2×10^6



Gerald Kothleitner



■ O ■ Ti ■ Al

3 images each around:

O K edge: @ 532 eV
Ti L₂₃ edge: @ 455 eV
Al K edge: @ 1560 eV

Color overlays, RGB images:

- assign a color to each elemental map: O red, Ti green and Al blue
- superimpose three color layers to form RGB composite

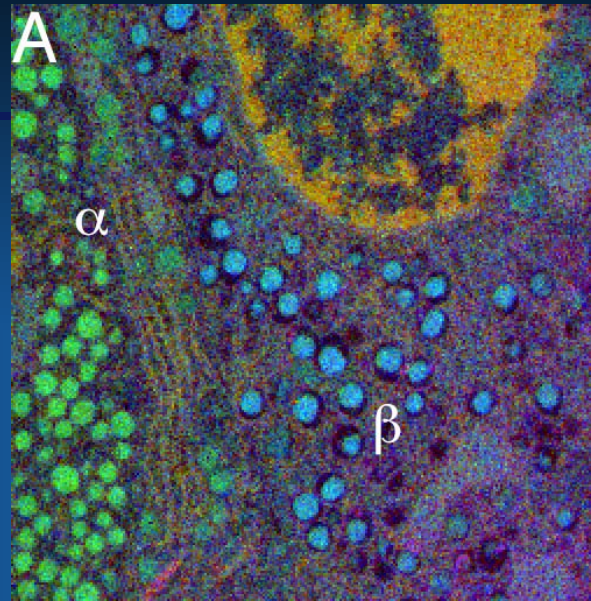
Leapman et al. (2003)

EFTEM elemental maps of mouse pancreatic islet cells

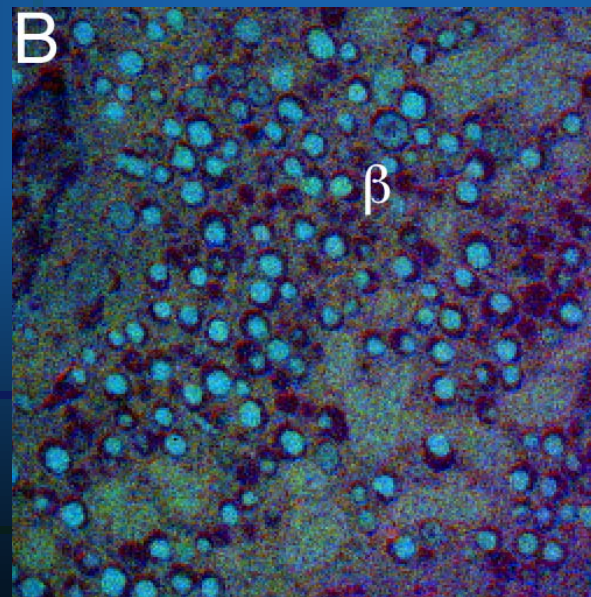
Shows sulfur-rich insulin granules in β cells

 Nitrogen
 Phosphorus
 Sulfur

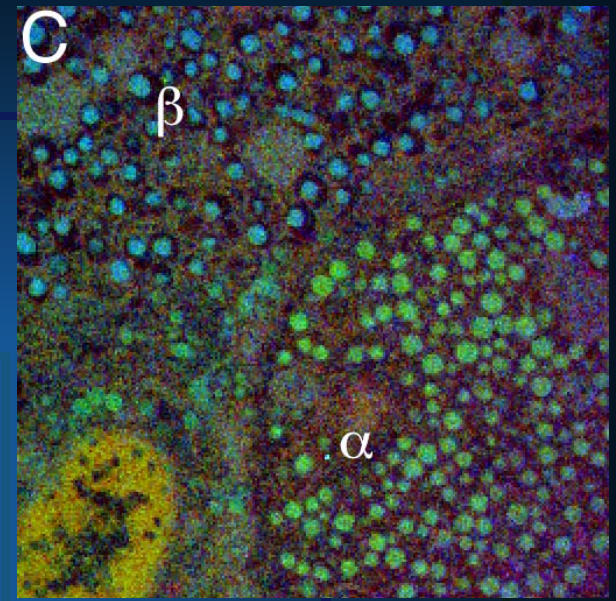
Mut



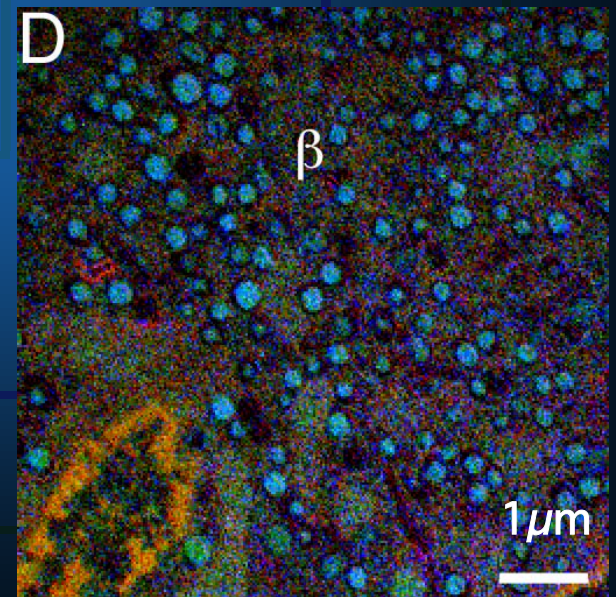
Mut



Cnt



Cnt



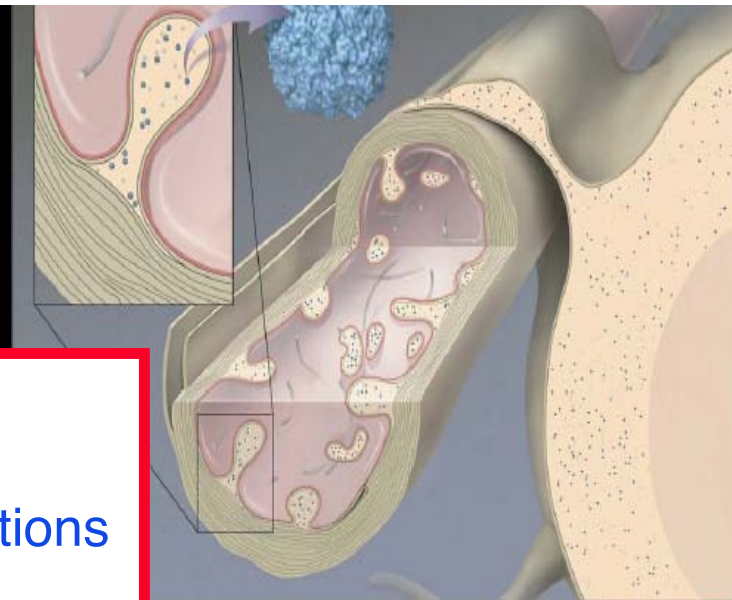
Mapping Ferritin in Brain: Misregulation of Iron Metabolism in IRP Knockout Mice

(P. Zhang et al., J. Struct. Biol. 2005)

Model of axon and oligodendrocyte showing anatomy of degeneration



Ferritin localized in invaginations of oligodendrocytes



STEM-EELS

Pre Fe L_{2,3}

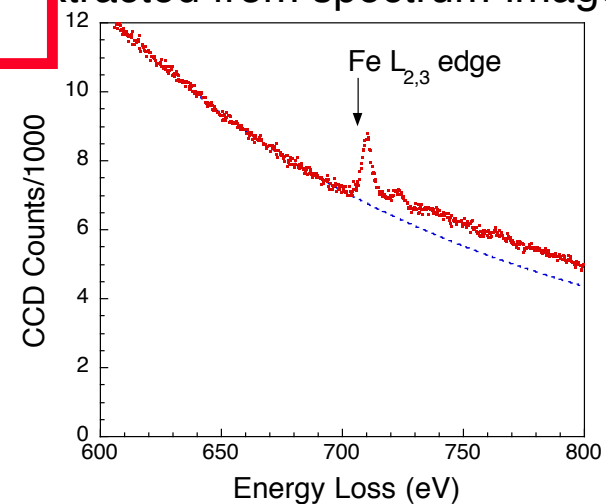
Post Fe L_{2,3}

Fe

Ferritin



EELS of ferritin molecule extracted from spectrum-image



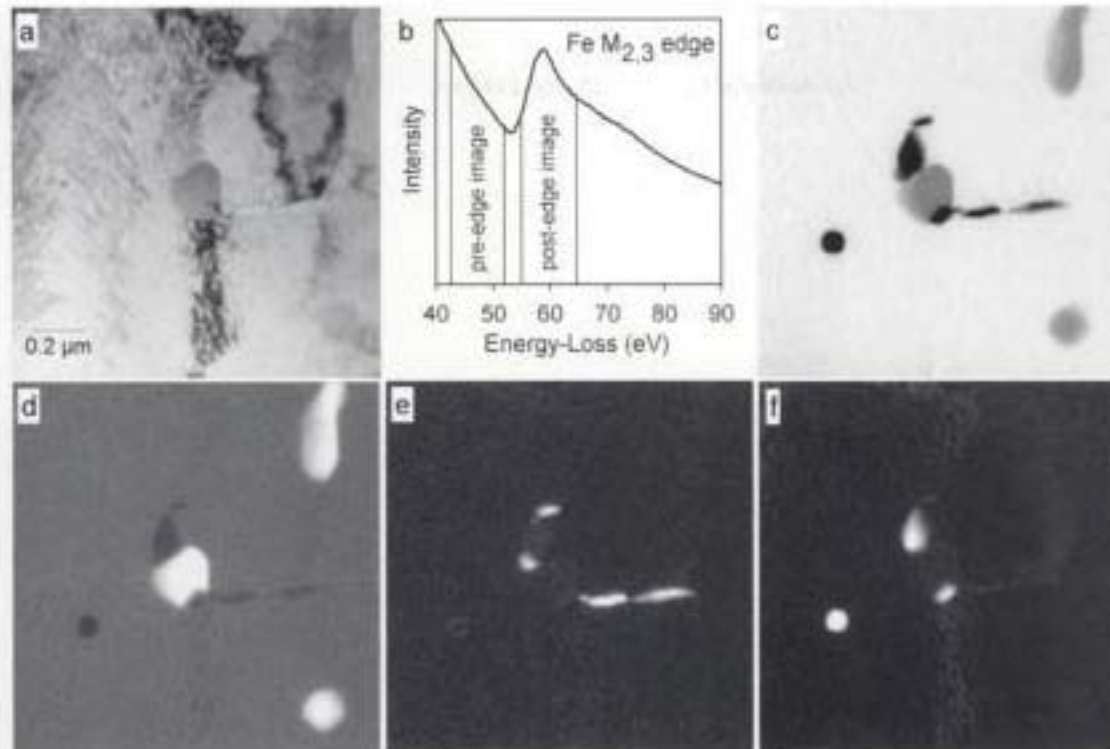


Fig. 6.14 Imaging of precipitates in a steel specimen; (a) TEM-bright field image of a 10% Cr steel with Cr_{23}C_6 , VN and Nb(C,N) precipitates; (b) EELS spectrum with the Fe $M_{2,3}$ edge; (c) Fe $M_{2,3}$ jump-ratio image recorded under rocking beam illumination; (d) Cr $L_{2,3}$ jump ratio image; (e) V $L_{2,3}$ jump ratio image; (f) Nb $M_{4,5}$ jump ratio image.

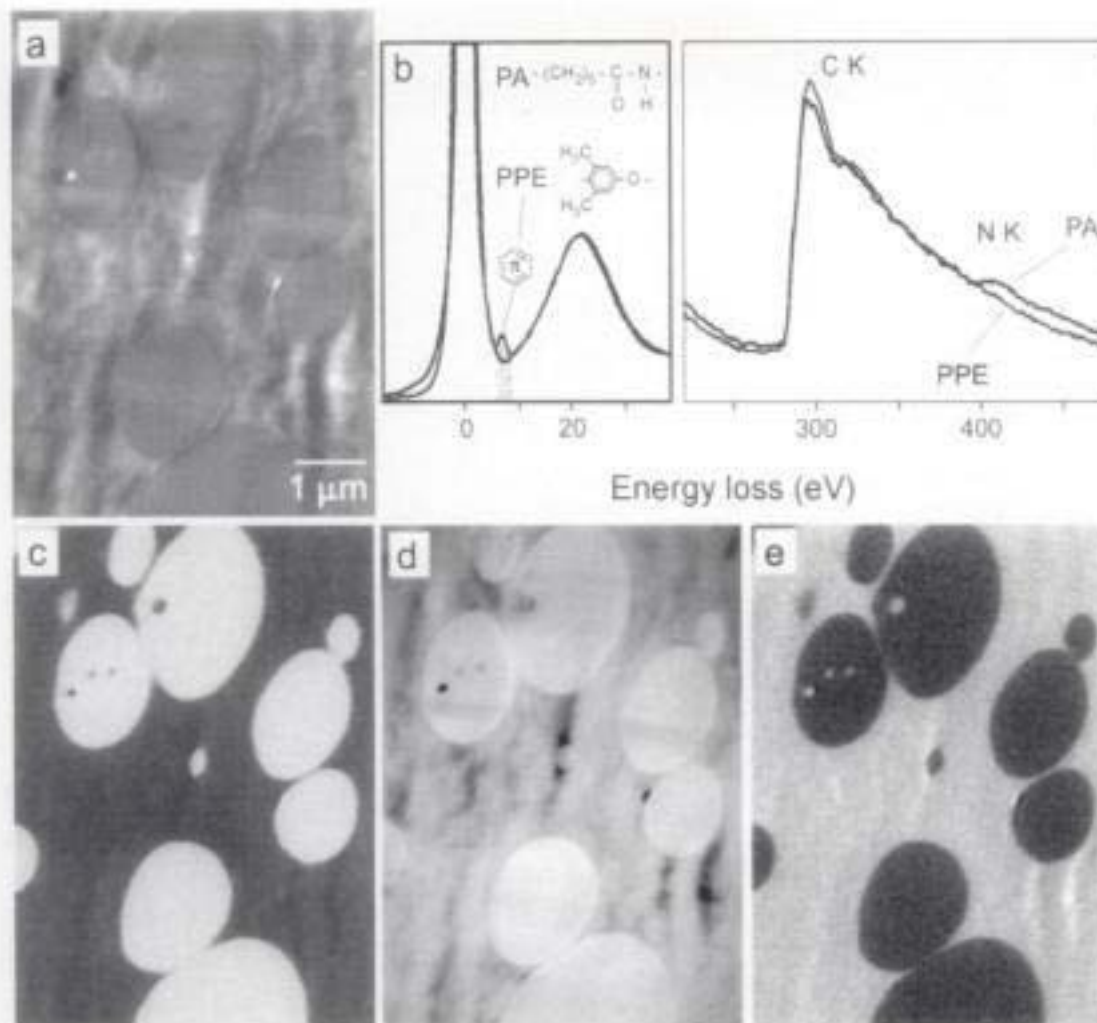


Fig. 6.23 Energy filtered imaging of polyamide/poly(phenylene ether) blend, (a) TEM-bright field image; (b) EELS spectra of PA and PPE; (b) π^* map in the low loss region revealing the PPE distribution; (c) carbon K elemental map; (d) nitrogen K elemental map revealing the polyamide; from [6.222].

Steps in Quantitative (Elemental) Analysis

Select the operating mode: Is it appropriate?

CTEM, STEM.....

Image Coupled, Diffraction Coupled

Obtain a typical spectrum

Optimize the experimental conditions

Accelerating Voltage (maximum consistent with your specimen)

Choose the best Edges to analyze (K, L, M,.....)

Optimize β for the weakest edges ($\theta_E = \delta E / 2E_0$)

Optimize α to minimize problems ($\alpha < \beta/2$)

Optimize the Acquisition Mode

Normal - High Concentrations

Difference - Low Concentrations

Optimize the Data Acquisition

Select Energy Resolution and Range

DQE & Statistics

Process the Data to Extract Intensities

Normal

Difference

Reference Spectra

Check the relative specimen thickness ($t/\lambda < 1$)

Calculate the compositions

Absolute # of atoms

Relative # of atoms

Standards/Standardless?

ReCheck for Artifacts/Problems

Diffraction

Orientation/Channeling

Unidentified Edges

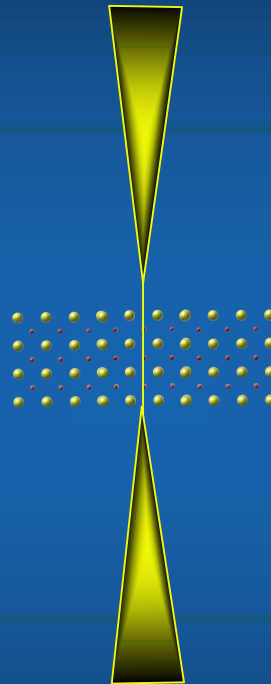
Spectral Overlaps

Radiation Damage

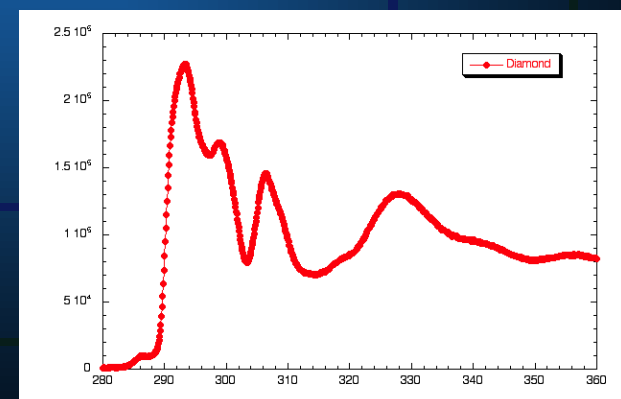
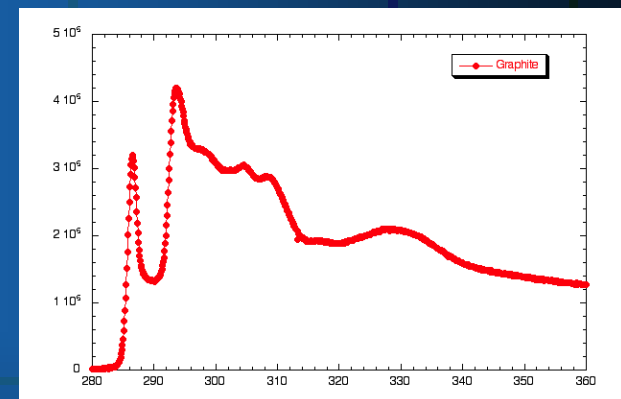
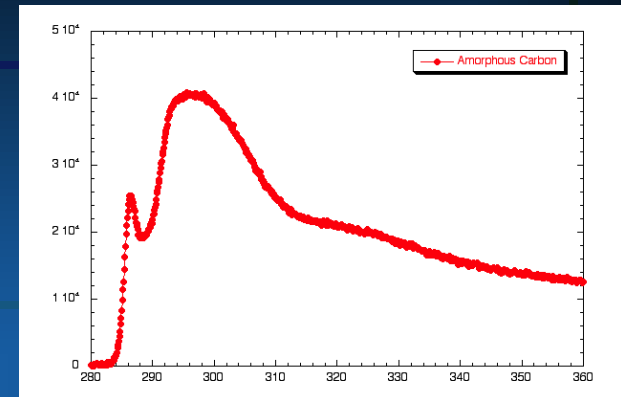
Linear Dichroism and Core Loss Electron Spectroscopy

Linear dichroism:

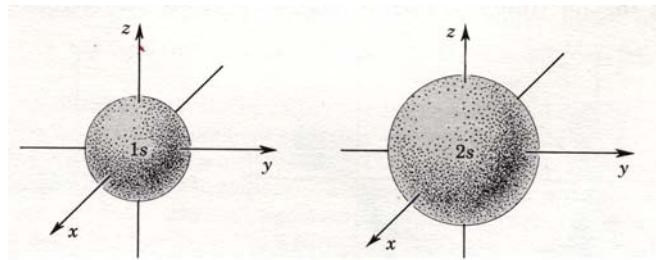
The linear polarization of the incident electrons parallel to the direction of momentum transfer. This polarization can be used to sense the anisotropy of the valence states involved in the core excitation process. It can detect the number or changes in the number of the valence holes in different directions of the atomic volume.



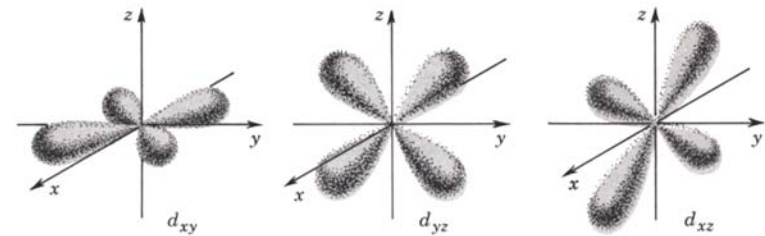
In many cases, the anisotropy of the charge in the atomic volume is caused by crystal-field interaction and is due to an anisotropy in the bonding.



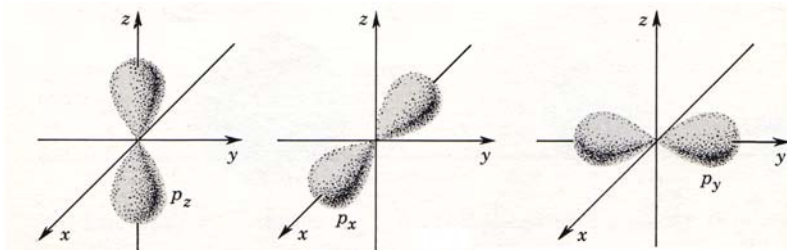
**Momentum Resolved EELS (MREELS) in Core Loss Spectroscopy
derives its information from transitions from initial to final states**



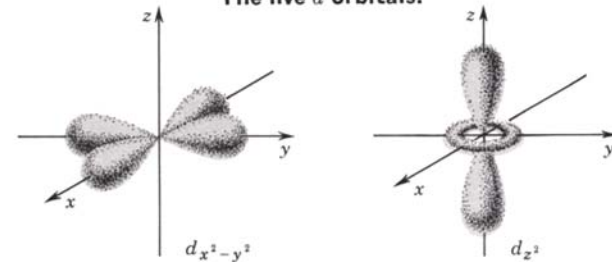
1s and 2s orbitals.



The five d orbitals.

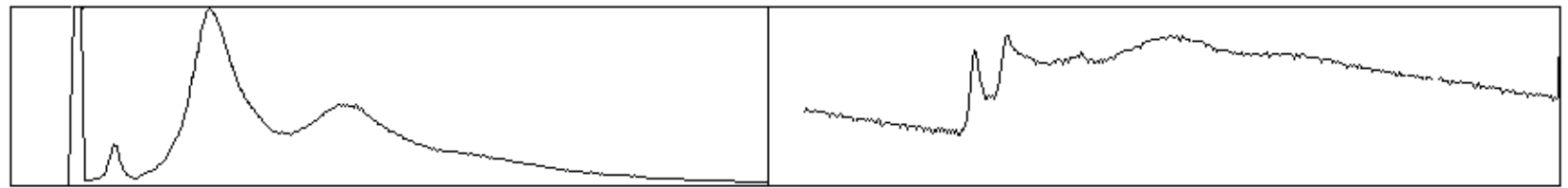
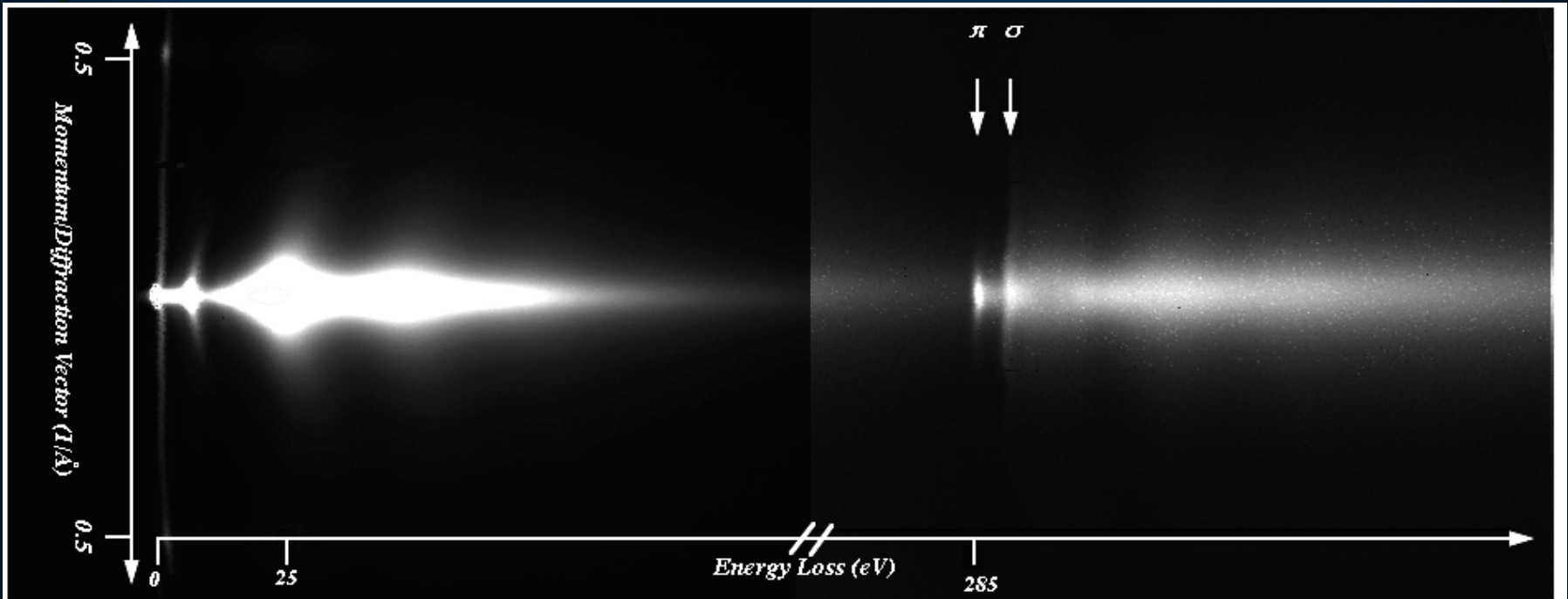


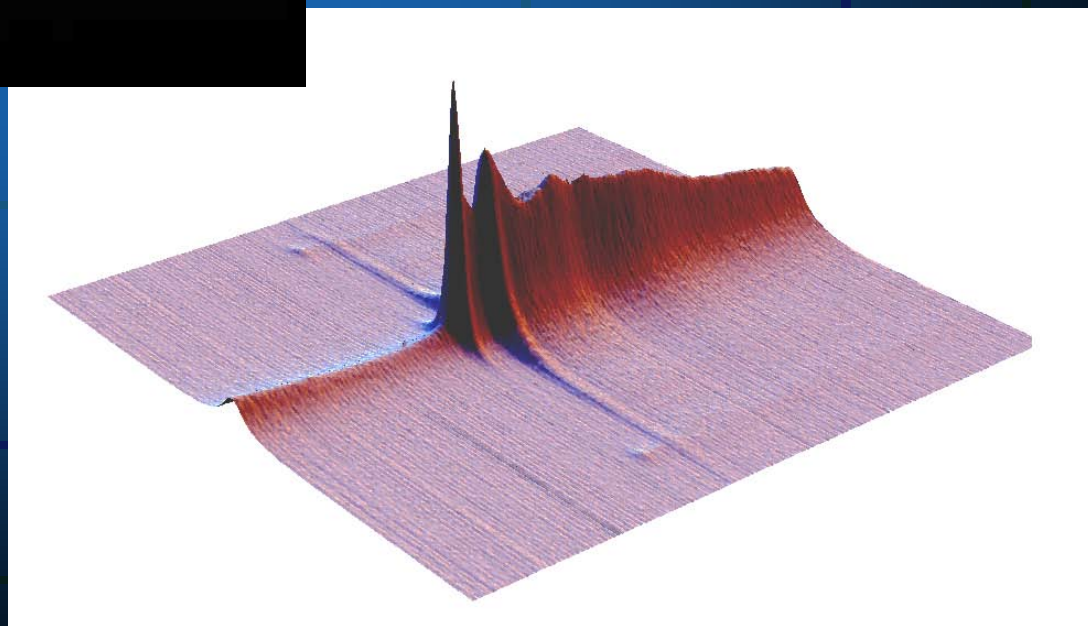
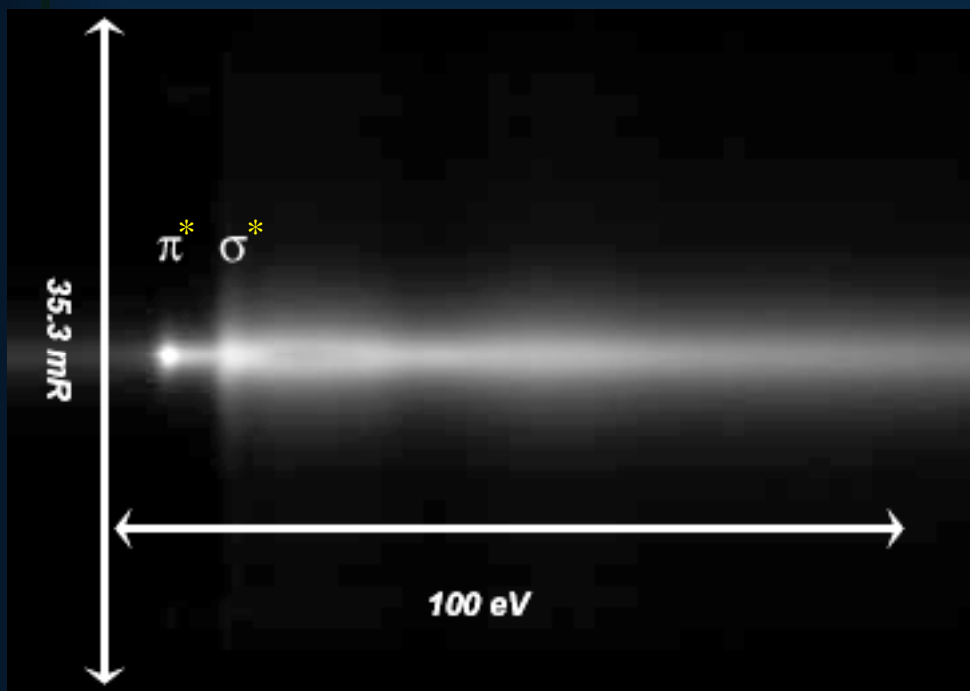
The p orbitals.

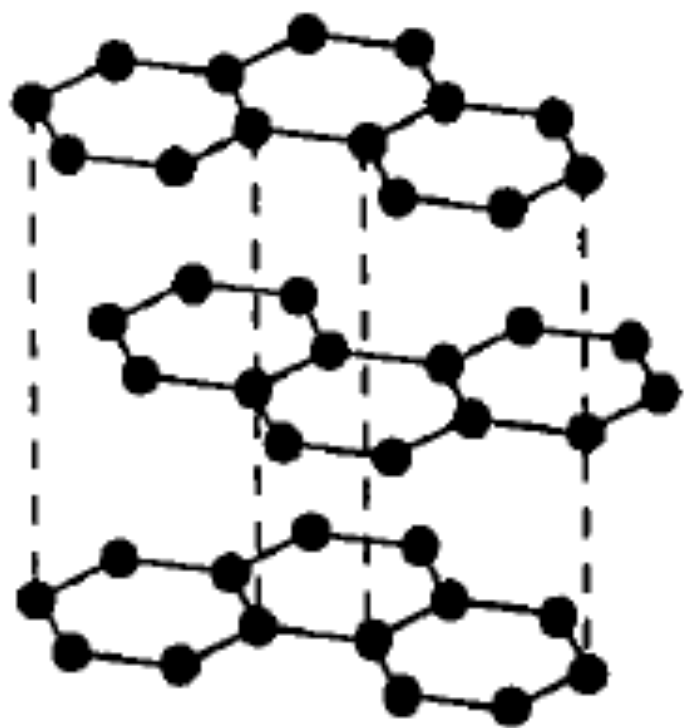


K shell p→s

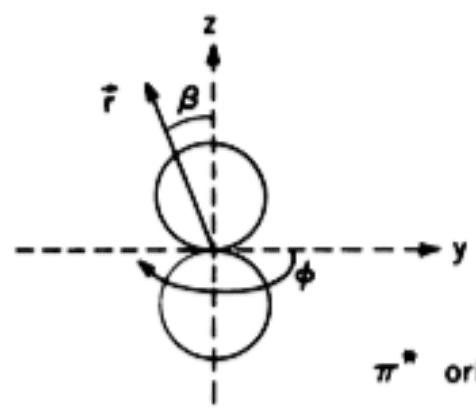
L shell p→s and p→d



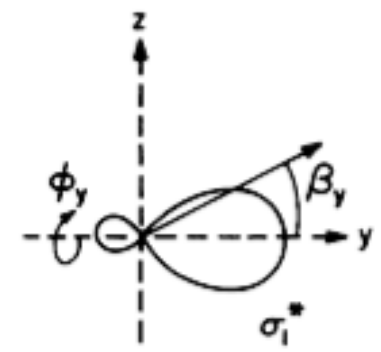
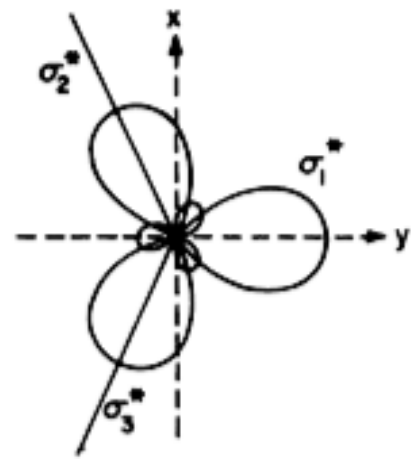




graphite C ●



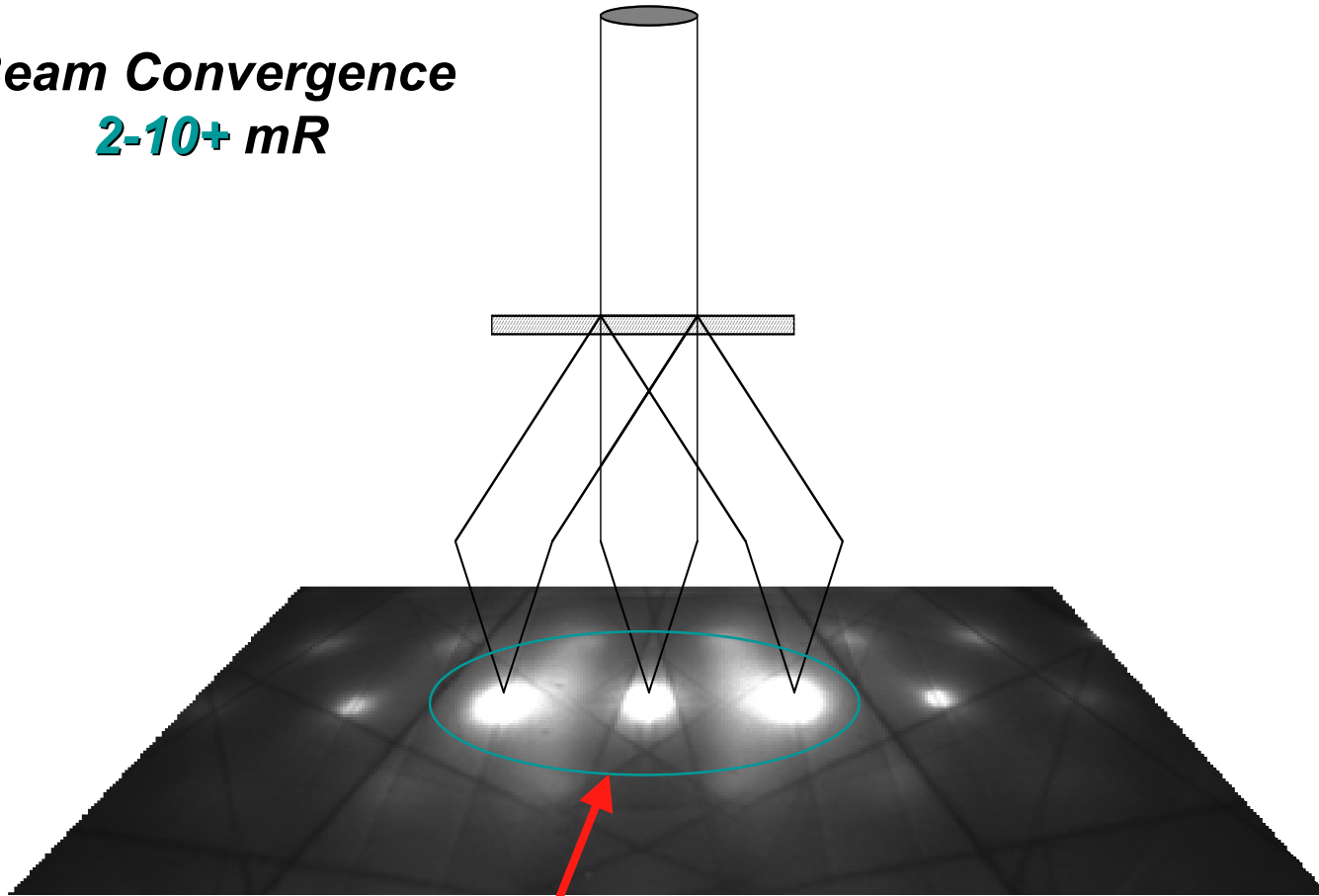
π^* orbital



σ^* orbitals

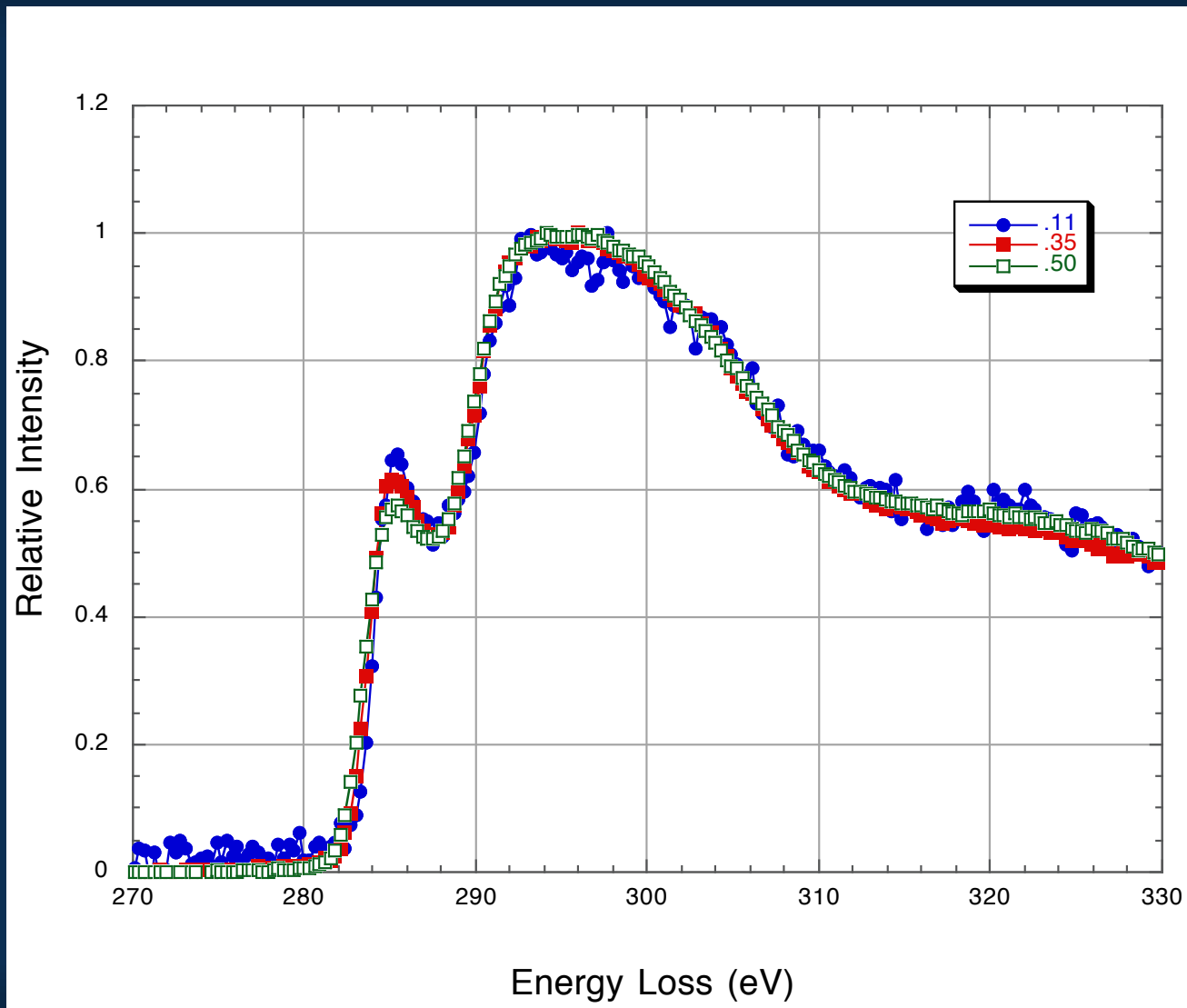
A Conventional EELS experiment in the TEM

Beam Convergence
2-10+ mR



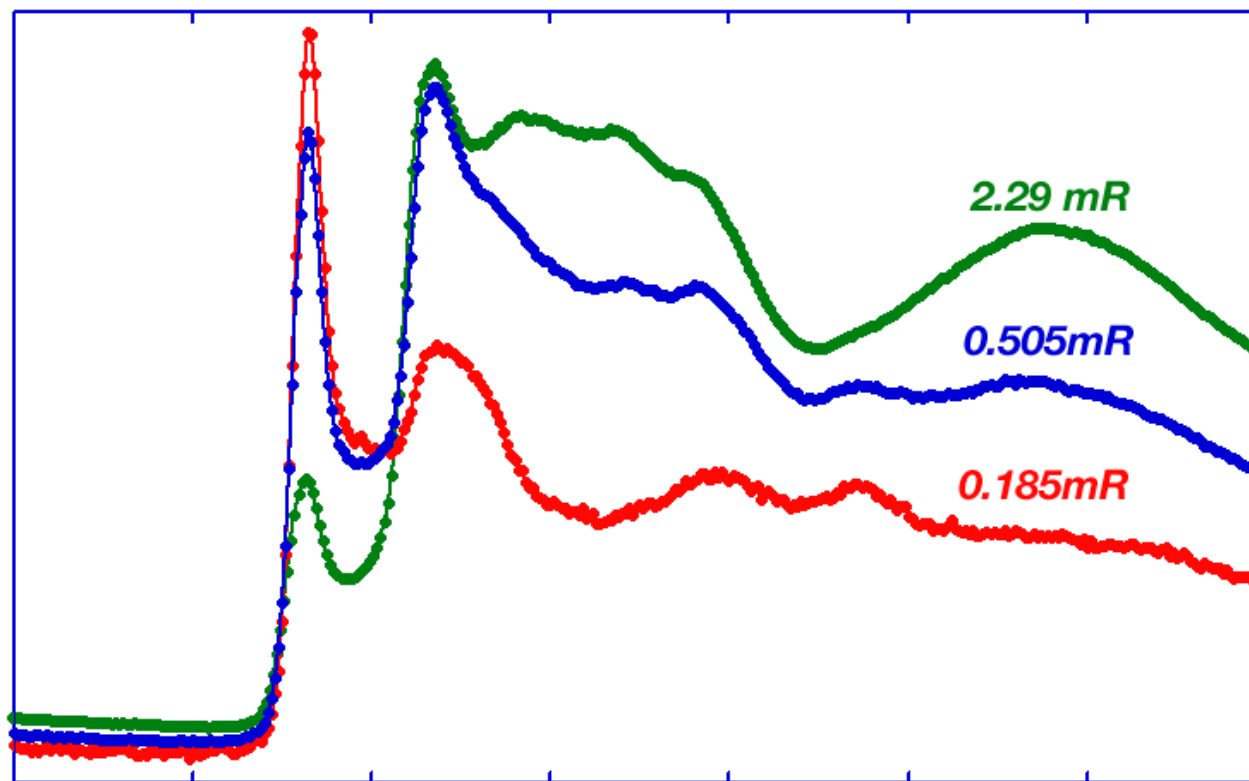
Angular Resolution typically 2-10 mR

Variation of Amorphous Carbon NES with Collection Angle (β)



In some systems/conditions the difference is subtle
But ... this also depends upon what your looking for.

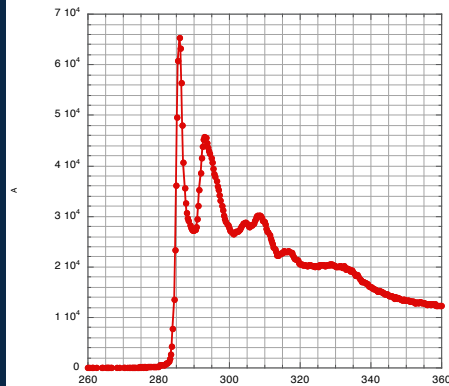
Variation of Graphite NES with Collection Angle (β)



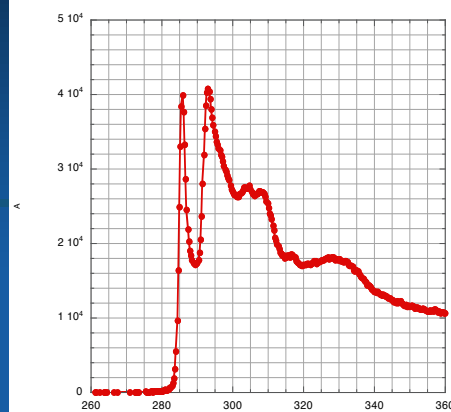
For Anisotropic Materials there can be large variations in the relative intensities of spectral features as a function of Angle (Momentum)

Variation of $C_K (\pi^* \sigma^*)$ in Graphite with Scattering Angle

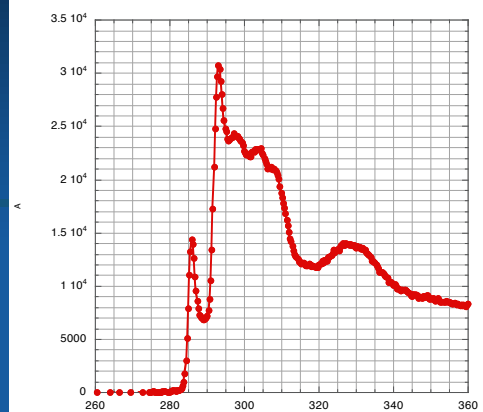
0 mR



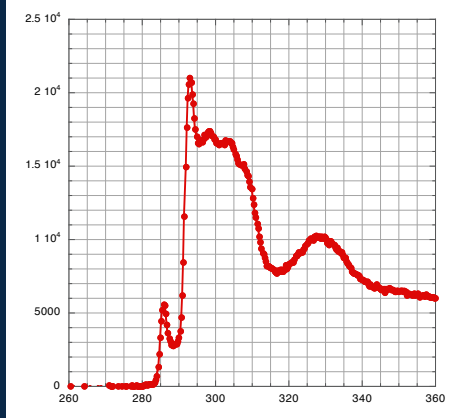
0.35 mR



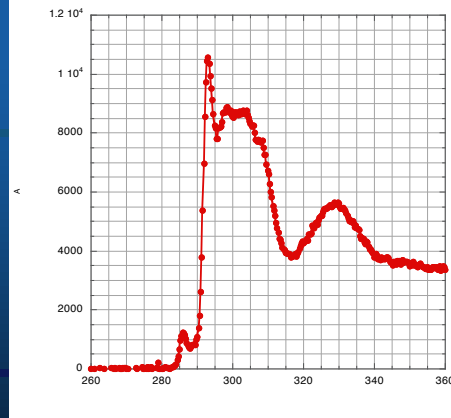
0.7 mR



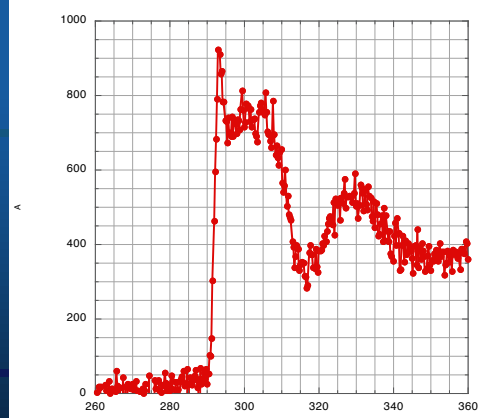
1.05 mR



1.73 mR



7 mR



$\alpha_{1/2} \sim 0.025 \text{ mR}$ $\beta_{1/2} \sim 0.1 \text{ mR}$

$\theta_E \sim 1.15 \text{ mR}$

Advanced Topics

Low Loss Spectroscopy

Plasmon Losses Studies

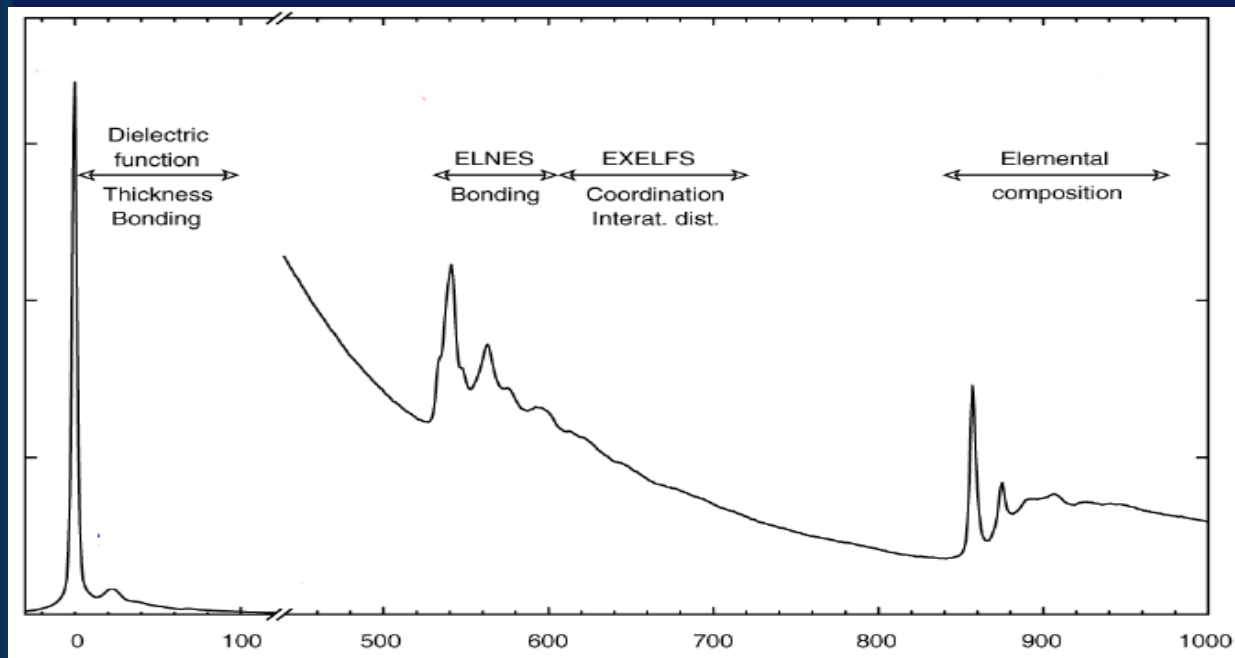
Dielectric Properties

Core Loss Spectroscopy

Near Edge Structure

Extended Fine Structure

Radiation Damage



Low Loss Regime

**Optical, Dielectric,
Electronic, Magnetic
Properties**

Core Loss Regime

**Composition, Bonding,
Electronic, Magnetic,
Structural Properties**

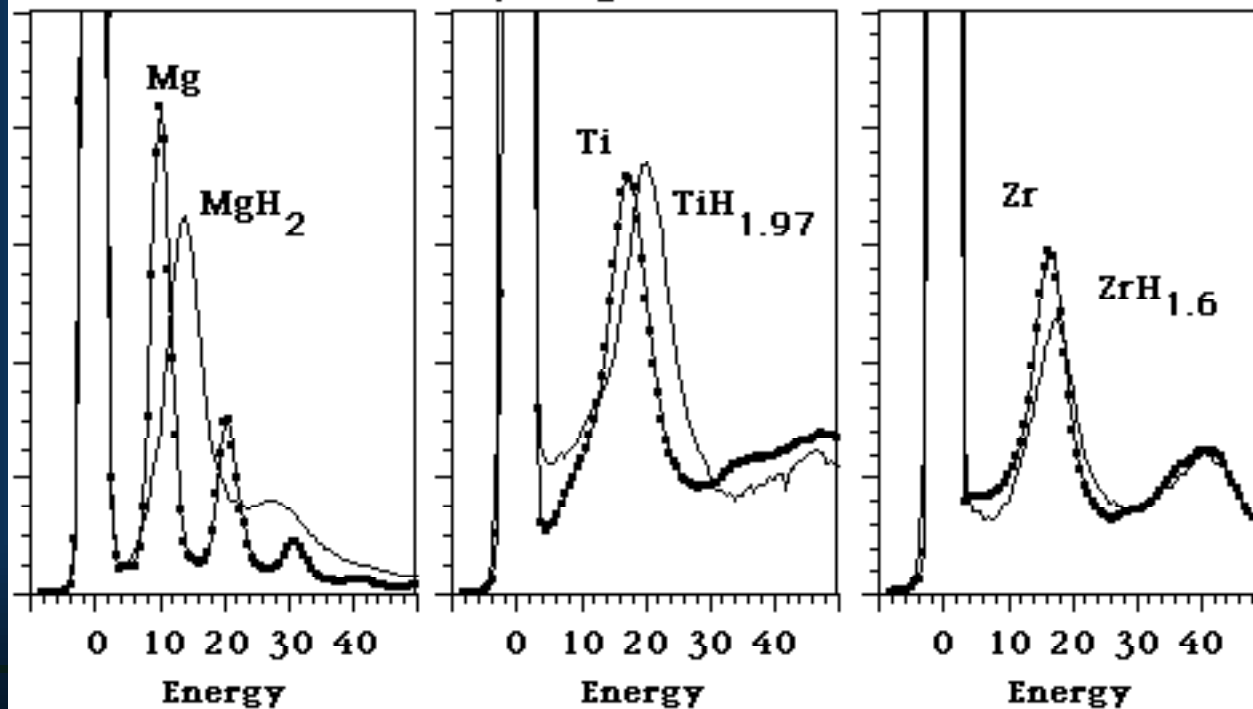
**Structure in EEL Spectra is a manifestation of:
Bonding (Chemistry/Physics) and/or Crystallography (Structure)**

EELS Measurements of Valence Electron Densities

$$\text{Plasmon Energy} = E_p = \hbar^2 \omega_p = \sqrt{\frac{\hbar^2 e^2}{\eta m \epsilon_0}}$$

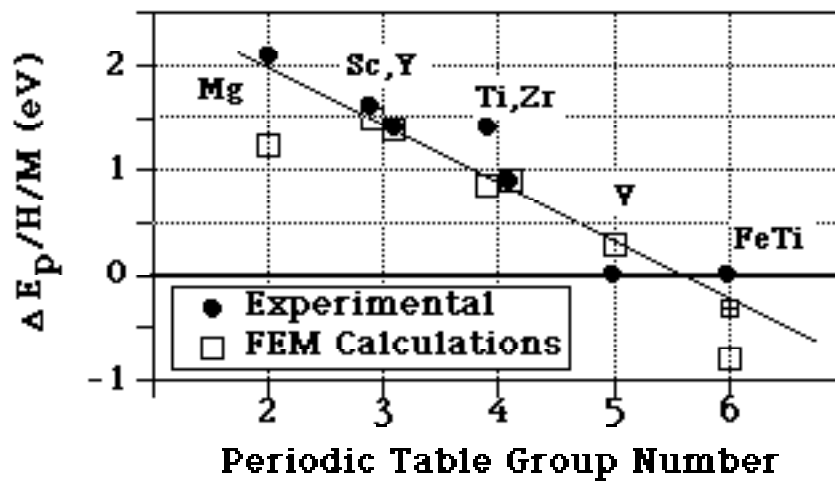
e is the electron charge,
 m its mass,
 ϵ_0 the vacuum dielectric constant,
 \hbar = Planck's constant/ 2π
 η the valence electron density

Hydrogen in Metals

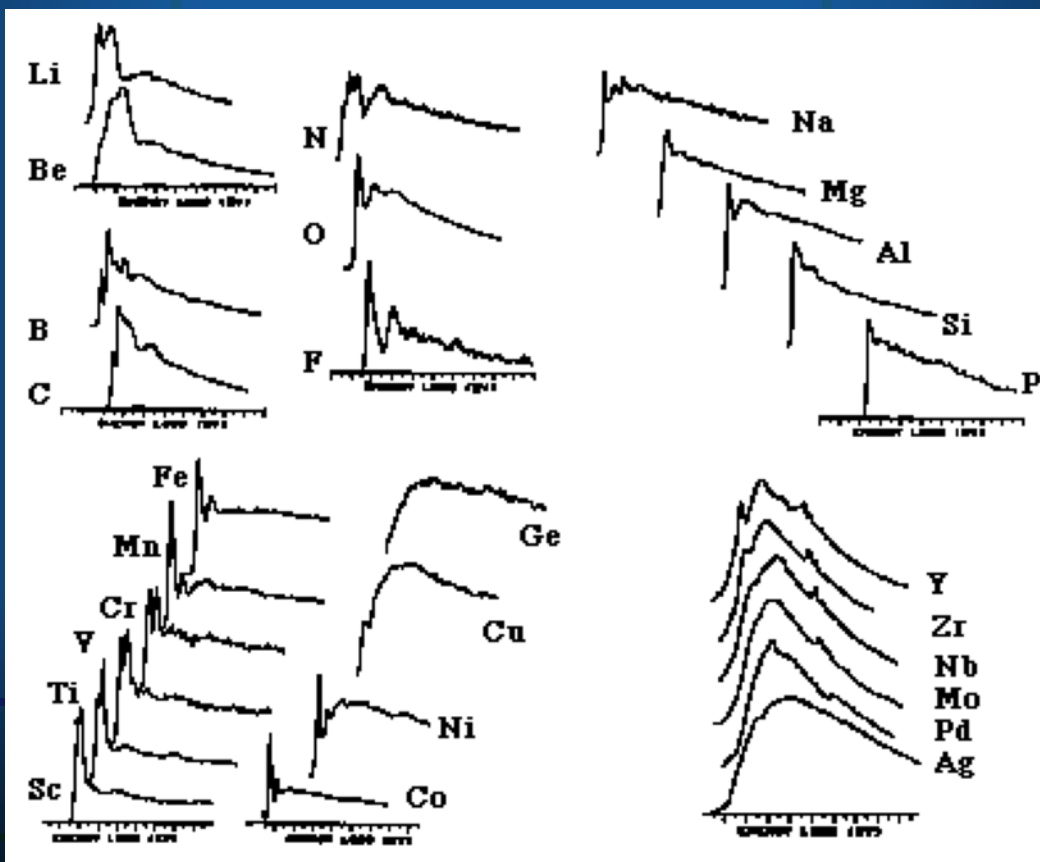
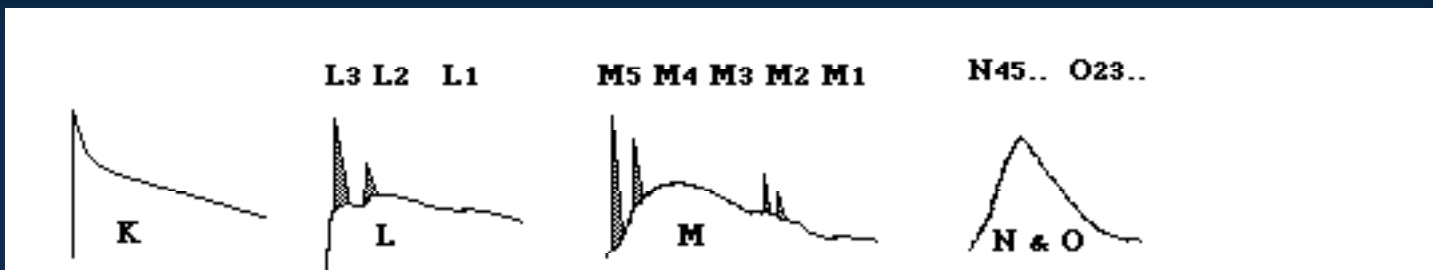


$$E_p = \sqrt{k^2 \omega_p^2} = \sqrt{\frac{-k^2 \epsilon^2}{\epsilon_0} \left(\frac{\eta_s}{m_s} + \frac{\eta_d}{m_d} \right)}$$

Normalized Plasmon Shift



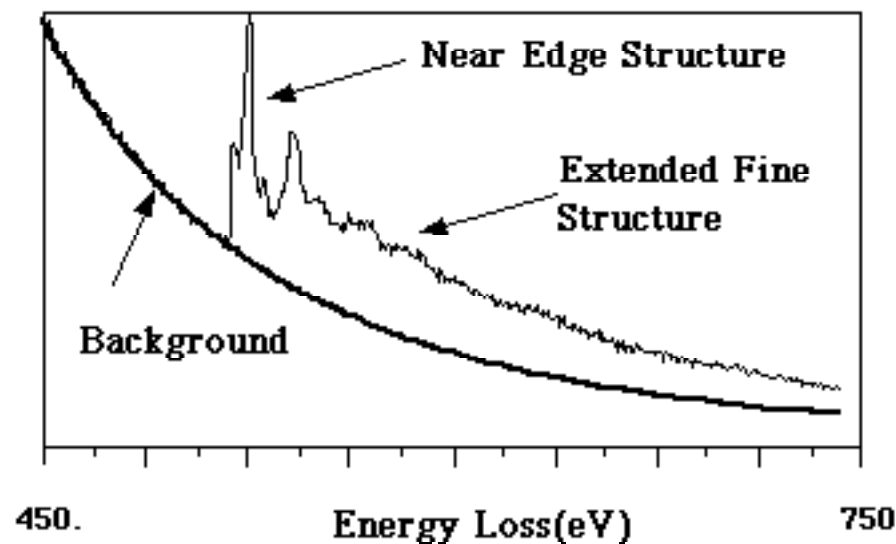
Information in Core-Loss Profiles



Additional EELS Information

Excitation of core levels by the transmitted electron beam can be used to measure the elemental composition of the solid, Near Edge Structure (NES) and EXtended Energy Loss Fine Structure (EXELFS) can be used to elucidate the density of states above the Fermi level and nearest neighbor configurations.

Oxygen K Shell in NiO



ELNES

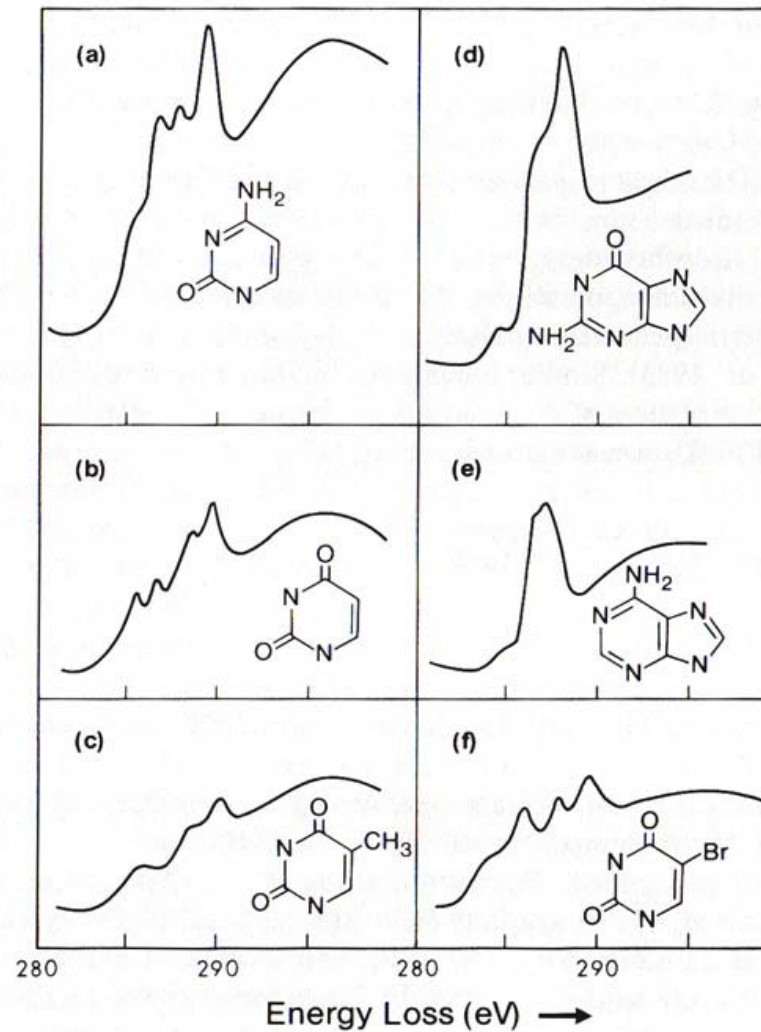
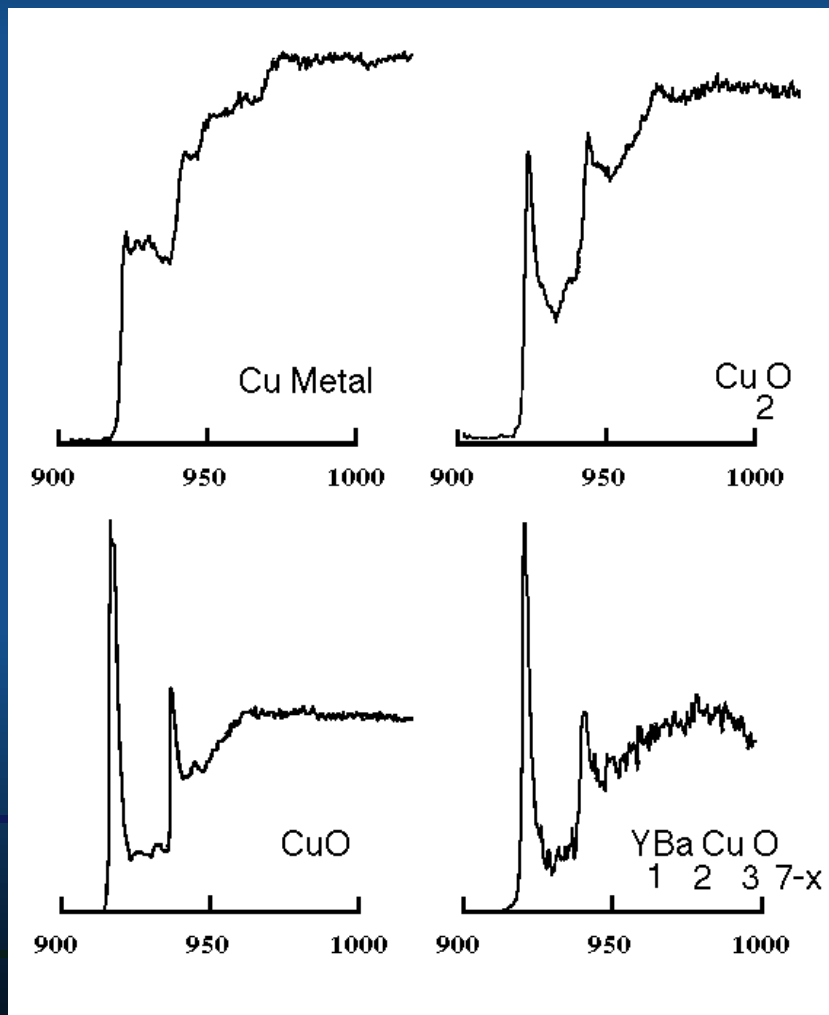


Figure 5.25. Carbon *K*-edge fine structure measured from thin films of (a) cytosine, (b) uracil, (c) thymine, (d) guanine, (e) adenine, and (f) bromothymine. Data from Isaacson (1972b) and Johnson (1972).

Copper L-shell Core Loss Spectroscopy in Metallic, Oxide and High T_c Superconductor Phases



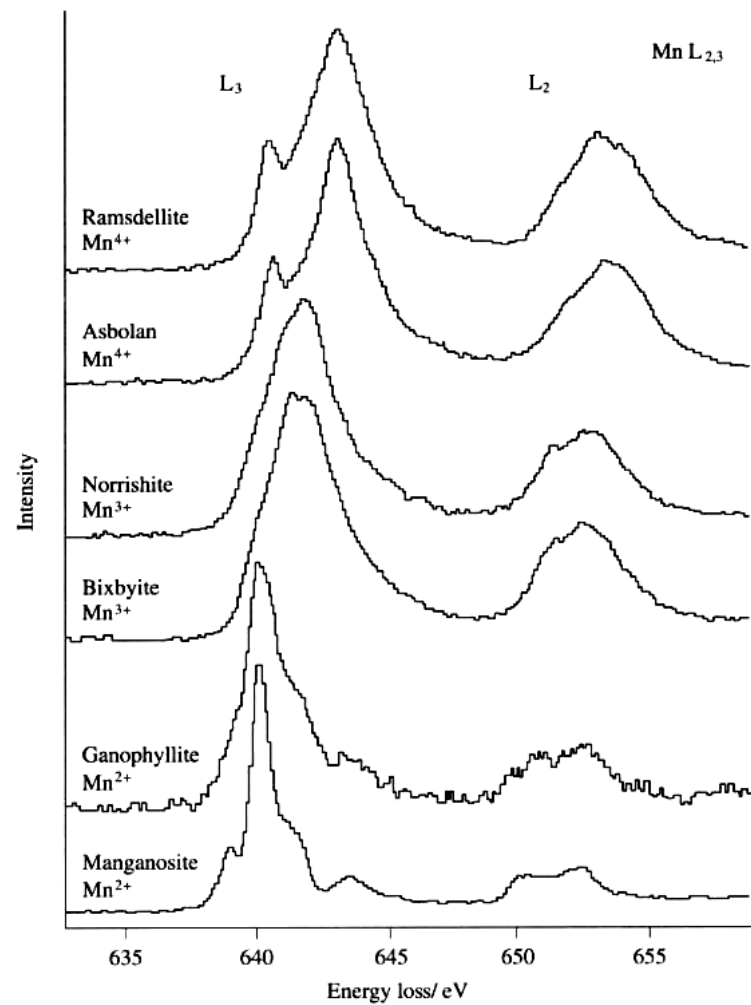
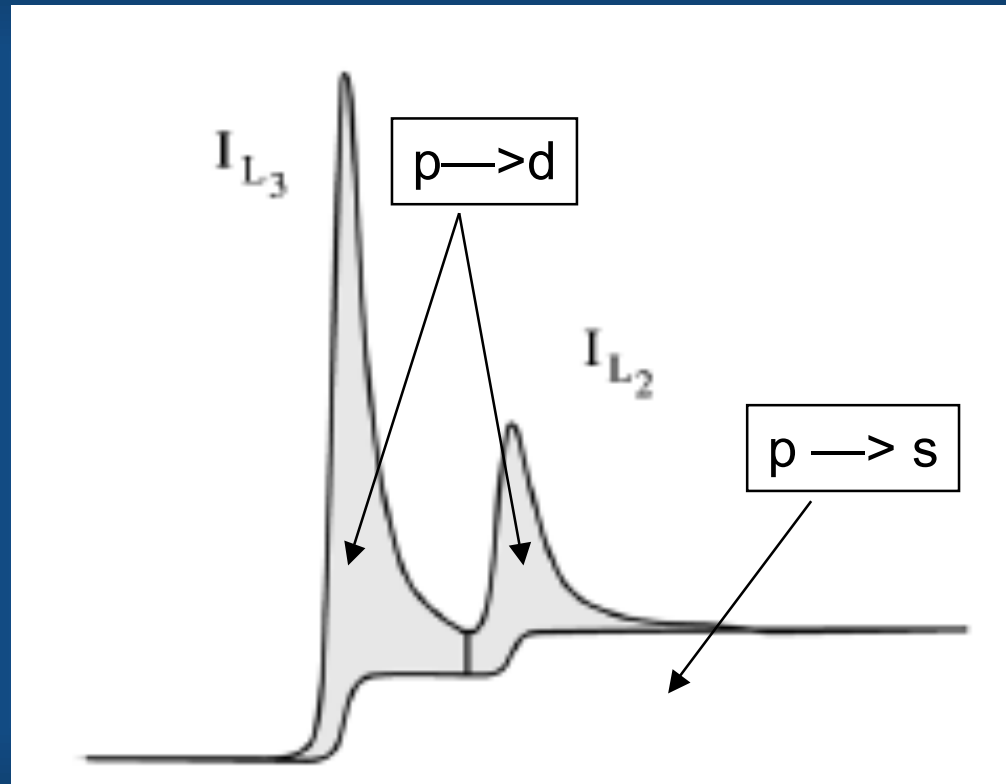


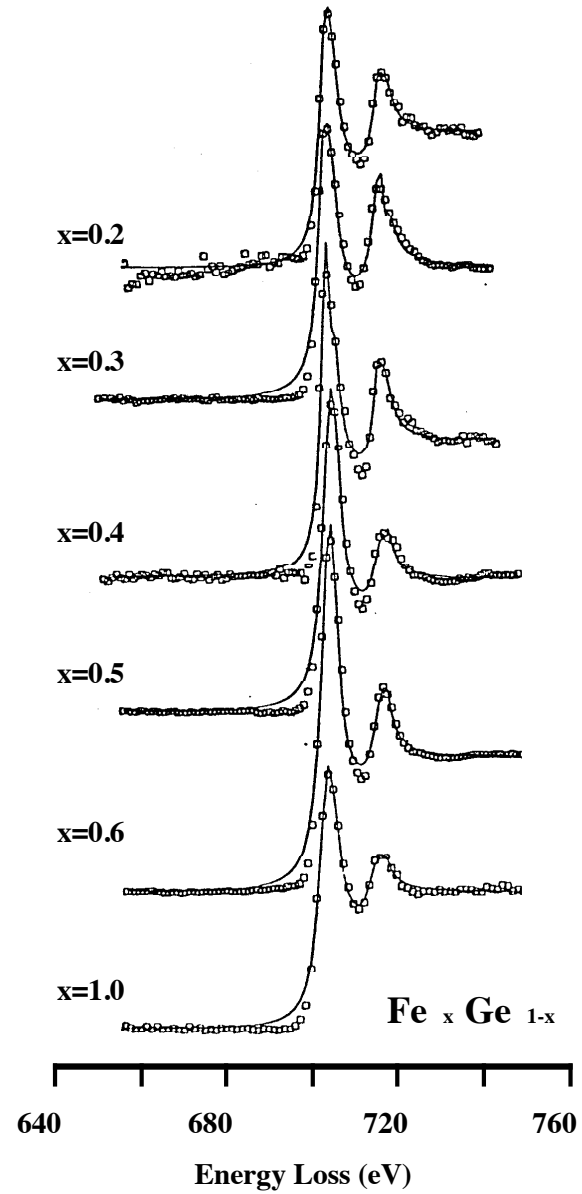
Figure 6.7. Comparison of Mn $L_{2,3}$ -ELNES from a range of manganese minerals showing the systematic change in the L_3 peak position, the L_3/L_2 white-line intensity ratio and the detailed fine structure as a function of the oxidation state of Mn.

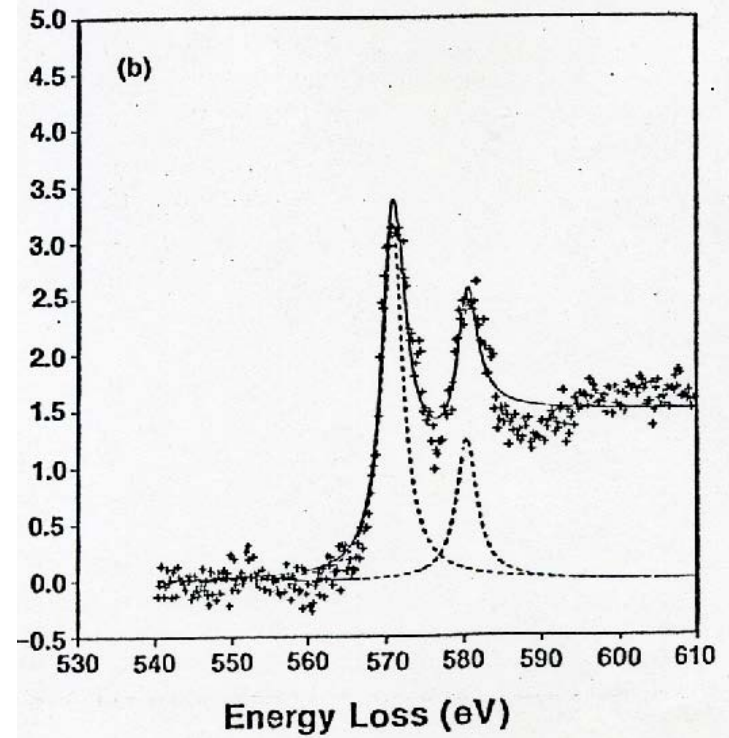
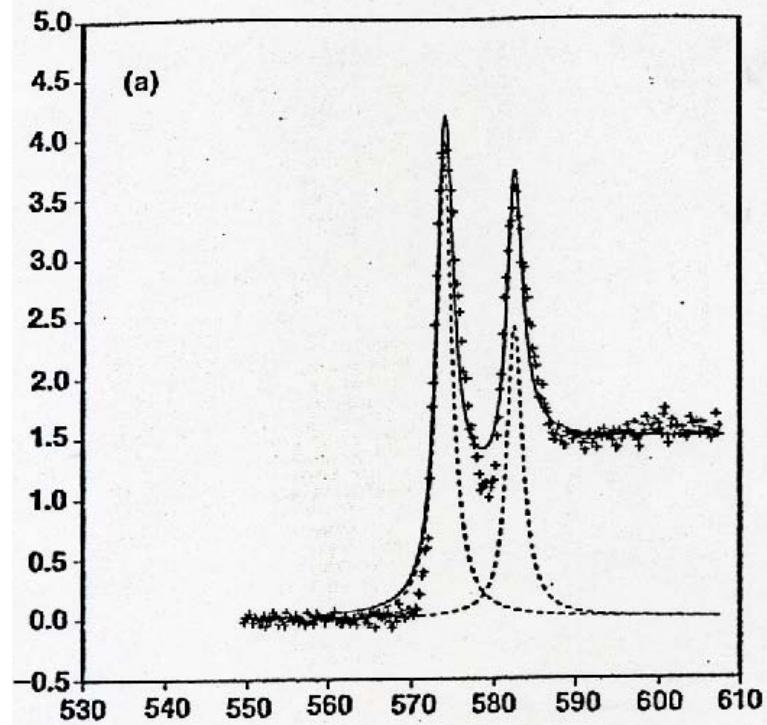
Magnetism in EELS is detectable
using the L shell transitions



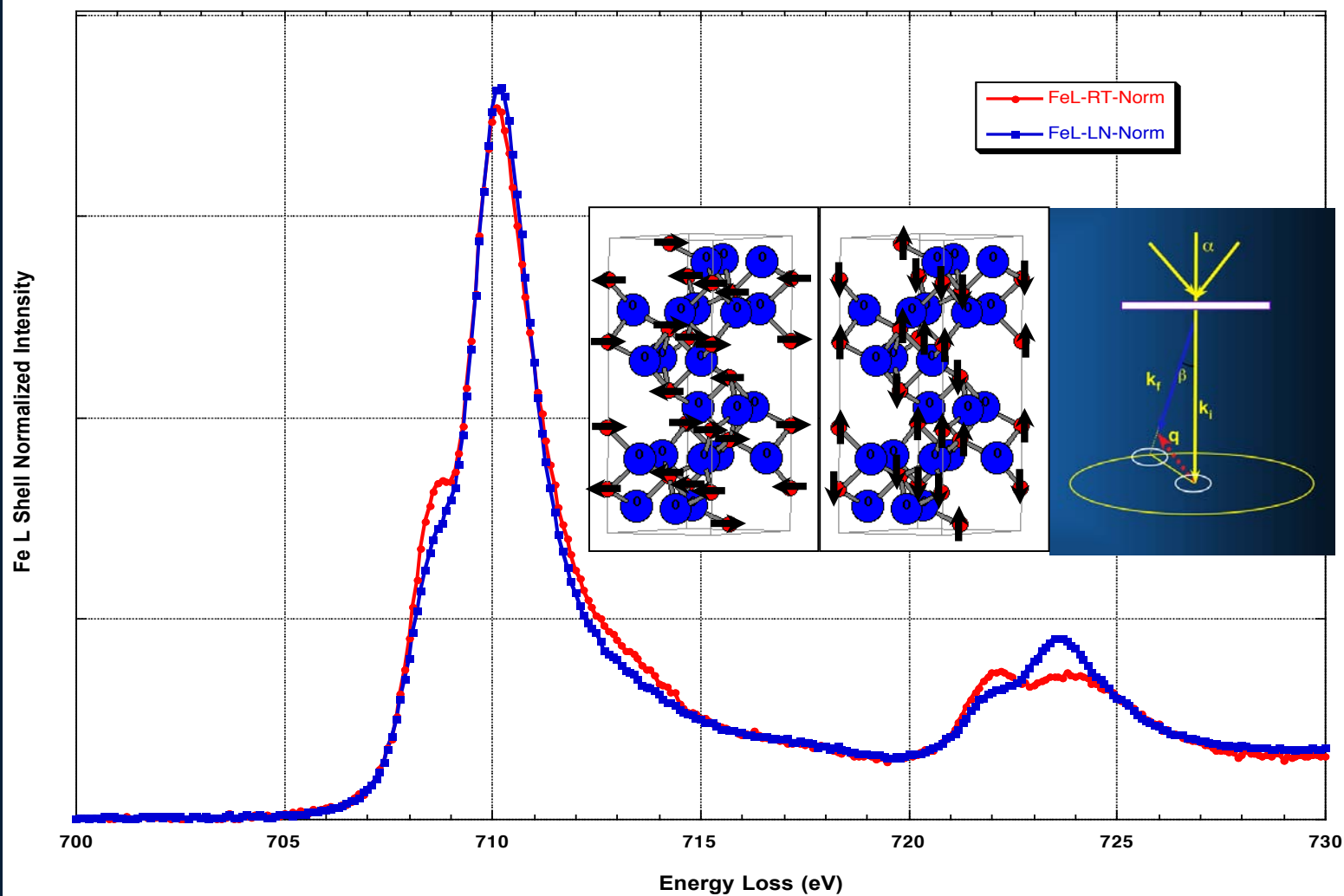
- d electrons are dominant in determining magnetic properties
- the L_3/L_2 "white lines" are the principle signals used to measure magnetism

**Amorphous
 $\text{Fe}_x\text{Ge}_{1-x}$ Magnetic
Materials**





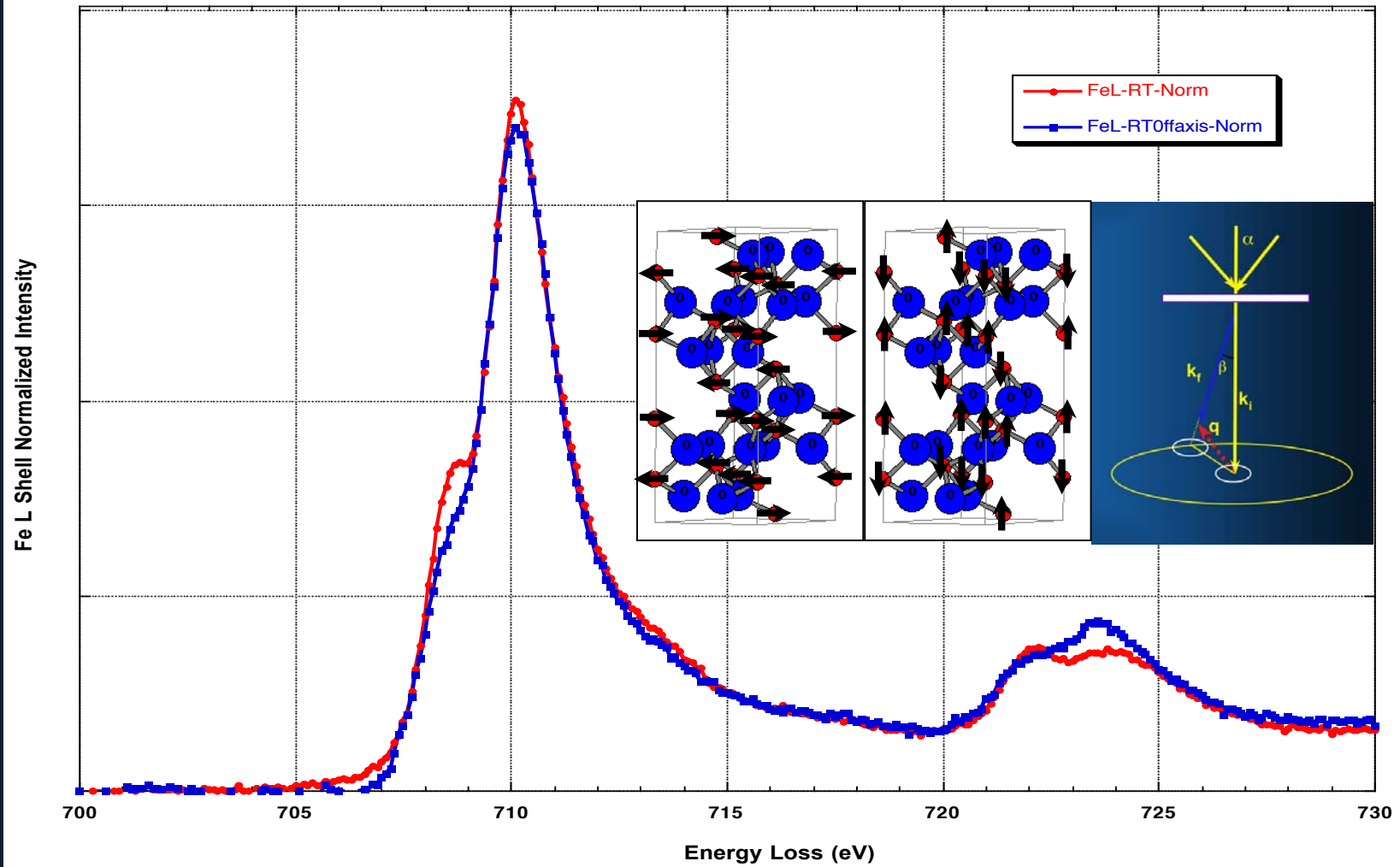
Fe_2O_3 (hematite)



Normalized to LShell Integral

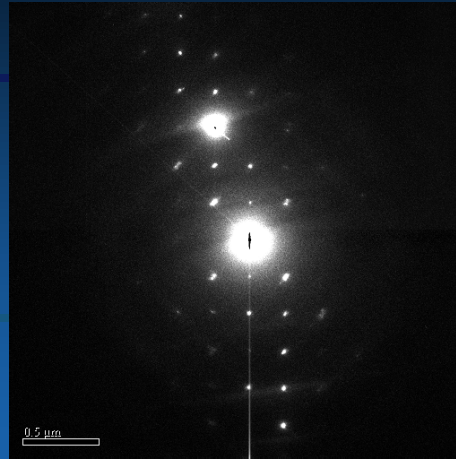
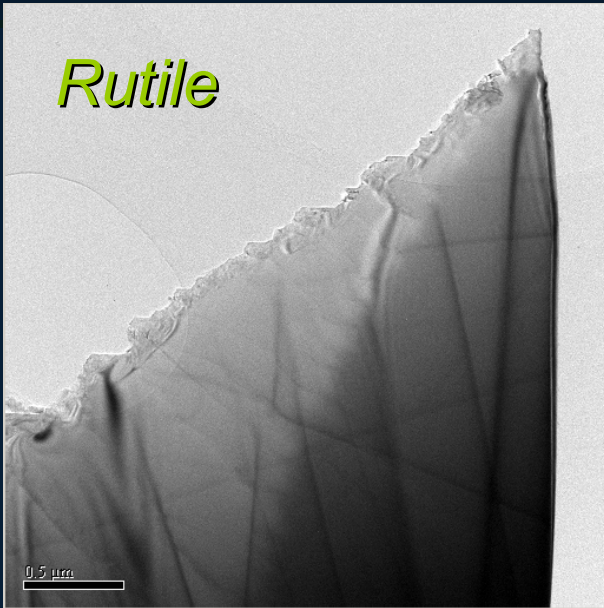
Summed Spectra 4 x 300 sec ~ 200KCnts at L3 Pk

Momentum Resolved On-Axis vs Off-Axis



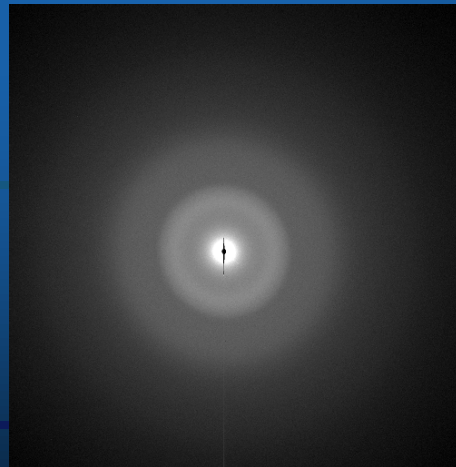
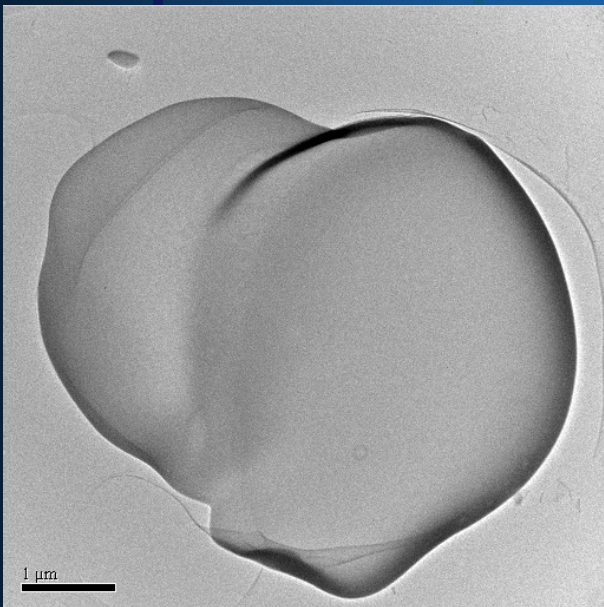
Normalized to LShell Integral

Rutile

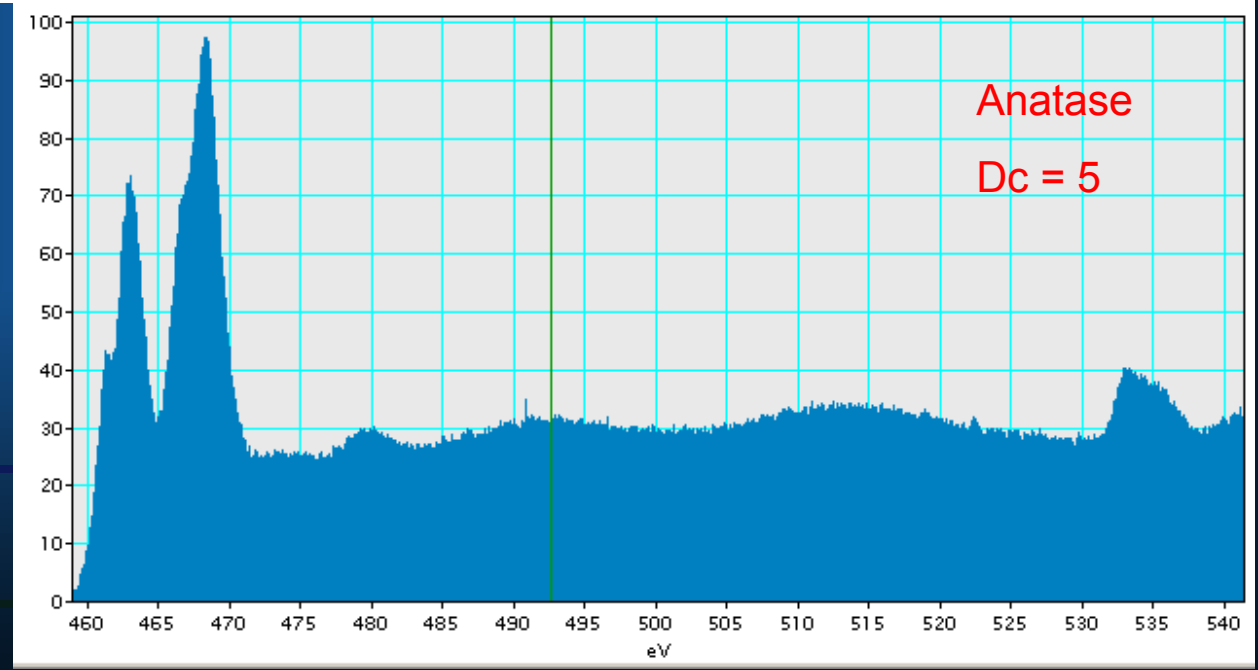
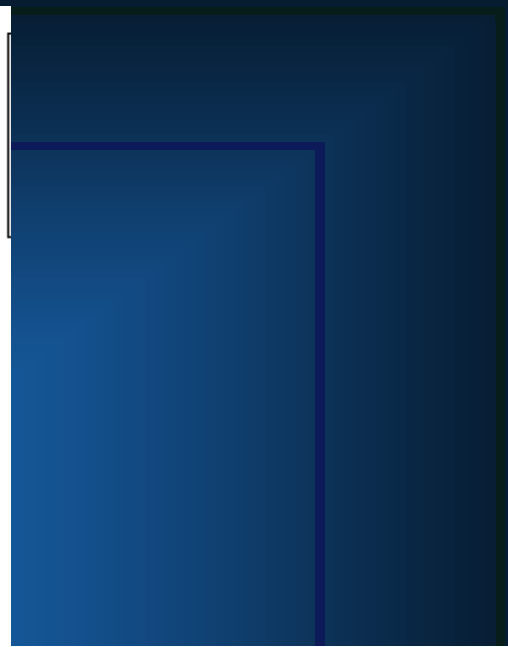
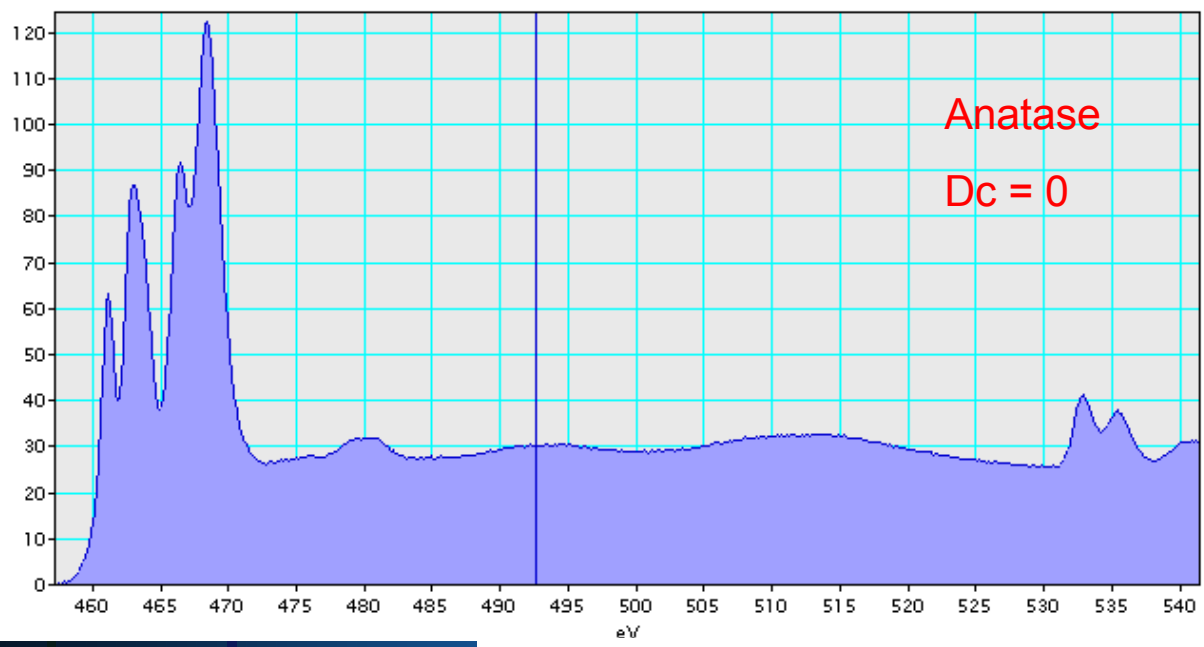


Typical Specimen
used in the EELS work

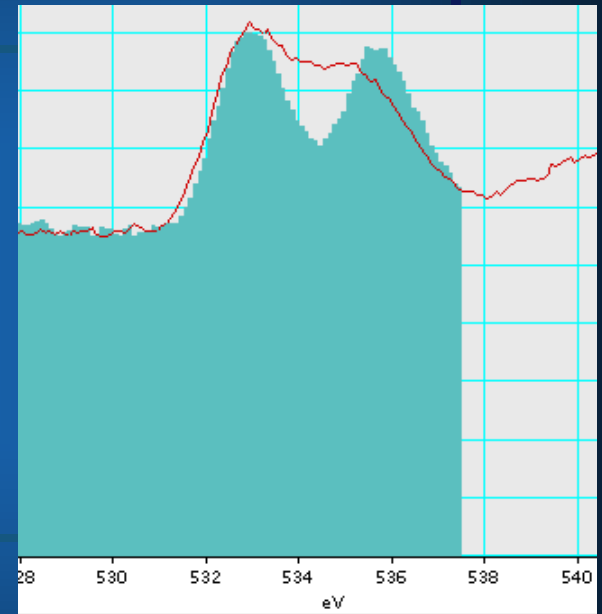
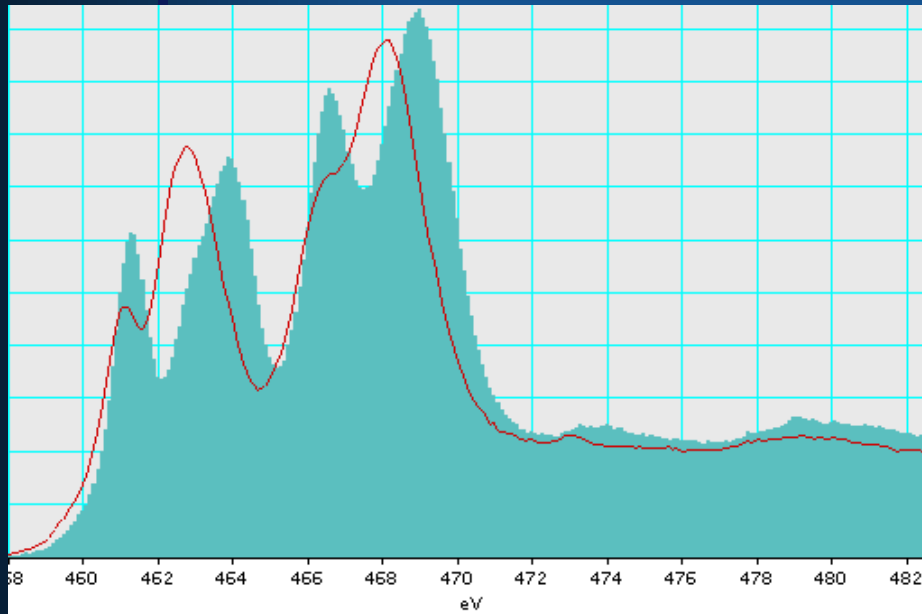
$D_c = 0$
Native
State



$D_c = 5$
Fully
Amorphized
State



Rutile Comparison Dc = 0 / 5



TiL

OK

Table 2.1. Summary of the analytical uses of EELS

Property determined	Spectral region	Processing required	Uses/limitations
Sample thickness	Full spectrum or low loss region	Integration of intensities	Rapid measure of relative thickness; need Λ (inelastic) for absolute values.
Valence electron density	Low loss – plasmon peak position	Peak fitting if required	Phase Identification/ Effects of alloying
Surface/interface states	Low loss – surface plasmons	Need model of dielectric function based on geometry	Surface properties
Joint DOS	Low loss – energy loss function	Deconvolution/fitting of ZLP/Kramers Kronig analysis/sum rules	Band gaps/interband transitions/comparison with optical results
Elemental concentration/ elemental distributions (EFTEM)	High loss – ionization edge intensities	Background subtraction/ deconvolution/ integration/calculation of partial cross-sections	Good for light elements with edges in range 0–2.5 keV/ often high detection limits/limited to thin sample areas
Element specific local coordination and/or valency	High loss – ELNES	Deconvolution/ comparison with reference materials – fingerprinting/peak fitting	Need good energy resolution and determination of absolute energy loss
Element specific unoccupied DOS	High loss – ELNES	Deconvolution/modelling of electronic structure	Need good energy resolution/effect of the core hole
Element specific radial distribution function	High loss – EXELFS	Standard EXAFS data processing	Low SNR – requires good statistics and large edge separations
Anisotropic DOS	High loss – ELNES/ low loss	Deconvolution/modelling of electronic structure	Need small collection angles and well-defined specimen orientation
Site specific DOS	High loss – ELNES/ALCHEMI	Deconvolution/modelling of electronic structure	Need well-defined diffraction and collection conditions
Ground state electron momentum distribution at large momentum transfer	Compton profile	Standard Compton scattering data processing	Low SNR/diffraction conditions